CHARACTERIZATION OF HYDROTHERMALLY ANNEALED LOW TEMPERATURE BIOACTIVE THIN FILM COATINGS OF HYDROXYAPATITE ON $TiAl_6V_4$ IMPLANT MATERIAL

Thesis submitted to

COCHIN UNIVERSITY OF SCIENCE AND TECHNOLOGY

In partial fulfilment of the requirements

for the award of the degree of

DOCTOR OF PHILOSOPHY

By

K.K.SAJU

DIVISION OF MECHANICAL ENGINEERING

SCHOOL OF ENGINEERING

COCHIN UNIVERSITY OF SCIENCE AND TECHNOLOGY

KOCHI-22, INDIA

July 2009

CHARACTERIZATION OF HYDROTHERMALLY ANNEALED LOW TEMPERATURE BIOACTIVE THIN FILM COATINGS OF HYDROXYAPATITE ON $TiAL_6V_4$ IMPLANT MATERIAL

PhD thesis in the field of materials science

Author:

K.K.Saju
Division of Mechanical Engineering
School of Engineering
Cochin University of Science and Technology
Kochi-682022,Kerala,India
Email :kksaju1970@gmail.com

Supervisor:

Dr P.S.Sreejith
Reader
Division of Mechanical Engineering
School of Engineering
Cochin University of Science and Technology
Kochi-682022,Kerala,India
Email:pssreejith2002@gmail.com

July 2009

Dedicated to my children, Krishna and Rahul

Dr. P.S.Sreejith
Reader
Division of Mechanical Engineering
School of Engineering
Cochin University of Science and Technology
Kochi-682022
Phone :91 484 556187
email pssreejith2002@gmail.com

9th July 2009

Certificate

Certified that the work presented in this thesis entitled "Characterization of Hydrothermally Annealed Low Temperature Bioactive Thin Film Coatings of Hydroxyapatite on $TiAl_6V_4$ Implant material" is based on the authentic record of research done by Shri K.K.Saju under my guidance in the School of Engineering, Cochin University of Science and Technology, Kochi-682022 and has not been included in any other thesis submitted for the award of any degree.

Dr P.S.Sreejith
(Supervising Guide)

DECLARATION

Certified that the work presented in this thesis entitled "*Characterization of Hydrothermally Annealed Low Temperature Bioactive Thin Film Coatings of Hydroxyapatite on $TiAl_6V_4$ Implant material*" is based on the original research work done by me under the supervision and guidance of Dr P.S.Sreejith, Reader ,Division of Mechanical Engineering, School of Engineering, Cochin University of Science and Technology,Kochi-682022 and has not been included in any other thesis submitted previously for the award of any degree.

Kochi-22

9th July 2009 **K.K.Saju**

ACKNOWLEDGEMENTS

The investigations in this thesis have been carried out under the supervision of Dr P.S.Sreejith, Reader, Division of Mechanical Engineering, School of Engineering, Cochin University of Science and Technology. I express my deep sense of gratitude for his excellent guidance, competent advice, keen observations and persistent encouragement as well as personal attention given to me during the entire course of work, without which the successful completion of this work would not have been possible. I am deeply indebted to him for all the above considerations.

It is with great pleasure that I acknowledge Dr M.K.Jayaraj, Reader Optoelectronics Lab, Department of Physics, Cochin University of Science and Technology for allowing me to use the facilities of the Department and providing me with great support and guidance during the entire course of my work.

I extend my sincere gratitude to Dr David Peter Principal School of Engineering and other former principals of the Department for allowing me to use the facilities of the Department. I acknowledge the help and guidance of my colleagues in my Department especially Dr Jayadas N.H.

I also thank Prof O.J.Lebba (Dean, Faculty of Engineering, CUSAT) for the support and encouragement given to me.

I wish to thank Dr.K.Prabhakaran Nair, Dean of post graduate studies, NIT Calicut for the support and constant encouragement given to me during the entire period of work.

I am totally thankful to Dr K.V.Menon of Ernakulam Medical Centre and Dr Harkrishna Varma SCTIMST, Thiruvananthapuram for giving me suitable guidance and motivation for the research work.

I express my gratitude to Dr Jackson James, Rajiv Gandhi Centre for Biotechnology, Thiruvanathapuram for helping me with the biological tests.

I am most thankful to Smt Geetha Devi Research scholar at IISc Bangaluru for helping with the contact angle studies.

Deep sense of appreciation is recorded for STIC,CUSAT,Kochi for helping me with the various analysis.

I remember all the research scholars of the Opto Elctronics Laboratory of the Department of Physics, especially Aneesh, Krishnaprasad, Saji, Reshmi, Anila Teacher, Sreeja, Arun, Anoop, Mini ,Joshy sir among others who have helped and supported me during my work.

I am indebted to my colleagues Tide.P.S, Bhasi.A.B, Dr Radhakrishna Panicker and C.A.Babu who were undergoing doctoral work at IISc and IIT's for helping me with various points during my work.

I express my sincere gratitude to all non teaching staff of CUSAT who have helped and supported me during the entire period of work.

I record my sincere and utmost gratitude to my parents and family for patience and tolerance during the entire period of my work

I thank all my well wishers.

I thank God almighty for blessing me with willpower and all qualities required for completion of my work as well as getting along with life.

K.K.Saju

CONTENTS

LIST OF TABLES

LIST OF FIGURES

PREFACE

Hydroxyapatite $Ca_{10}((PO)_4)_6(OH)_2$ (HA) has been widely used as a biomaterial for many applications in orthopaedics since it is chemically similar to the mineral component of bone and tooth minerals in mammals. However due to the poor mechanical properties of bulk HA, it cannot be use as an implant-device material for load bearing applications. Hence HA is applied as coatings on Titanium and Titanium based alloy implant materials by which the mechanical properties of the implants are supported by the metallic structure while the osseointegration is promoted by the bioactive surface of HA. To date plasma spray coating is the only commercially available technique for coating implants with HA. However there are issues affecting the long-term stability and the coating-substrate adhesion of plasma coated implants which are related to the properties of the coating layer, low density and the presence of amorphous and other crystalline calcium phosphate phases. As an alternative method for HA deposition, Pulsed laser deposition has been investigated to produce thin HA films with high crystallanity and good adhesion. Many research efforts have reported on the influence of the process parameters on the crystal structure of the deposited film. Except for crystalline HA all amorphous phases of calcium phosphate are found to have poor adhesion on to the substrate and exhibit a faster dissolution rate in body fluids. Substrate temperatures over 400^0 C in water vapour atmosphere is found to be required in deposition of crystalline HA. However it is found that this high temperature induced an oxide layer on the substrate prior to

deposition which reduced the adhesion of the coated films on to the substrate. Hence many studies are focussed on the deposition of crystalline HA on to Titanium alloy based implant materials at lower temperatures to get a highly adhesive film suitable for clinical applications.

This thesis summarizes the results on the growth and characterisation of thin films of HA grown on $TiAl_6V_4$ (Ti) implant material at a lower substrate temperature by a combination of Pulsed laser deposition and a hydrothermal treatment to get sufficiently strong crystalline films suitable for orthopaedic applications. The comparison of the properties of the coated substrate has been made with other surface modification techniques like anodization and chemical etching. The in-vitro study has been conducted on the surface modified implants to assess its cell viability. A molecular level study has been conducted to analyze the adhesion mechanism of protein adhesion molecules on to HA coated implants.

Chapter 1 gives an introduction to orthopaedic implants and the surface modification techniques used for inducing biocompatibility of implants. A brief description of the properties of implants, materials used for implants highlighting the use of titanium alloys is given in this section. An insight into the tissue response to implant material and the use of hydroxyaptite as thin film coatings on implants are also highlighted here. The limitations of the present coating methods like plasma spraying along with the scope for deposition by pulsed laser process is also mentioned in this chapter.

Chapter 2 describes in detail the pulsed laser deposition of thin films which has been employed for the growth of HA thin films on Ti Al_6 V_4 substrates. A short description on rf magnetron sputtering, electron beam deposition are also mentioned here. The method of anodization of TiAl6V4 implants are described in this section. The various characterization tools used for surface profilometry, morphology, compositional analysis, adhesion tests and mechanical property measurements are detailed here. The set up and procedure for wettability studies are also briefed in this chapter.

Chapter 3 deals with the theoretical mechanism of protein adhesion on to an implant surface. The adhesion of cells are directly related to cell adhesion molecules which are proteins and they are known to attach to proteins adsorbed on to implant surfaces by a ligand receptor binding mechanism. The various surface parameters which will lead to favourable protein adhesion are highlighted in this chapter.

Chapter 4 presents an insight to the in vitro cell viability study adopted here. The cell viability of the various surface modified implant material was studied using the growth of osteosarchoma cells on to them and analyzed by an MTT assay. The optical studies using confocal imaging for cell viability assessment is also briefed in this chapter

Chapter 5 describes the growth and characterization of polycrystalline hydroxyapatite thin films on $TiAl_6V_4$ substrates. The PLD of HA was carried out using an isostatically pressed HA target sintered at 200^0C. After deposition the films were subjected to a standard hydrothermal treatment for a period of one hour. The morphological and

compositional analysis confirmed the growth of a polycrystalline HA film at a low substrate temperature of 200^0C followed by a hydrothermal treatment at 100^0C. The adhesion tests indicated good adhesion characteristics and the wettability study results gave favourable conditions for protein adhesion leading to good osseointegration. These parameters were checked by actual cell viability studies in vitro which yielded a higher cell viability of 40 % more than uncoated samples.

Chapter 6 describes the anodization of $TiAl_6V_4$ substrates at different voltages to different degree of anodization. The samples were anodized at 55V, 60V and 75V to get anodized surfaces with different layers of anodization thickness. The surface morphological studies, wettability studies and mechanical analysis of the substrates showed that the surface anodized at a higher voltage had surface properties to give good osseointegration. The samples were subjected to in-vitro cell viability tests which confirmed good osseointegration for the substrate anodized at a voltage of 75 V.

Chapter 7 compares the surface parameters of etched, anodized and HA Coated Ti substrates for suitability for good osseointegration. It is seen that HA coated surface showed most favourable properties for maximum protein adhesion. The surface anodized at 75V also showed properties close to HA coated surfaces, whereas the other surfaces presented surface condition for a lower protein adhesion than the above surfaces. The order of cell viability was ascertained for all surfaces using MTT assay and the surfaces presented cell adhesion as evaluated by their surface properties.

Chapter 8 presents the molecular level study of the adhesion mechanism of proteins on to binding sites of HA using quantum chemical calculations. In this chapter the electrostatic attraction and the tendency of adhesion of protein molecules on to a HA coated surface due to HOMO–LUMO interactions of various molecules done in a qualitative manner using the commercial quantum chemical package Spartan 04, Wavefunction USA has been described. The semi-empirical method PM3 used for the quantum chemical studies are mentioned. HOMO-LUMO maps and electrostatic potential maps used to identify binding sites are described. The protein strands of fibronectin with the Argine-Glycine-Aspartic acid highlighted chosen for the study are also depicted. The HA molecular pattern gave a favourable binding protocol for binding of Extracellular matrix proteins on to the surface thereby providing a case for good cell adhesion.

Chapter 9 summarizes the main results in the thesis and the scope for future work.

Part of the thesis has been published/accepted for publication in internationally Refereed journals

1. K.K.saju, Sasidharan Vidyanand, N.H.Jayadas, Jackson James, M.K.Jayaraj, Effect of surface characteristics of anodized Ti-6Al-4V implant material on osteoblast attachment and proliferation-Journal of orthopaedics 2009; 6(1)e5.
2. K.K.Saju, Reshmi R, JayadasN.H., Jackson James, M.K.Jayaraj-Polycrystalline coating of hydroxyapatite on $TiAl_6V_4$ implant material grown at lower substrate temperatures by hydrothermal annealing after pulsed laser deposition-accepted for publication in the Journal of engineering in medicine (Ref: JEIM568R1).
3. K.K.Saju, Jayadas .N.H, M.K.Jayaraj, Jackson james, Comparison of cell Adhesion Characteristics of Anodized and Hydroxyapatite coated $TiAl_6V_4$ implant material based on wet ability and in-vitro studies-under review with the Journal of adhesion science and technology (Ref: JAST-S-09-00012).

Conference Proceedings:

1. K.K.Saju, Naishan.K.George, P.S.Sreejith, Bioactive coatings of hydroxyapatite on titanium substrates for body implants-presented in the International conference on Advanced Materials and Composites (ICAMC 2007)

Chapter 1

INTRODUCTION TO ORTHOPAEDIC IMPLANTS AND SURFACE MODIFICATION TECHNIQUES ADOPTED FOR BIOCOMPATIBILITY

This chapter *gives an overview of orthopaedic implants and the surface modification techniques used on implants. A brief description of the properties of implants and materials used for implants are given in this section. An insight into the tissue response to implant material and the use of hydroxyaptite as thin film coatings on implants are also highlighted here.*

1.1Introduction to Orthopaedic Implants

An orthopaedic implant is a device surgically placed into the body designed to restore function by replacing or reinforcing a damaged structure. The material used in orthopaedic implants must be biocompatible to avoid rejection by the body [1]. The implant helps in repair and reunion of bone mass quickly and effectively so that the patient can return to a normal healthy lifestyle [1]. The design principles and manufacturing criteria are the same as for any other engineering applications requiring a dynamic load-bearing member. Bone is unique among the tissues of the body, in the level of its resistance to compressive forces. Factors contributing to the overall mechanical behaviour of bone include constituent volume fraction, mechanical properties, orientation and interfacial bonding interactions. Interfacial bonding interactions between the mineral and organic constituents is based in part on electronic interactions between negatively charged organic domains and the positively

charged mineral surface [2]. Phosphate and fluoride ions have demonstrated to offer mineral organic interactions, thereby influencing the mechanical properties of bone in tension. The implant material fall into two categories: (1) Temporary fixation devices and (2) Permanent prosthetic devices [1, 2].

1.1.1 Properties of implants

The proper function of orthopaedic devices is dependent on a number of factors, defect in any of which may result in failure of the implants [3,4]. The implanted device is expected to withstand applied physiological forces without substantial stress corrosion. The device has to have proper design for sufficient strength. Materials selection has to be critical in order to ensure biocompatibility, corrosion resistance, long term stability and adequate strength. Thermodynamic stability of the implant is the ideal condition and requires an equivalent replacement material in an identical structure to that of natural bone. In order to function as intended, all replacements must transmit forces into or from one part to another part of the skeleton. The mechanical problems resulting from this force transmission depends on

1. The mechanical reliability of the implant itself
2. The response of the bony tissues to the stresses and strains created by the insertion of the implant
3. The mechanics of the interface between implant and bone.

Once an implant is in place the natural physiological response of wound healing, callous formation and remodelling must take place for the implant to be successful. Therefore the geometry of the implant should not interfere with the transport processes and cellular responses required for repair.

1.1.2 Implant materials

The implanted material is expected to withstand applied physiological forces without substantial dimensional change, catastrophic brittle fracture or fracture in the longer term from creep, fatigue or stress corrosion [5]. Thermodynamic stability is only achieved in the ideal situation of an equivalent replacement material in an identical structure to that of the natural tissue. Any departure from this may create a different stress state in the remaining tissue and hence the potential for bone resorption and implant loosening. Presently, more inert implant materials are most frequently used, while others are designed to possess combinations of mechanical and surface chemical properties required to meet specific physiological properties. Materials with high strength and inertness such as metal alloys, alumina and high density polyethylene are in clinical use. Metallic alloys and alumina are stiffer than cortical bone while polymers are less stiff [5]. With respect to fracture toughness the metallic alloys are considerably stronger than cortical bone, while alumina is at the lower band of the values of cortical bone. Hydroxyapatite (HA) which is of the same composition as of the mineral component of bone is used as coating material on metallic implants to improve its biocompatibility. Titanium and its alloys are the most widely used implant material in recent times. Among the Titanium alloys $TiAl_6V_4$ is the most common orthopaedic implant material chosen for its higher biocompatibility and osseointegration [5]. Table 1.1 shows properties and uses of some common implant materials along with the properties of bone [3].

Table1.1: Properties and uses of some common implant materials along with the properties of bone

Material	Ultimate Tensile Strength (MPa)	Modulus (GPa)	Biological Properties	Disadvantages	Common Applications
Cortical Bone	30-211	16-20	---	---	---
Cancellous Bone	51-193	4.6-15	---	---	---
Synthetic rubber	10-12	4	Easy to fabricate. Low density	Low mechanical strength, tissue reactions	Space filling devices, middle ear prosthesis
Steel	480-655	193	High Impact strength, high resistance to wear, absorption of high strain energy	Lower biocompatibility, corrosion in physiological environment, mismatch in mechanical properties with connective tissues	Orthopaedic load bearing and fixation devices, dental implants
Cobalt – Chromium alloy	655-1400	195			
Titanium	550-860	100-105			
Platinum	152-485	147	Resistance to wear	High cost, lower strength	Dental applications
Hydroxyapatite	600	19	Good biocompatibility	Lower load bearing capacity	Hip and knee prosthesis, increase biocompatibility

1.1.3 Temporary fixation devices

The purpose of temporary fixation devices is to stabilize fractured bone until natural healing processes have restored sufficient strength so that the implant can be removed [1]. These devices include pins, nails, wires, screws, plates and intramedullary devices. Bone plates are used for joining bone fragments together during healing of load-bearing bones. The later provides rigidity for the fixation of the fracture. Screws are used with the plates to secure them to bone. Figs 1.1 show the use of temporary fixation devices.

a) b)

Fig 1.1(a) shows a lower jaw bone fixed with the help of a miniplate and screw (b) Shows a miniplate and miniscrew used as temporary fixation devices.

1.1.4 Permanent Prosthetic Devices

Synovial joints are mobile joints which include human hip, knee, elbow, ankle, finger and shoulder joints. In case of degenerative bone and joint diseases these joints require replacements which are done by permanent prosthetic devices [1]. However, the delicate articulation of joints and complicated load transfer dynamics pose some additional problems as compared to long bone fracture repairs. If the replacement fails for any reason, it is much more difficult to replace the joint a second time since a large portion of the natural tissue has already been destroyed. For these reasons orthopaedic surgeons try to salvage the joints whenever possible and use implants as a last resort. Many different type of joints are routinely replaced. This include knee, shoulder, elbow, wrist and hip joints. Current hip prosthetic devices and techniques claim a high success rate. A permanent hip prosthesis is shown in fig 1.2. A nearly inert metal surface ($TiAl_6V_4$) articulates against an UHMWPE (Ultra high molecular weight polyethylene) surface. These components are

fixed in place using PMMA (Polymethylmethacrylate) [6]. The common biomaterials used for total joint replacements are shown in table 1.2 [3].

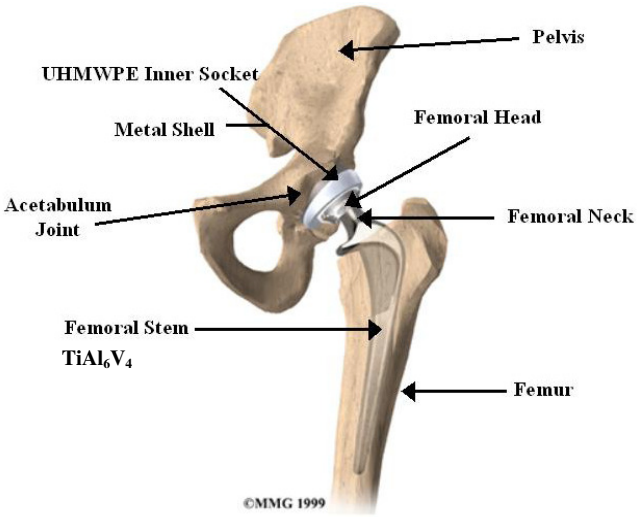

Fig 1.2: Model of a total hip prosthesis

Table 1.2: Biomaterials used in total joint replacement

Material	Application
Metals: Stainless steels 316 L, Cobalt based alloys, Co-Cr-Mo ,Co-Ni-Cr-MO,Co-Cr-W-Ni Titanium based material CP Ti ,Ti-6Al-4V,Ti-5Al-2.5Fe,Ti-Al-nb	Femoral stems, heads, tibial and femoral components, Porous coatings. Porous coatings second phase in ceramic and PMMA composites, Femoral stems, heads
Ceramics: Bioinert carbon Alumina,Zirconia Bioactive Calcium phosphates,Bioglasses	Coatings on metallic femoral stems,second phase in composites and bone cement. Femoral stems, heads, acetabular cups Coatings on metallic and ceramic femoral stems,cafold materials,second phase in PMMA and UHMWPE composites.
Polymers: PMMA UHMWPE/HDPE PTFE	Bone cement Acetablar cups,tibial and patellar components, porous coatings on metallic and ceramic femoral stems
Composites: Polymer based-Polysulflone–carbon,Polycarbonate-Carbon,Polysulflone-Kevar,Polycarbonate-Kevlar	Femoral stems

1.2 Biocompatibility of Implants

1.2.1 Introduction

The term 'biocompatible' suggests that the material described displays good or harmonious behaviour in contact with tissue and body fluids[6].

Biocompatibility describes the interactions between the living system and the material introduced into this system. A material is bioinert when the material-tissue interface is stable, i.e., constituents of the tissue and material neither react chemically with each other nor dissolve into each other. When the interface is not in equilibrium, that is, when the interface is unstable, host-material relationships characterized by irritation, inflammation, damage, immunogenicity, pyrogenicity, toxicity, or carcinogenicity evince a state of bio incompatibility while a state of biocompatibility exists in their absence. Biomaterials which cannot be eliminated by the body are biotolerant when they are fibrotically encapsulated and bioactive when they evoke a critical host reaction. Bioactive hydroxyapatite is a case in point in as much as it stimulates proliferation and differentiation of fibroblasts and osteoblasts and induces collagen synthesis by these cells [1-6].

1.2.2 Tissue Response to implant material

Peri-implantar tissue is the body response to implantation of medical devices. The site of implantation is an important factor that influences the tissue response to biomaterials. The main differentiation has to be done between soft and hard tissue.

a) Soft Tissue

The tissue response to biomaterials in soft tissue is always characterized by the presence of a fibrous tissue capsule enveloping the implant and by the presence of interfacial cells like macrophages and foreign body giant cells. The

thickness of the capsule seems to be related to the biocompatibility of the material and to its chronic inflammatory response.

b) Hard Tissue

Histological evaluations of tissue reactions to materials implanted in hard tissues (bone) have identified the direct apposition of new bone to biomaterial. In some cases bone may be found directly apposed to one portion of an implant, while the remaining surface is encapsulated by fibrous tissue similar to that seen in soft tissue. In this case the fibrous tissue capsule takes an additional significance because it reduces the stability of the implant, leading to implant loosening. Many histological evaluations have been made on this membrane. Since 1975 attention has been focused on two histological parameters: the inflammatory infiltrate and the presence of material debris [6-7]. The inflammatory reaction is diffused in the peri-implantar tissue: in the acute phase polymorphonuclear cells are predominant, while in the chronic phase lymphocytes and giant cells are more prevalent.

The peri-implantar membrane is composed of three layers: near the prosthesis it has macrophages and giant cells, in the middle layer it is fibrous and poor in cells, and, finally, near the bone it looks like a granulation tissue rich in fibroblasts, macrophages, round cells and blood vessels. Macrophages show in the cytoplasm phagocyted particles of metal and corrosion product. More recent studies describe the membrane as consisting of an external compact fibrous layer and an internal layer richer in cells. The external layer has a thickness ranging from 3 to 5 μm formed by orientated fibres. Blood vessels of various size, few fibroblastic cells and small wear debris may be recognized. The internal layer, less than 1 μm thick, is derived from fibroblastic differentiation.

1.2.3 Surface Properties that influence biocompatibility

Cells are sensitive and responsive to the topography and surface chemistry of the material substrates with which they interact. Several factors (such as surgical techniques, implant design, surface topography, surface chemistry, and wetability are known to influence bone growth on an implant; the later three have become key areas in the development of improved orthopaedic devices [8]. One of the major research topics in orthopaedic tissue engineering is topography, particularly with respect to optimizing cell colonization. Topography is often seen to have a significant effect on both proliferation and differentiation of osteoblastic cells. The most commonly observed trend is that as the roughness and disorder of surface features increase, differentiation and/or extracellular matrix synthesis increase, with a corresponding reduction in cell proliferation. Improved osteoinduction of titanium was observed on micro porous structures compared with non-microporous titanium which did not induce bone formation at all. Several studies have further suggested that other microstructural features (such as grain and particle size) promote osteoblast functions compared with smooth surfaces. In addition to topography, implant surface chemistry plays an important role in protein adsorption and subsequent cell adhesion. For example, the surface oxide layer of titanium has many qualities regarded as important for promoting bone growth [8]. This oxide layer of titanium can be manipulated chemically. The electrochemical method of anodization or anodic oxidation is a well-established surface modification technique for titanium that produces protective layers. Anodization has been successfully used as a surface treatment for orthopedic implants and has reported to increase bone growth. Other strategies for improving the biocompatibility and osteogenic capacity of metal implants include surface modification with inorganic mineral coatings, particulates, or

cements containing a diversity of calcium salts (mainly calcium phosphates, sulphates or carbonates). The idea behind all of these strategies is to make the metal surface more acceptable to bone cells and by doing so, trick the body into rapid integration of the implanted structure rather than fibrous encapsulation.

Another feature that is widely observed is that protein adsorption that determines cell adhesion on to an implant favours a more hydrophobic surface compared to a lesser one. Therefore the wetability of the surface is detrimental in the final biocompatibility of the implant.

1.2.4 Techniques adopted to increase biocompatibility of implants

Various techniques have been adopted to change the surface topography as well as surface chemistry of the implant surfaces [7-11]. Table 1.3 summarizes some of the techniques adopted for the surface modification of Titanium implants [12].

Table 1.3 Overview of surface modification techniques for implants of titanium and its alloys

Surface modification methods	Modified Layer	Objective
Mechanical methods Machining Grinding Polishing Blasting	Rough or smooth surface formed by subtraction process	Produce specific surface topographies: clean and roughen surface: improve adhesion in bonding
Chemical methods Chemical treatments Acidic treatment Alkaline treatment	< 1nm of surface oxide layer ~ I μm of sodium titanate	Remove oxide layers, contamination. Improve biocompatibility

Hydrogen peroxide treatment	~5nm of dense inner oxide and porous layer	Improve biocompatibility
Sol gel methods	~10nm of thin films such as calcium phosphate	Improve biocompatibility
CVD	~1μm of TiC, TiN etc	Improve wear resistance ,corrosion resistance
Anodic oxidation	~10nm to40 μm of TiO_2 layer	Specific surface topographies, improve biocompatibility
Biochemical methods	Modifications through silanized titania, photochemistry etc	Induce specific cell and tissue response
Physical methods Thermal spray Flame spray Plasma spray HVOF DGUN	~30 TO ~200 μm of coatings like HA, calcium silicate etc	Improve biological properties
PVD Evaporation Ion plating Sputtering	~1μm ofTiN, TiC, diamond like carbon thin films etc	Improve wear resistance ,corrosion resistance ,biocompatibility
Ion Implantation Beam- line ion implantation	~10 nm of surface modified layer	Modify surface composition and biocompatibility
Glow discharge plasma	~ 1nm to ~100 nm of surface modified layer	Clean, sterilize, oxide, nitride surface, remove native oxide layer

1.3 Hydroxyapatite as bone substitute

Hydroxyapatite is a bioactive ceramic material that mimics the mineral composition of natural bone [13-16]. This material does not possess acceptable mechanical properties for use as a bulk biomaterial; however, it does

demonstrate significant potential for use as a coating on metallic orthopaedic and dental prostheses. Hydroxyapatite, fluorapatite, monetite, tricalcium phosphate, tetracalcium phosphate, and octacalcium phosphate belong to a family of minerals known as apatites. These materials have similar structures (hexagonal system, P63/m), and formulae ($X_3Y_2(TO_4)Z$) [13-16].

Apatites of interest in medicine and dentistry possess the followingstructures: X=Y=Ca, T=P, and Z=OH. Of these, hydroxyapatite ($Ca_{10}(PO_4)_6(OH)_2$) is the most widely used compound. The calcium:phosphate ratio determines the activity of calcium phosphorus compounds within the human body. In pure compounds, the ratio between calcium and phosphate ranges from0.5 to 2.0. Hydroxyapatite exhibits calcium: phosphorus ratio of 1.67 (5/3). Table 1.4 contains the several physical properties for hydroxyapatite [13]. Crystalline powders of this material may be obtained using aqueous precipitation and solid state processes. X-ray and infrared spectroscopy studies have shown that hydroxyapatite is fully hydroxylated after sintering at 900 °C. The reverse process of dehydroxylation may occur if the sintering temperature is greater than 900 °C [13]. A slight deviation from the 1.67 Calcium: phosphorus ratio may occur during thermal processing, which can lead to the formation of α-tricalcium phosphate, β-tricalcium phosphate, or other compounds. Table 1.4 also contains information on several bioactive calcium phosphate compounds, which are similar to the naturally occurring apatites that provide strength to the skeleton and act as a storehouse for calcium, phosphorus, and other minerals [13].

Table1. 4: Biologically relevant calcium phosphate compounds

Name	Chemical formula	Calcium: phosphate ratio
Hydroxyapatite (HA)	$Ca_{10}(PO_4)6(OH)_2$	1.67
Fluorapatite (FA)	$Ca_{10}(PO_4)6F_2$	1.67
Calcium-deficient hydroxyapatite (CDHA)	$Ca_{10-x}(HPO_4)x(PO_4)_{6-x}(OH)_{2-x}(0 < x < 2)$	1.33–1.67
Biological apatite (BA BA = carbonated CDHA(x = 1.7)	$Ca_{8.3}(PO_4)_{4.3}(CO_3–HPO_4)_{1.7}(OH)_{0.3}$	1.38–1.93
Oxyhydroxyapatite (OHA)	$Ca_{10}(PO_4)6(OH)_{2-2x}O_x\Upsilon_x(0 < x < 1)$	1.67
Oxyapatite (OA	$Ca_{10}O(PO_4)_6$	1.67
Monocalcium phosphate monohydrate (MCPM)	Ca(H2PO4)2·H2O	0.5
Monocalcium phosphate anhydrate (MCPA)	Ca(H2PO4)2	0.5
Dicalcium phosphate dehydrate (brushite) (DCPD)	$CaHPO_4{\cdot}2H_2O$	1
Dicalcium phosphate anhydrate (monetite) (DCPA)	$CaHPO_4$	1
Octacalcium phosphate (OCP)	$Ca_8(HPO_4)_2(PO_4)_{4\cdot5}H_2O$	1.33
Tricalcium phosphate (phase α (α-TCP)	$Ca_3(PO_4)_2$ (monoclinic)	1.5
Tricalcium phosphate (phase β, whitlockite) (β-TCP	$Ca_3(PO_4)_2$ (rhombohedral)	1.5
Tetracalcium phosphate (TTCP)	$Ca_4O(PO_4)_2$	2
Dicalcium phosphate (phase α) (α-DCP)	$Ca_2P_2O_7$ (orthorhombic)	1
Dicalcium phosphate (phase β) (calcium pyrophosphate)(β-DCP)	$Ca_2P_2O_7$ (tetragonal)	1
Amorphous calcium phosphate (ACP)	$Ca_x(PO_4)_y\ nH_2O$	1.2–2.2
The symbol Υ represents a vacancy in the crystallographic lattice.		

Hydroxyapatite forms crystals that are best described as hexagonal rhombic prisms [14]. The lattice parameters for hydroxyapatite are a=9.432 Å and c=6.881 Å (Fig: 1.3). Hydroxyl ions (OH^-) occur at the corners of the basal plane. These ions are positioned at every 3.44 Å (one half the unit cell), parallel to the c-axis and perpendicular to the basal plane. Thus, 60% of calcium ions in the unit cell are associated with the hydroxyl ions. The density of this material is 3.219 g/cm^3.

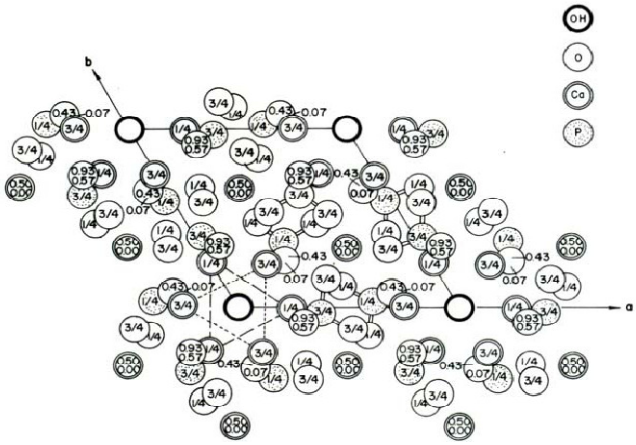

(a)

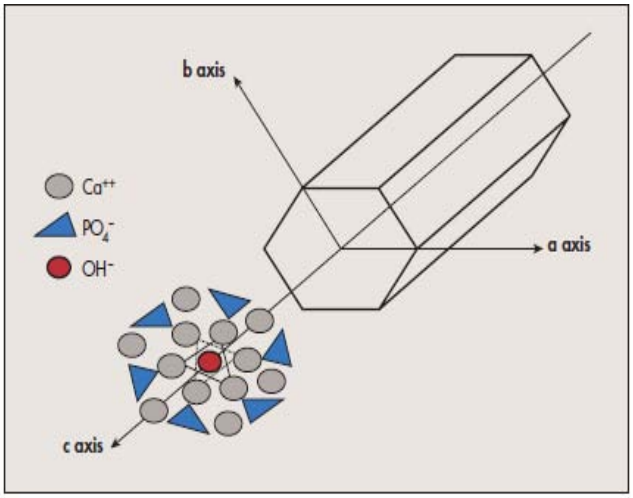

(b)

Fig 1.3 (a&b): Hydroxyapatite structure projected down c axis onto basal plane

1.3.1 Hydroxyapatite coated implants

There are many techniques that have been used to create hydroxyapatite coatings on metallic implant materials. Dip coating, electrophoretic deposition, hot isotatic pressing, pulsed laser deposition, sol-gel processing, and sputter coating have been used to deposit hydroxyapatite coatings [18]. Table 1.5 shows the characteristics of the different coating techniques adopted for coating HA on implants.

Table 1.5: Hydroxyapatite deposition techniques

Name	Thickness	Remarks
Plasma Spraying	1mm -10 mm	Can coat complex substrates Requires high melting temperatures. Thermal expansion mismatch is common. Phase non-uniformity
Electrophoretic Deposition	0.1-2.0mm	Can coat complex substrates Cannot produce crack-free coatings without difficulty Requires high sintering temperatures
Hot Isostatic Pressing	0.2-2.0mm	HIP cannot coat complex substrates High temperature required, producing thermal expansion mismatch Produces dense coatings
Sol-Gel	$< 1\mu m$	Complex shapes at low processing temperatures Expensive raw materials
Sputter Coating	0.02-1μm	Line of sight technique Produces amorphous coatings Uniform coating thickness on flat substrates
Thermal Spraying	30-200μm	High processing temperature and rapid cooling leads to amorphous coatings Line of sight technique
Pulsed Laser Deposition	$< 5\ \mu m$	Stoichiometric transfer of material Water vapour atmosphere requirement Phase purity

1.3.2 Limitations posed by present coating methods.

Plasma spraying is the most commonly used technique producing hydroxyapatite coatings, which involves heating hydroxyapatite powder above its melting point in order to form a plasma-gas stream [13]. The plasma-gas stream is then accelerated towards the substrate. Plasma-sprayed coatings contain a mixture of crystalline hydroxyapatite, amorphous hydroxyapatite and tricalcium phosphate phases. There are several drawbacks to this process, which include poor adhesion, nonuniform thickness, poor crystallinity, poor integrity, uneven resorption, mechanical failure at the coating/substrate interface, and increased implant wear [19, 20]. For example, the amorphous hydroxyapatite phase, which generally makes up between 5% and 20% of plasma-sprayed coatings, degrades much more rapidly than the crystalline hydroxyapatite phase. In addition, plasma sprayed coatings contain large numbers of molten particles, defects, porosities, and cracks, which act to degrade coating integrity. Furthermore, plasma-sprayed coatings also contain stresses that result from the large coefficient of thermal expansion (CTE) mismatch between the hydroxyapatite coating and the metal substrate. For example, the CTE mismatch between hydroxyapatite(15×10^{-6} K^{-1}) and $TiAl_6V_4$ alloy (8.8×10^{-6} K^{-1}) is significant [13]. In addition, plasma spraying of many metals and all polymers is precluded due to the high processing temperatures. As a result, a high proportion of plasma-sprayed hydroxyapatite coatings exhibit mechanical failure at the coating–substrate interface [21]. Pulsed laser deposition presents the case of stoichiometrically correct and pure coatings of HA. However it is seen that the coatings have to be done either at elevated temperatures ranging from 400-800^{0}C. The condition of high substrate temperatures promoted the oxidation of the substrate surface prior to the growth of the HA layer .The oxidation layer degraded the adhesion of the coating to the substrate [21].

1.3.3 Scope for improvement of HA coatings

PLD has several characteristics that distinguish it from other growth methods and provide special advantages for the growth of chemically complex (multielement) and composite materials [22, 23]. The advantages of technique are the capability for reactive deposition, energetic evaporants, fast deposition times, flexibility, improved film quality at lower temperatures, maintenance of stoichiometry, and simplicity for the growth of multilayered structures [22-23].

However, there are problems associated with pulsed laser deposition of hydroxyaptite thin films. Previous work suggests pulsed laser deposition of fully crystalline hydroxyapatite thin films requires temperatures greater than 400°C and deposition in an Ar/H_2O gas environment [21]. Deposition at lower temperatures produces amorphous films, which resorb too rapidly to provide *in vivo* implant-bone bonding. In addition, films deposited by PLD using an excimer laser on $TiAl_6V_4$ substrates either at room temperature or at elevated temperature in inert gases gave very poor adhesion. This may be due to the formation of an intermediate titanium oxide layer between the hydroxyapatite film and the $TiAl_6V_4$ substrate prior to deposition or due to softening of the $TiAl_6V_4$substrate during after deposition annealing. This necessitates the study for deposition of crystallized HA coatings by PLD at lower temperatures in order to obtain a high adhesive coating suitable for clinical purposes [21,24].

1.4 Conclusion

Implant loosening in bone fixation is an unresolved complication associated with internal fixation. It is generally accepted that this problem can be overcome by modifying the implant bone interface for improved osseointegration. This is achieved in part by hydroxyapatite coatings on implant materials. The benefits of these coatings are constrained by not only the

generally low strength of adhesion to the implant surface but also by the variation in crystalinity across the coatings. Pulsed laser deposition of HA presents a case of depositing stoichiometrically correct phase pure HA coatings. However the higher processing temperatures needed for obtaining polycrystalline HA coatings lead to lower adhesion of the coatings on the substrates and can fail in implant applications. This opens a case for deposition of HA on implant materials at a lower processing temperature in order to produce highly adhesive coatings of clinical acceptability.

References:

[1] S.V. Bhat-Biomaterials,(2005) Narosa publishing house Mumbai, ISBN 81-7319-626-5 186-208.

[2] S.H Park, A. Llinás, and V. K. Goel, Bone Repair and Joint Implants, Biomaterials: principles and applications, (2003) CRC Press LLC-ISBN 0-8493-1491-7 173-178.

[3] S V. Bhat-Biomaterials, (2005), Narosa publishing house Mumbai, ISBN 81-7319-626-5 4-5.

[4] J. B. Park and J. D. Bronzino, Biomaterials: principles and applications, (2003)CRC Press LLC-ISBN 0-8493-1491-7 1-5.

[5] P. Korkusuz, F. Korkusuz, Hard Tissue-Biomaterial Interactions, Biomaterials inOrthopedics, (2004) Marcel Dekker ,USA, ISBN: 0-8247-4294-X 1-40.

[6] J. H. Boss, Biocompatibility: Review of the Concept and Its Relevance to Clinical Practice (2000), CRC ,USA 978-0824703189 1-54.

[7] M.Ninomi, Mechanical biocompatibilitie of titanium alloys for biomedical applications, Journal of medical behaviour of biomedical materials, 1 (2008) 30-42

[8] G. Balasundaram, T. J Webster, A perspective on nanophase materials for orthopaedic implant applications, Journal of materials chemistry **16** (2006) 3737-3745.

[9] S. A. Catledge, M D. Fries, Y.K. Vohra, W.R. Lacefield, J.E. Lemons, S. Woodard, and R.Venugopalan- Nanostructured Ceramics for Biomedical Implants, Journal of Nanosci. Nanotech **2** (2002) 1–20.

[10] A.J. García and C.D. Reyes, Bio-adhesive Surfaces to Promote Osteoblast Differentiation and Bone Formation, J Dent Res (2005) **84(5)** 407-413.

[11] L. C. Baxter, V. Frauchiger, M. Textor, I. Gwynn and R. G.Richards, Fibroblast and Osteoblast Adhesion and morphology on calcium phosphate surfaces, European cells and materials **4** (2002) 1-17.

[12] X. Liua, P. K. Chub, C. Ding, Surface modification of titanium, titanium alloys, and related materials for biomedical applications, Materials Science and Engineering **R 47** (2004) 49–121.

[13] C.F. Koch, S. Johnson , D. Kumar , M. Jelinek , D.B. Chrisey , A. Doraiswamy ,C. Jin , R.J. Narayan , I.N. Mihailescu -Pulsed laser deposition of hydroxyapatite thin films, Materials Science and Engineering **C 27** (2007) 484–494.

[14] S. Johnson, M. Haluska, R. J. Narayan , Robert L. Snyder, In situ annealing of hydroxyapatite thin films, Materials Science and Engineering **C 26** (2006) 1312 – 1316.

[15] S.W.K. Kweha, K.A. Khora, P. Cheang, The production and characterization of hydroxyapatite (HA) powders, Journal of Materials Processing Technology **89** (1999) 373-377.

[16] Y.W. Gua, N.H. Loha, K.A. Khora, S.B. Tora, P. Cheang, Spark plasma sintering of hydroxyapatite powders, Biomaterials. **23** (2002) 37–43.

[17] S Bharati, M K Sinha and D Basu, Hydroxyapatite coating by biomimetic method on titanium alloy using concentrated SBF, Bull. Mater. Sci. **28 No. 6** (2005) 617–621.

[18] K.S. RajaT, M. Misra, K. Paramguru, Deposition of calcium phosphate coating on nanotubular anodized titanium, Materials Letters. **59** (2005) 2137–2141.

[19] M. Fini, A. Cigada, G. Rondelli, R. Chiesa, R. Giardino, G. Giavaresi, N. N. Aldini, P. Torricelli, B.Vicentini, In vitro and in vivo behaviour of Ca-and P-enriched anodized titanium, Biomaterials **20** (1999) 1587-1594.

[20] F. J. Garcia-Sanz, M. B. Mayor, J. L. Arias, J. Pou, B. Leon,M. Perez, Amor-Hydroxyapatite coatings: a comparative study between plasma-spray and pulsed laser deposition techniques, Journal of Materials Science: Materials in Medicine **8** (1997) 861- 865.

[21] M Katto, K Ishibashi, K Kurosawa, A Yokotani, S Kubodera, A Kameyama, T Higashiguchi, T Nakayama, H Katayama, M Tsukamoto and N Abe, Crystallized hydroxyapatite coatings deposited by PLD with targets of different densities, Journal of Physics: Conference Series. **59** (2007) 75–78

[22] D.P. Norton-Pulsed Laser Deposition of Complex Materials: Progress Toward Applications, Pulsed laser deposition of thin films, applications-led growth of functional materials, Wiley-Interscience publication,USA (2007) ISBN-13: 978-0-471-44709-2,1-28.

[23] V.Nelea, I.N.Mihailescu, and M. Jelinek, Biomaterials: New Issues and Breakthroughs for Biomedical Applications Pulsed laser deposition of thin films, applications-led growth of functional materials, Wiley-Interscience publication,USA (2007) ISBN-13: 978-0-471-44709-2,421-456.

[24] H.-Lee Kim, S.W. Lee, Y.S.Kim, D.J. Kim and W.J. Lee, Influence of Substrate Temperature on the Growth Rate and the Composition of Calcium Phosphate Films Prepared by Using Pulsed Laser Deposition, Journal of the Korean Physical Society. 49 No 6 D (2006) 2418-2422.

Chapter 2

THIN FILM DEPOSITION TECHNIQUES, ANODIZATION OF IMPLANTS AND CHARACTERIZATION TOOLS USED

This chapter presents the pulsed laser deposition technique used for the growth of hydroxyapatite thin films on $TiAl_6V_4$ implant material. The chapter gives an overview of the anodization process used. The various characterization tools employed for analyzing the films are also described here.

2.1 Classification of Deposition Technologies

Basically, thin-film deposition technologies are either purely physical, such as evaporative methods, or purely chemical, such as gas- and liquid-phase chemical processes. A considerable number of processes that are based on glow discharges and reactive sputtering combine both physical and chemical reactions; these overlapping processes can be categorized as physical-chemical methods [1, 2].

A classification scheme is presented in Table 2.1 [1], where thin-film deposition technologies are grouped according to evaporative methods, glow discharge, gas-phase chemical, and liquid-phase chemical processes.

Table 2.1: Classification of the deposition processes.

Classification	Type
Evaporative methods (Vacuum Evaporation)	Conventional vacuum evaporation
	Molecular–beam epitaxy (MBE)
	Electron Beam evaporation
	Pulsed laser deposition
Glow –Discharge Processes (Sputtering-Plasma process)	Diode sputtering
	Reactive sputtering
	Plasma oxidation
	Bias sputterng
	Plasma anodization
	Magnetron sputtering
	Ion beam sputter deposition
	Microwave ECR plasma
	CVD Cluster beam depostion
Gas-phase chemical process (Chemical vapour deposition)	CVD Epitaxy thermal oxidation
	Atmospheric-pressure CVD
	Thermal nitridation
	Low-pressure CVD
	Thermal polymerization
	Metalorgainc CVD
	Laser-induced CVD (PCVD)
	Electron-enhanced CVD
	Ion implantation
Liquid phase chemical techniques (Electro Processes - Mechanical Techniques)	Electroplating
	Spary pyrolysis
	Electroless plating
	Spray-on techniques
	Electrolytic anodization
	Chemical reduction plating
	Electrophoretic deposition
	Liquid phase epitaxy

2.1.1 Overview of various thin film deposition process.

A brief description of the principles, salient features and applications for some of the important thin-film deposition processes are given below.

i) Evaporative Technologies

One of the oldest techniques used for depositing thin films, thermal evaporation or vacuum evaporation is still widely used in the laboratory and in industry for depositing metal and metal alloys [1,3]. The following sequential basic steps take place: (*i*) a vapor is generated by boiling or subliming a source material (*ii*) the vapor is transported from the source to the substrate and (*iii*) the vapor is condensed to a solid film on the substrate surface. Evaporants cover an extraordinary range of varying chemical reactivity and vapor pressures. This variety leads to a large diversity of source components including resistance-heated filaments, electron beams; crucibles heated by conduction, radiation, or rf-induction; arcs, exploding wires, and lasers. Additional complications include source-container interactions, requirements for high vacuum, precise substrate motion (to ensure uniformity) and the need for process monitoring and control.

a) **Molecular Beam Epitaxy.** MBE is a sophisticated, finely controlled method for growing single-crystal epitaxial films in a high vacuum. The films are formed on single-crystal substrates by slowly evaporating the elemental or molecular constituents of the film from separate Knudsen effusion source cells (deep crucibles in furnaces with cooled shrouds) onto substrates held at a temperature appropriate for chemical reaction, epitaxy, and re-evaporation of excess reactants [3]. The furnaces produce atomic or molecular beams of relatively small diameter, which are directed at the heated substrate, usually silicon or gallium arsenide. Fast shutters are interposed between the sources and the substrates. By controlling these

shutters, one can grow super lattices with precisely controlled uniformity, lattice match, composition, dopant concentrations, thickness, and interfaces down to the level of atomic layers.

b) **Electron beam evaporation:** In electron beam evaporation (EBE) a stream of electrons is accelerated through fields of typically 5–10kV and focussed onto the surface of the material for evaporation. The electrons lose their energy very rapidly upon striking the surface and the material melts at the surface and evaporates. That is, the surface is directly heated by impinging electrons, in contrast to conventional heating modes. Direct heating allows the evaporation of materials from water-cooled crucibles. Such water-cooled crucibles are necessary for evaporating reactive and in particular reactive refractory materials to avoid almost completely the reactions with crucible walls. This allows the preparation of high purity films because crucible materials or their reaction products are practically excluded from evaporation. Electron beam guns can be classified into thermionic and plasma electron categories. In the former type the electrons are generated thermionically from heated refractory metal filaments, rods or disks. In the latter type, the electron beams are extracted from plasma confined in a small space.

c) **Laser Induced Evaporation/Laser Ablation/Pulsed Laser Deposition (PLD).**This technique with many names was first used by Smith and Turner in 1965 to deposit thin films in a vacuum chamber using a pulsed ruby laser [1, 3]. In this technique, material is vaporized and ejected from the surface of a target as it irradiated by a laser beam. Films are formed by condensing the material ablated from the target onto a solid substrate. Absorption characteristics of the material to be evaporated determine the laser wavelength to be used. To obtain the high power density required in many

cases, pulsed laser beams are generally employed. Pulse width, repetition rate, and pulse intensity are selected for specific applications.

ii) Glow-Discharge Technologies

The electrode and gas-phase phenomena in various kinds of glow discharges (especially rf discharges) represent a rich source of processes used to deposit and etch thin films[1,4,5]. Creative exploitation of these phenomena has resulted in the development of many useful processes for film deposition (as well as etching), as listed in Table 2.1.

a) Sputtering. The most basic and well-known of these processes is sputtering, the ejection of surface atoms from an electrode surface by momentum transfer from bombarding ions to surface atoms. From this definition, sputtering is clearly an etching process, and is, in fact, used as such for surface cleaning and for pattern delineation. Since sputtering produces a vapor of electrode material, it is also (and more frequently) used as a method of film deposition similar to evaporative deposition. *Sputter deposition* has become a generic name for a variety of processes.

Diode Sputtering. Diode sputtering uses a plate of the material to be deposited as the cathode (or rf-powered) electrode (target) in a glow discharge. Material can thus be transported from the target to a substrate to form a film. Films of pure metals or alloys can be deposited when using noble gas discharges (typically Argon) with metal targets.

Reactive Sputtering. Compounds can be synthesized by reactive sputtering, that is, sputtering elemental or alloy targets in reactive gases; alternatively, they can be deposited directly from compound targets.

Bias Sputtering. Bias sputtering or ion-plating is a variant of diode sputtering in which the substrates are ion bombarded during deposition and prior to film

deposition to clean them. Ion bombardment during film deposition can produce one or more desirable effects, such as resputtering of loosely-bonded film material, low-energy ion implantation, desorption of gases, conformal coverage of contoured surface, or modification of a large number of film properties. The source material need not originate from a sputtering target, but can be an evaporation source, a reactive gas with condensable constituents, or a mixture of reactive gases with condensable constituents and other gases that react with the condensed constituents to form compounds.

All glow discharge processes involve sputtering in one form or another, since it is impossible to sustain a glow discharge without an electrode at which these processes occur. In "electrodeless" discharges, rf power is capacitively coupled through the insulating wall of a tubular reactor. In this case, the inside wall of the tube is the main electrode of the discharge.

Magnetron Sputtering. Another variant in sputtering sources uses magnetic fields transverse to the electric fields at sputtering-target surfaces. This class of processes is known as *magnetron sputtering*. Sputtering with a transverse magnetic field produces several important modifications of the basic processes. Target-generated secondary electrons do not bombard substrates because they are trapped in cycloidal trajectories near the target, and thus do not contribute to increased substrate temperature and radiation damage. This allows the use of substrates that are temperature-sensitive (for example, plastic materials) and surface sensitive(for example, metal-oxides-semiconductor devices) with minimal adverse effects. In addition, this class of sputtering sources produces higher deposition rates than conventional sources and lends itself to economic, large-area industrial application. There are cylindrical, conical, and planar magnetron sources, all with particular advantages and disadvantages for specific applications. As with other forms of sputtering, magnetron sources can

be used in a reactive sputtering mode. Alternatively, one can forego the low-temperature and low radiation-damage features and utilize magnetron sources as high-rate sources by operating them in a bias-sputtering mode.

Ion-Beam Sputtering. Ion beams, produced in and extracted from glow discharges in a differentially pumped system, are important to scientific investigations of sputtering, and are proving to be useful as practical film-deposition systems for special materials on relatively small substrate areas. There are several advantages of ion-beam sputtering deposition. The target and substrate are situated in a high-vacuum environment rather than in a high-pressure glow discharge. Glow discharge artifacts are thereby avoided, and higher-purity films usually result. Reactive sputtering and bias sputtering with a separate ion gun can be used.

iii) Plasma Processes

The fact that some chemical reactions are accelerated at a given temperature in the presence of energetic reactive-ion bombardment is the basis of processes for surface treatments such as plasma oxidation, plasma nitriding, and plasma carburizing [1, 6, 7]. A metal to be oxidized, nitrided or carburized is made the cathode of a glow discharge and is simultaneously heated by radiant or rf-induction means. Protective coatings on a variety of metals can be produced in this way to render surfaces hard and/or corrosion resistant.

a) Anodization. Plasma anodization is a technique for producing thin oxide films (less than 100 nm) on metals such as aluminium, tantalum, titanium, and zirconium, collectively referred as *valve metals.* In this case, a dc discharge is set up in an oxygen atmosphere and the substrates (shielded from the cathode to avoid sputter deposition) are biased positively with respect to the anode. This bias extracts negative oxygen ions from the discharge to the surface, which is also bombarded with

electrons that assist the reaction. The process produces very dense, defect-free, amorphous oxide films that are of interest as gate material in compound semiconductor devices such as in microwave field-effect transistors.

b) ***Microwave Electron Cyclotron Resonance Deposition.*** ECR plasma deposition employs an electron cyclotron resonance (ECR) ion source to create high-density plasma. The plasma is generated by resonance of microwaves and electrons through a microwave discharge across a magnetic field. The main feature of this recently introduced process is the high rate of deposition obtained at a low temperature of deposition.

c) ***Cluster Beam Deposition.*** Ionized cluster beam deposition (ICB) or cluster beam deposition is one of the most recent emerging technologies for the deposition of thin films with growth-control capabilities not attainable by other processes. ICB deposition is one of several techniques classified as ion-assisted thin-film formation. The material to be deposited emerges and expands into a vacuum environment from a small nozzle of a heated confinement crucible, usually constructed of high-purity graphite. The vapor pressure within the crucible is several orders of magnitude higher than the pressure of the vacuum chamber so that the expanding vapour super cools. Homogeneous nucleation results in the generation of atomic aggregates or clusters of up to a few thousand atoms held together by weak inter atomic forces. The clusters passing through the vacuum towards the substrate can, in part, be positively charged by impact ionization with electron beam irradiation. Closely controlled accelerating voltages add energy to the ionized clusters which then impinge on the substrate, diffuse or migrate along

the plane of the surface, and finally form a thin film of exceptional purity.

iv) Gas-Phase Chemical Processes

Methods of film formation by purely chemical processes in the gas or vapor phases include chemical vapor deposition and thermal oxidation.Chemical vapor deposition (CVD) is a materials synthesis process whereby constituents of the vapor phase react chemically near or on a substrate surface to form a solid product [1,8,9,10]. The deposition technology has become one of the most important means for creating thin films and coatings of a very large variety of materials essential to advanced technology, particularly solid-state electronics where some of the most sophisticated purity and composition requirements must be met. The main feature of CVD is its versatility for synthesizing both simple and complex compounds with relative ease at generally low temperatures. Both chemical composition and physical structure can be tailored by control of the reaction chemistry and deposition conditions. Fundamental principles of CVD encompass an interdisciplinary range of gas-phase reaction chemistry, thermodynamics, kinetics, transport mechanisms, film growth phenomena, and reactor engineering.Chemical reaction types basic to CVD include pyrolysis (thermal decomposition), oxidation, reduction, hydrolysis, nitride and carbide formation, synthesis reactions, disproportionation, and chemical transport. A sequence of several reaction types may be involved in more complex situations to create a particular end product. Deposition variables such as temperature, pressure, input concentrations, gas flow rates and reactor geometry and operating principle determine the deposition rate and the properties of the film deposit. CVD has become an important process technology in several industrial fields and CVD

has long been used for coating of substrates at reduced pressure, often at high temperatures.

a) **Vapor-Phase Epitaxy.** Vapor-phase epitaxy (VPE) and metal-organic chemical vapor deposition (MOCVD) are used for growing epitaxial films of compound semiconductors in the fabrication of optoelectronic devices. Composite layers of accurately controlled thickness and dopant profile are required to produce structures of optimal design for device fabrication.

b) **Photo-Enhanced Chemical Vapor Deposition (PHCVD).** PHCVD is based on activation of the reactants in the gas or vapour phase by electromagnetic radiation, usually short-wave ultraviolet radiation. Selective absorption of photonic energy by the reactant molecules or atoms initiates the process by forming reactive free-radical species that then interact to form a desired film product. Mercury vapor is usually added to the reactant gas mixture as a photosensitizer that can be activated with the radiation from a high-intensity quartz mercury resonance lamp (253.7 nm wavelength). The excited mercury atoms transfer their energy kinetically by collision with the reactants to generate free radicals

c) **Laser-Induced Chemical Vapor Deposition (LCVD).**LCVD] utilizes a laser beam for highly localized heating of the substrate that then induces film deposition by CVD surface reactions. Another mode of utilizing laser (or electron radiation) is to activate gaseous reactant atoms or molecules by their absorption of the specific wavelength of the photonic energy supplied. The resulting chemical gas phase reactions are very specific, leading to highly pure film deposits.

v) Liquid-Phase Chemical Formation

The growth of inorganic thin films from liquid phases by chemical reactions is accomplished primarily by electrochemical processes (which include anodization and electroplating), and by chemical deposition processes(which include reduction plating, electroless plating, conversion coating, and displacement deposition) [1,11]. A number of extensive reviews of these film formation processes discuss theory and practice. Another class of film forming methods from the liquid phase is based on chemically reacting films that have been deposited by mechanical techniques. Finally, liquid phase epitaxy is still being used for growing a number of single-crystal semiconductors.

a) **Electrolytic Anodization.** In anodization, as in thermal oxidation, an oxide film is formed from the substrate. The anode reacts with negative ions from the electrolyte in solution and becomes oxidized, forming an oxide or a hydrated oxide coating on semiconductors and on a few specific metals, while hydrogen gas is evolved at the cathode. Nonporous and well adhering oxides can be formed on aluminium, tantalum, niobium, titanium, zirconium, and silicon. The most important applications are corrosion protective films and decorative coatings with dyes on aluminium and its alloys, and layers for electrical insulation for electrolyte capacitors on aluminium and tantalum.

b) **Electroplating.** In electroplating a metallic coating is electrodeposited on the cathode of an electrolytic cell consisting of a positive electrode (anode), a negative electrode (cathode), and an electrolyte solution (containing the metal ions) through which electric current flows. The quantitative aspects of the process are governed by Faraday's laws. Important electroplating variables include current efficiency, current

density, current distribution, pH, temperature, agitation, and solution composition. Numerous metals and metal alloys have been successfully electroplated from aqueous solutions.. Electroplating is widely used in industry and can produce deposits that range from very thin films to very thick coatings (electroforming).

c) **Chemical Reduction Plating.** Chemical reduction plating is based on reduction of a metal ion in solution by a reducing agent added just before use. Reaction is homogeneous, meaning that deposition takes place everywhere in the solution, rather than on the substrate only. Silver, copper, nickel, gold, and some sulfide films are readily plated. The oldest application of the process is the silvering of glass and plastics for producing mirrors using silver nitrate solutions and one of various reducing agents, such as hydrazine.

d) **Electroless Plating.** Autocatalytic or electroless plating is a selective deposition plating process in which metal ions are reduced to a metallic coating by a reducing agent in solution. Plating takes place only on suitable catalytic surfaces, which include substrates of the same metal being plated, hence the definition autocatalysis. Electroless (or electrodeless) plating offers a number of advantages over electroplating, such as selective (patterned) deposition, but is limited to a few metals and some alloys.

e) **Electrophoretic Deposition.** Electrophoretic coating is based on deposition of a film from a dispersion of colloidal particles onto a conductive substrate. The dispersion in a conductive liquid dissociates into negatively charged colloidal particles and positive ions (cations), or the reverse. On application of an electric field between the positive

substrate electrode (anode), the colloidal particles migrate to the substrate, become discharged, and form a film.

f) **Immersion Plating.** Deposition of a metal film from a dissolved salt of the coating metal on a substrate by chemical displacement without external electrodes is known as displacement deposition or immersion plating. Generally, a less noble (more electronegative) metal displacesfrom solution any metal that is more noble, according to the electromotive force series. Actually, different localized regions on the metal surface become anodic and cathodic, resulting in thicker films in the cathodic areas. The industrial uses of this process are limited to a few applications, mainly thin coatings on copper and its alloys.

vi) Mechanical Methods

Mechanical techniques for depositing coatings from liquid media that are subsequently reacted chemically to form the inorganic thin film product are spraying, spinning, dipping and draining, flow coating, roller coating, pressure-curtain coating, brushing, and offset printing of reagent solutions[1,12]. Chemical reaction of the coating residue, often by thermal oxidation, hydrolysis, or pyrolysis (in the case of metal organics) produces the desired solid film. Spin-on deposition of film-forming solutions is widely used in solid-state technology. Liquid spray coating is probably the most versatile mechanical coating technique of the deposition techniques noted, and it is particularly well-suited for high-speed automated mass production. Deposition of very thin films is possible by judicious selection and optimization of spray machine parameters for forming “atomized” droplets and the reagent and solvent systems used to formulate the spray liquid. Spray deposition encompasses several other types of spraying processes that are based on either liquid sources, such as harmonic electrical spraying, or on dry source reactants

that include flame spraying, arc plasma spraying, electric arc spraying, and detonation coating.

a) **Liquid-Phase Epitaxy.** LPE is used for the thermally-controlled overgrowth of thin single-crystalline films of compound semiconductors and magnetic garnets from the melt on a single-crystal substrate. This relatively old and simple technique has been successfully applied in the semiconductor industry for fabricating optoelectronic devices.

Procedures adopted in the present work: Pulsed laser deposition was utilised for depositing thin film of hydroxyapatite on $TiAl_6V_4$ substrates and electrolytic anodizing was adopted for anodization of the $TiAl_6V_4$ substrates. A detailed description of the above two methods are given below.

2.1.2 Pulsed laser deposition (PLD)

Pulsed laser deposition, is a very effective thermal evaporation technique for the preparation of epitaxial films under moderate vacuum, or ultrahigh vacuum conditions [1, 3, 13]. PLD is the deposition method of choice in the case of phase pure growth of multicomponent compositions. PLD technique requires a UV nanosecond pulsed laser source such as the frequency tripled (355 nm) or quadrupled (266 nm) solid state Nd:YAG laser, or the KrF (248 nm) or ArF (193 nm) excimer laser. In a typical PLD process, a focused train of high energy laser pulses, derived from a UV nanosecond pulsed laser source, is rastered over the target. A suitable substrate, often heated, is brought into contact with the laser plume (formed by the high pulse energy beam–target interaction) comprising of atomic and molecular species ablated from the target.

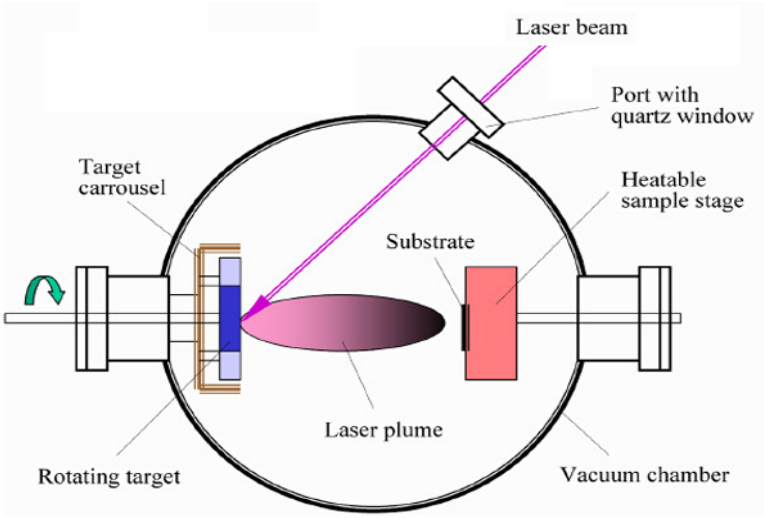

Fig: 2.1. Schematic diagram of a PLD chamber

Figure 2.1. shows a schematic view of a pulsed laser deposition chamber. Provisions are made for controlling the ambient atmosphere within the chamber and substrate heating. Short wavelength irradiation of the target material creates an ablation plume that contacts the substrate

i) Mechanisms of PLD

The mechanism of pulsed laser deposition, in contrast to the simplicity of the set-up, is a very complex physical phenomenon[13,14,15,16]. It not only involves the physical process of laser-material interaction under the impact of high-power pulsed radiation on solid target, but also the formation of plasma plume with highly energetic species and even the transfer of the ablated material through the plasma plume onto the heated substrate surface. Thus the thin film formation process in PLD generally can be divided into the following four stages.

a) Laser radiation interaction with the target

b) Dynamics of the ablated materials.

c) Deposition of the ablation materials on the substrate.

d) Nucleation and growth of a thin film on the substrate surface

Each stage in PLD is critical to the formation of quality epitaxial, crystalline, stoichiometric and uniform thin film.

In the first stage, the laser beam is focused onto the surface of the target. At sufficiently high flux densities and short pulse duration, all elements in the target are rapidly heated up to their evaporation temperature. Materials are dissociated from the target surface and ablated out with stoichiometry as in the target. The instantaneous ablation rate is highly dependent on the fluences of the laser shining on the target. The ablation mechanisms involve many complex physical phenomena such as collisional, thermal, and electronic excitation, exfoliation and hydrodynamics.

During the second stage, the emitted materials tend to move towards the substrate according to the laws of gas-dynamics. The spot size of the laser and the plasma temperature has significant effects on the deposited film uniformity. The target-to-substrate distance is another parameter that governs the angular spread of the ablated materials. A mask placed close to the substrate could reduce the spreading. The third stage is important to determine the quality of the thin film. The ejected high-energy species impinge onto the substrate surface and may induce various type of damage to the substrate. These energetic species sputter some of the surface atoms and a collision region is formed between the incident flow and the sputtered atoms. Film grows after a thermalized region is formed. The region serves as a source for condensation of particles. When the condensation rate is higher than the rate of particles ejected

by the sputtering, thermal equilibrium condition can be reached quickly and film grows on the substrate surface.

The effect of increasing the energy of the adatoms has a similar effect of increasing substrate temperature on film growth[14]. Typical power densities involved in PLD are approximately 50 MW cm-2 for a reasonable growth rate (> 1 A^o/shot). The plasma is formed initially during laser target interaction in vacuum or in air and then again an explicit laser – plasma interaction occurs. Due to which ions in the plasma are accelerated to as much as 100 – 1000 eV . Nucleation-and-growth of crystalline films depends on many factors such as the density, energy, ionization degree, and the type of the condensing material, as well as the temperature and the physio-chemical properties of the substrate. The two main thermodynamic parameters for the growth mechanism are the substrate temperature T and the supersaturation Dm of laser plasma. They can be related by the following equation

$$Dm = kT \ln(R/Re) \quad \text{---------- (2.1)}$$

where k is the Boltzmann constant, R is the actual deposition rate, and Re is the equilibrium value of deposition rate of the thin film at the temperature T. The nucleation process depends on the interfacial energies between the three phases present – the substrate, the condensing material and the vapour. The critical size of the nucleus depends on the driving force, i.e. the deposition rate and the substrate temperature. For the large nuclei, a characteristic of small supersaturation, they create isolated patches (islands) of the film on the substrate, which subsequently grow and coalesce together. As the supersaturation increases, the critical nucleus shrinks until its height reaches on atomic diameter and its shape is that of a two-dimensional layer. For large supersaturation, the layer-by-layer nucleation will happen for incompletely wetted foreign substrates. The crystalline film growth depends on the surface

mobility of the adatom (vapour atoms). Normally, the adatom will diffuse through several atomic distances before sticking to a stable position within the newly formed film. The surface temperature of the substrate determines the adatom's surface diffusion ability. High temperature favours rapid and defect free crystal growth, whereas low temperature or large supersaturation crystal growth may be overwhelmed by energetic particle impingement, resulting in disordered or even amorphous structures.The mean thickness (N99) at which the growing thin and discontinuous film reaches continuity, is given by the formula

N99 = A(1/R)1/3 exp (-1/T) ----------(2.2)

where R is the deposition rate (supersaturation related) and T is the temperature of the substrate and A is a constant related to the materials.

In the PLD process, due to the short laser pulse duration (~10 ns) and hence the small temporal spread (~10 ms) of the ablated materials, the deposition rate can be enormous (~10 nm/s). Consequently a layer-by-layer nucleation is favoured and ultra-thin and smooth film can be produced. In addition the rapid deposition of the energetic ablation species helps to raise the substrate surface temperature. In this respect PLD tends to demand a lower substrate temperature for crystalline film growth.

Pulsed laser deposition is the main growth technique used in the present study. The deposition was carried out in a vacuum chamber pumped by a turbo-molecular pump (Pfeiffer Vacuum Inc, Germany). The laser used was the third harmonics (355 nm) of Nd:YAG laser (Spectra Physics model GCR 150). In this study $TiAl_6V_4$ substrates have been coated by PLD method at different substrate temperatures ranging from 150-500^oC in O_2 atmosphere and the films were subjected to a hydrothermal process at 100^oC to get polycrystalline films.

2.2 Anodizing

Anodizing is an electrochemical process in which the part is made the anodic (positive) electrode in a suitable electrolyte [11,17,18,19]. Sufficiently high voltage is deliberately applied to establish the desired polarization to deposit oxygen at the surface (O2 overvoltage). The metal surfaces or ions react with the oxygen to produce adherent, oxide coatings.

Industrial anodizing processes are confined mainly to aluminium and to a much lesser extent to magnesium and titanium alloys.

Anodic coating applications include:

a. Protection corrosion, wear and abrasion resistance.
b. Decorative clear coatings on polished or brightened surfaces, dyed (color) coatings.
c. Base for subsequent paint or organic coating.
d. Base for plating aluminium.
e. Special based on some specific property or the coating, e.g. thermal barrier films, refractory films, electrolytic condensers, capacitors (dielectric films).

Titanium anodizing standards such as AMS 2487 define film properties and quality requirements for an electrochemical process that does not exceed 12.4 pH. This pH range covers acid and neutral salt solutions. The acid or neutral salt anodized films are classified as abrasion resistant. AMS 2488 specifics alkaline anodizing solutions with a pH of 13 or greater. Alkaline anodizing creates a thicker oxide film and may be specified as an anti-galling coating for severe wear applications. The composition and structure of alkaline anodized films are unique and some are considered proprietary [19].

The anodic films are classified according to the solvent action of the electrolyte. The films produced in sulphuric or chromic acids are porous type films. Phosphoric acid has even greater solvent action, resulting in oxides with a greater degree of porosity; these coatings are used for adhesive bonding and for plating on aluminium processes to provide deposit adhesion by mechanical locking in the enlarged pores. Less aggressive mild electrolytes such as tartaric acid, ammonium tartarate, boric acid, borate compounds, citric acid, etc., have little or no ability to attack the anodic oxide. These films are essentially non-porous and thin and are considered barrier type coatings.

In an air or moisture containing environment, titanium dioxide (TiOz) spontaneously forms on the surface of CP(Commercially Pure) titanium. The oxide is typically 2 to 5 nanometers thick and this passive layer is responsible for the excellent corrosion resistance of titanium .Anodizing is a well recognized surface modification for titanium and titanium alloys used in the aerospace, chemical processing, and consumer product industries. In the last few years, anodizing has been successfully used as a surface treatment for orthopaedic implants.

Titanium and its alloys are anodized to provide [19]:

1) Protection from galvanic corrosion when assembled or in contact with dissimilar metals by reducing or minimizing potential differences.
2) Anti-galling, anti-fretting properties to the surfaces of parts in moving assemblies.
3) Part identification using a range of integral colors produced by the particular anodizing process.

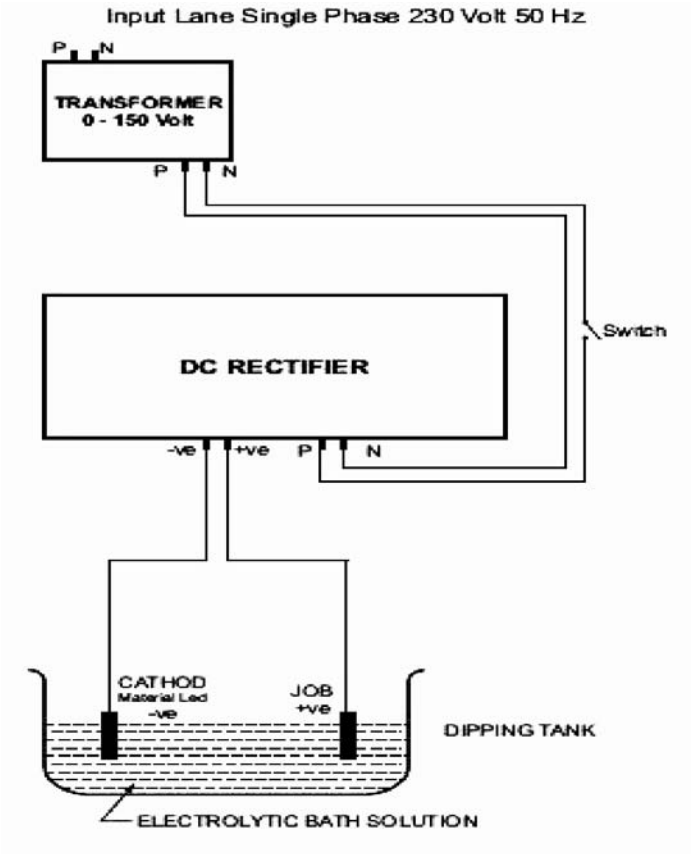

Fig 2.2 Set up utilized for the anodization treatments of Ti substrates

$TiAl_6V_4$ was anodized in 200 g/L sulfuric acid, 5% trisodium phosphate, and 5% sodium bicarbonate (baking soda) at voltages of 55,60 and 75 volts to yield anodized surfaces of different surface topographies with the set up as shown in figure 2.2.

2.3. Characterization tools

2.3.1. Thin film thickness

Thickness is one of the most important thin film properties to be characterized since it plays an important role in the film properties unlike a bulk

material [20,21]. Reproducible properties are achieved only when the film thickness and the deposition parameters are kept constant. Film thickness may be measured either by in-situ monitoring of the rate of deposition or after the film deposition. The thicknesses of the thin films prepared for the work presented in this thesis were measured by a stylus profiler (Dektak 6M).

i) Stylus profiler

The stylus profiler takes measurements electromechanically by moving the sample beneath a diamond tipped stylus. The high precision stage moves the sample according to a user defined scan length, speed and stylus force. The stylus is mechanically coupled to the core of a linear variable differential transformer (LVDT). The stylus moves over the sample surface. Surface variations cause the stylus to be translated vertically. Electrical signals corresponding to the stylus movement are produced as the core position of the LVDT changes. The LVDT scales an ac reference signal proportional to the position change, which in turn is conditioned and converted to a digital format through a high precision, integrating, analog-to-digital converter [22]. The film whose thickness has to be measured is deposited with a region masked. This creates a step on the sample surface. Then the thickness of the sample can be measured accurately by measuring the vertical motion of the stylus over the step.

2.3.2 Surface morphology

Surface morphology is an important property since while going for multilayer devices roughness of the thin film surface play an important role. Some of the characterization tools which clearly demonstrates an idea about the surface of the thin films is described below.

i) Scanning electron microscope (SEM)

The scanning electron microscope (SEM) is a microscope that uses electrons rather than light to form an image. There are many advantages for using the SEM instead of a light microscope [23,24]. The SEM has a large depth of field, which allows a large amount of the sample to be in focus at the same time. The SEM also produces images of high resolution, which means that closely spaced features can be examined at a high magnification. Preparation of the samples is relatively easy since most SEMs only require that sample should be conductive. The combination of higher magnification, larger depth of focus, greater resolution, and ease of sample observation makes SEM one of the most heavily used instruments in the research field. The electron beam comes from a filament, made of various types of materials. The most common is the Tungsten hairpin gun. This filament is a loop of tungsten that functions as the cathode. A voltage is applied to the loop, causing it to heat up. The anode, which is positive with respect to the filament, forms powerful attractive forces for electrons. This causes electrons to accelerate toward the anode. The anode is arranged, as an orifice through which electrons would pass down to the column where the sample is held. Other examples of filaments are lanthanum hexaboride filaments and field emission guns.

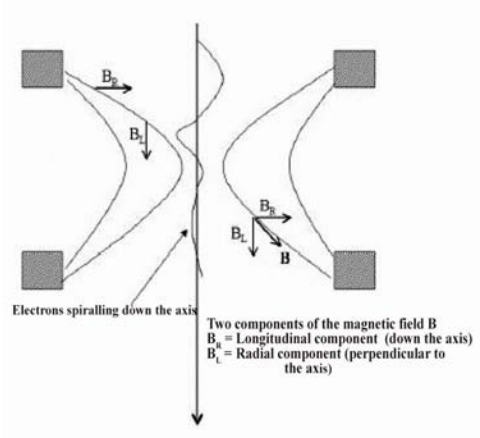

Fig: 2.3 The focusing of electrons in SEM

The streams of electrons that are attracted through the anode are made to pass through a condenser lens, and are focused to very fine point on the sample by the objective lens (figure 2.3). The electron beam hits the sample, producing secondary electrons from the sample. These electrons are collected by a secondary detector or a backscatter detector, converted to a voltage, and amplified. The amplified voltage is applied to the grid of the CRT that causes the intensity of the spot of light to change. The image consists of thousands of spots of varying intensity on the face of a CRT that correspond to the topography of the sample. In the present thesis, JEOL JSM 5600 was used for SEM analysis.

2.3.3 Average roughness with stylus profilometer:

The average roughness Ra is measured using a stylus profilometer [22] using the formula

$$R_a = \frac{1}{L}\int_{x=0}^{x=L} lyldx$$

Where L is the total length of the coated film

2.3.4 Compositional analysis

In order to check the stoichiometry of the deposited films, compositional analysis is essential and the characterization tool used in the present investigation is described below.

i) Energy dispersive x-ray (EDX) analysis

EDX analysis stands for energy dispersive x-ray analysis. It is sometimes referred to also as EDS or EDAX analysis. It is a technique used for identifying the elemental composition of the specimen, on an area of interest thereof. The EDX analysis system works as an integrated feature of a scanning electron microscope (SEM), and can not operate on its own without the latter [23,24].

During EDX Analysis, the specimen is bombarded with an electron beam inside the scanning electron microscope. The bombarding electrons collide with the specimen atom's own electrons, knocking some of them off in the process. A position vacated by an ejected inner shell electron is eventually occupied by a higher-energy electron from an outer shell. To be able to do so, however, the transferring outer electron must give up some of its energy by emitting an X-ray. The amount of energy released by the transferring electron depends on which shell it is transferring from, as well as which shell it is transferring to. Furthermore, the atom of every element releases X-rays with unique amounts of energy during the transferring process. Thus, by measuring the energy of the X-rays emitted by a specimen during electron beam bombardment, the identity of the atom from which the X-ray was emitted can be established.

The output of an EDX analysis is an EDX spectrum, which is a plot of how frequently an X-ray is received for each energy level. An EDX spectrum normally displays peaks corresponding to the energy levels for which the most X-rays had been received. Each of these peaks are unique to an atom, and therefore corresponds to a single element. The higher a peak in a spectrum, the more concentrated the element is in the specimen. An EDX spectrum plot not only identifies the element corresponding to each of its peaks, but the type of X-ray to which it corresponds as well. For example, a peak corresponding to the amount of energy possessed by X-rays emitted by an electron in the L-shell going down to the K-shell is identified as a K_α peak. The peak corresponding to X-rays emitted by M-shell electrons going to the K-shell is identified as a K_β peak as shown in figure 2.4.

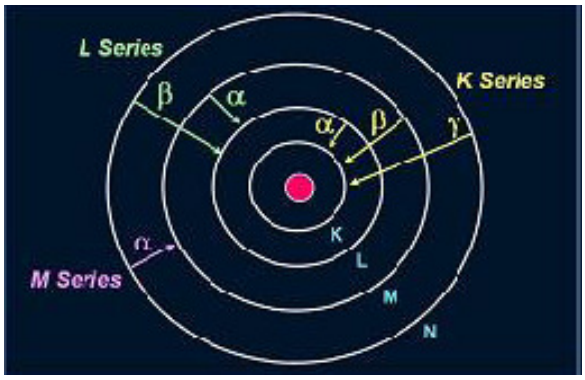

Fig: 2.4 The emission of x rays

2.3.5 Structural characterization

i) X-ray diffraction

The structural characterization was done by recording the X-ray diffraction (XRD) pattern of the samples. XRD pattern was taken using Rigaku X-ray diffractometer with Cu-K_α radiation (λ=1.5414A^0). A given substance always produces a characteristic diffraction pattern whether that substance is present in the pure state or as one constituent of a mixture of substances. This fact is the basis for the diffraction method of chemical analysis. The particular advantage of X-ray diffraction analysis is that it discloses the presence of a substance, as that substance actually exists in the sample and not in terms of its constituent chemical elements. Diffraction analysis is useful whenever it is necessary to know the state of chemical combination of the elements involved or the particular phase in which they are present. Compared with ordinary chemical analysis the diffraction method has the advantage that it is usually much faster, requires only very small quantity of sample and is non destructive [25, 26].

The basic law involved in the diffraction method of structural analysis is the Bragg's law. When monochromatic beam of x-rays impinge upon the atoms in a crystal lattice, each atom acts as a source of scattering. The crystal acts as series of parallel reflecting planes. The intensity of the reflected beam at certain angles will be maximum when the path difference between two reflected waves from two different crystal planes is an integral multiple of λ. This condition is termed as Bragg's law and is given by n λ = 2d sinθ, where n is the order of diffraction, λ is the wavelength of X-rays, d is the spacing between consecutive parallel planes and θ is the glancing angle (or the complement of the angle of incidence) [27].

X-ray diffraction studies give a whole range of information about the crystal structure, orientation, average crystalline size and stress in the powder. Experimentally obtained diffraction patterns of the sample are compared with the standard powder diffraction files published by the international centre for diffraction data (ICDD). The average grain size of the film can be calculated using the Scherrer's formula[25]

$$d = \frac{0.9\lambda}{\beta \cos\theta} \quad \text{..... (2.3)}$$

where, λ is the wavelength of the x-ray and β is the full width at half maximum intensity in radians. The lattice parameter values (a and c) for hexagonal system can be calculated from the following equations using the (hkl) parameters and the interplanar spacing d.

$$\frac{1}{d^2} = \frac{4}{3}\left(\frac{h^2 + hk + k^2}{a^2}\right) + \frac{l^2}{c^2} \quad \text{.....(2.4)}$$

X-ray diffraction measurements of the films in the present studies were done using Rigaku automated X-ray diffractometer. The filtered copper Kα (λ=1.5414A^0) radiation was used for recording the diffraction pattern.

2.3.6 Measurement of contact angles

The contact angle is defined as the angle made by the intersection of the liquid/solid interface and the liquid/air interface. It can be alternately described as the angle between solid sample's surface and the tangent of the droplet's ovate shape at the edge of the droplet. A high contact angle indicates a low solid surface energy or chemical affinity [28, 29, 30]. This is also referred to as a low degree of wetting. A low contact angle indicates a high solid surface energy or chemical affinity, and a high or sometimes complete degree of wetting. The three degrees of wetting are shown in fig 2.5. For example, a contact angle of zero degrees will occur when the droplet has turned into a flat puddle; this is called complete wetting. Young proposed that the contact angle represents the vectorial balance of three tensors, the surface tension of the solid in air, the surface tension of the liquid in equilibrium with the vapour and the interfacial tension between the solid and the liquid . The solid-vapor interfacial energy is denoted as γ_{SV}, the solid-liquid interfacial energy as γ_{SL} and the liquid-vapor energy as simply γ, we can write an equation that must be satisfied in equilibrium (known as the Young's Equation 2.5):

$$0 = \gamma_{sv} - \gamma_{sL} - \gamma cos\theta_C \text{ ---------- (2.5)}$$

where θ_C is the equilibrium contact angle.

The simplest way of measuring the contact angle is with a goniometer shown in fig 2.6 using the static sessile drop method [30], which allows the user to measure the contact angle visually. When a drop of liquid is placed on a surface of a solid that is smooth, planar, and level, the liquid either spreads out

to a thin surface film, or it forms a sessile droplet on the surface. The droplet has a finite between the solid and the liquid and the surface tension of the liquid. The contact angle equilibrium has received a great deal of attention, principally because it is perhaps the simplest direct experimental approach to the thermodynamic work of adhesion. The droplet is deposited by a syringe pointed vertically down onto the sample surface, and a high resolution camera captures the image, which can then be analyzed either by eye (with a protractor) or using image analysis software. The size of the droplet can be increased gradually so that it grows proportionally, and the contact angle remains congruent. By taking pictures incrementally as the droplet grows, the user can acquire a set of data to get a good average. If necessary, the receding contact angle can also be measured by depositing a droplet via syringe and recording images of the droplet being gradually sucked back up.

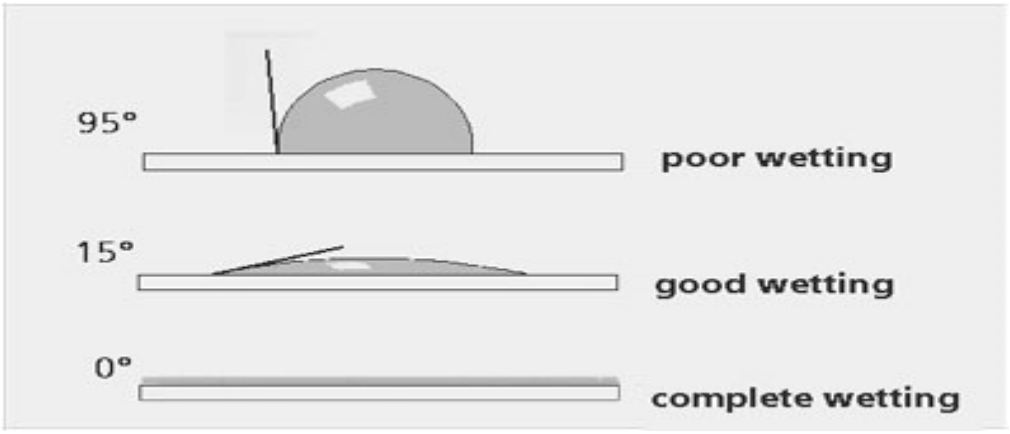

Fig 2.5 A sketch of three degrees of wetting and the corresponding contact angles

Fig 2.6 A photograph of a standard goniometer

An alternative method for measuring the contact angle is the Whilemy method, which employs a sensitive force meter of some sort to measure a force that can be translated into a value of the contact angle. In this method, a small plate-shaped sample of the solid in question, attached to the arm of a force meter, is vertically dipped into a pool of the probe liquid (in actuality, the design of a stationary force meter would have the liquid being brought up, rather than the sample being brought down), and the force exerted on the sample by the liquid is measured by the force meter. This force is related to the contact angle by the equation 2.6:

---------- 2.6

Where F is the total force measured by the force meter, Fb is the force of buoyancy due to the solid sample displacing the liquid, I is the wetted length, and sigma is the known surface tension of the liquid.The contact angles of the samples with three different fluids were measured using a contact angle goniometer (NRL) using the sessile drop method [30] in three well characterized liquids, water, formamide and di-iodomethane as per previous studies.

2.3.7 Hardness testing

Hardness is the ability of a material to resist permanent indentation or deformation when in contact with an indenter under load. Generally a hardness test consists of pressing an indenter of known geometry and mechanical properties into the test material. The hardness of the material is quantified using one of a variety of scales that directly or indirectly indicate the contact pressure involved in deforming the test surface[31,32]. Since the indenter is pressed into the material during testing, hardness is also viewed as the ability of a material to resist compressive loads. The indenter may be spherical (Brinell test), pyramidal (Vickers and Knoop tests), or conical (Rockwell test). In the Brinell, Vickers and Knoop tests, hardness value is the load supported by unit area of the indentation. In the Rockwell tests, the depth of indentation at a prescribed load isdetermined and converted to a hardness number (without measurement units), which is inversely related to the depth. In microindentation hardness testing, a diamond indenter of specific geometry is impressed into the surface of the test specimen using a known applied force.

Vickers Hardness Test.This indentation test employs a square-based pyramidal-shaped indenter made from diamond. Fig 2.7 shows examples of Vickers indents to illustrate the influence of test force on indent size.

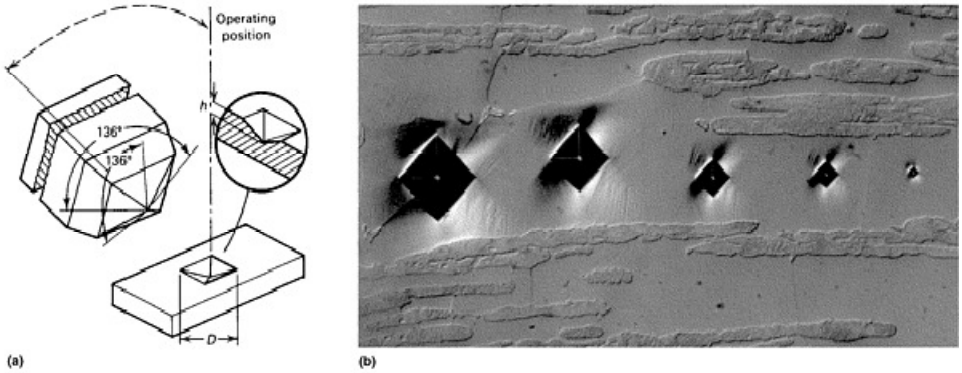

Fig. 2.7 Vickers hardness test. (a) Schematic of the square-based diamond pyramidal indenter used for theVickers test and an example of the indentation it produces. (b) Vickers indents made in ferrite in a ferritic-martensitic high-carbon version of 430 stainless steel using (left to right) 500, 300, 100, 50, and 10gf test forces (differential interference contrast illumination, aqueous 60% nitric acid, 1.5 V dc). 250× Magnification

In this test, the force is applied smoothly, without impact, and held in contact for 10 to 15 s. The force must be known precisely (refer to ASTM E 384 for tolerances). After the force is removed, both diagonals are measured and the average is used to calculate the HV according to equation 2.7:

$$HV = \frac{200Psin(\frac{\alpha}{2})}{d^2} = \frac{1854.4P}{d^2} \quad \text{---------- (2.7)}$$

where *d* is the mean diagonal in μ m, *P* is the applied load in gf, and α is the face angle .

2.3.8 Microscratch adhesion testing

One of the primary requirements of a PVD coating is excellent adhesion of the coating to the substrate, a property that can be defined as the interfacial forces between two surfaces. The most common method of assessing PVD coating adhesion is the scratch tester [33, 34, 35].The scratch tester moves a Rockwell diamond tip with a radius of 200µm across the coated surface of a

substrate at a constant velocity while an increasing normal force is applied with a constant loading rate. The scratch test introduces stresses to the interface between coating and substrate causing delamination or chipping of the coating. The critical normal force at which the first failure of the coating is detected is termed the critical load Lc.

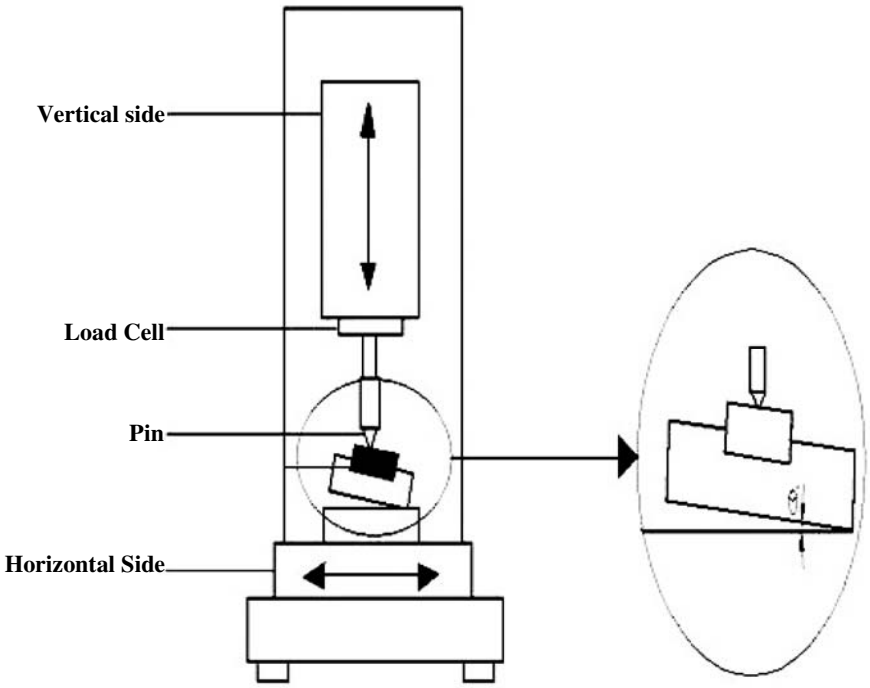

Fig 2.8 Set up of a scratch test procedure

The typical scratch tester has three methods of detecting coating failure; a load cell to measure the change in friction, acoustic emission or observation of the scratch channel using an attached optical microscope. The best scratch adhesion testers use all three methods of coating failure detection. The intensity of the acoustic emission is dependent on the type of coating failure during the adhesion test e.g. cracking, chipping (cohesive failure) and delamination (adhesive failure). It is therefore important to observe the coating failure after

the adhesion test using an optical microscope to confirm the critical load. Figure 2.7 shows a set up for the scratch test.

In this work the change of frictional coefficient was measured to assess the adhesion strength of HA on Ti. The normal and tangential forces were continuously acquired using a computer with data acquisition electronics. The tests were conducted under ambient conditions of 28 ◦C and Relative humidity of 40%.The coefficient of friction was calculated using the formula given by Eq. 2.8

$$\mu = \frac{T}{N} = \frac{FT\cos\theta - FN\sin\theta}{FT\sin\theta + FN\cos\theta} \text{----------2.8}$$

where 'θ' is the angle of inclination of the sample, *FT* the recorded traction force and *FN* the recorded normal force at any instance.

2.3.9 Thermogravimetric analysis

Thermogravimetric analysis (TGA) is an analytical technique used to determine a material's thermal stability and its fraction of volatile components by monitoring the weight change that occurs as a specimen is heated [36, 37]. The measurement is normally carried out in air or in an inertatmosphere, such as Helium or Argon, and the weight is recorded as a function of increasing temperature. Sometimes, the measurement is performed in a lean oxygen atmosphere (1 to 5% O_2 in N_2 or He) to slow down oxidation. In addition to weight changes, some instruments also record the temperature difference between the specimen and one or more reference pans(differential thermal analysis, or DTA) or the heat flow into the specimen pan compared to that of the reference pan (differential scanning calorimetry, or DSC). The latter can be used to monitor the energy released or absorbed via chemical reactions during the heating process.

Analysis is carried out by raising the temperature gradually and plotting weight against temperature. The temperature in many testing methods routinely reaches 1000°C or greater, but the oven is so greatly insulated that an operator would not be aware of any change in temperature even if standing directly in front of the device. After the data is obtained, curve smoothing and other operations may be done such as to find the exact points of inflection. In this study TGA was conducted on HA to assess its water loss temperature.

References

[1] W. Kern and K. K. Schuegraf, Deposition Technologies and Applications: Introduction and Overview -Handbook of Thin-Film Deposition Processes and Techniques - Principles, Methods, Equipment and Applications (2nd Edition) William Andrew Publishing/Noyes (2002) ISBN: 978-0-8155-1442-8 .11-40.

[2] R. F. Bunshah, Deposition Technologies: An Overview , Handbook of Deposition Technologies for Films and Coatings, Noyes Publications Mill Road, Park Ridge, New Jersey (1994), ISBN: 0-8155-1337-2, 1-40.

[3] R. F. Bunshah, Evaporation: Processes, Bulk Microstructures and Mechanical Properties, Handbook of Deposition Technologies for Films and Coatings, Noyes PublicationsMill Road, Park Ridge, New Jersey 07656,(1994) ISBN: 0-8155-1337-2,157-258.

[4] J. A. Thornton and J.E. Greene, Sputter Deposition Processes, Handbook of Deposition Technologies for Films and Coatings, Noyes Publications Mill Road, Park Ridge, New Jersey 07656,(1994) ISBN: 0-8155-1337-2,275-337.

[5] S. Rossnagel, Sputtering and Sputter Deposition, Handbook of Thin-Film Deposition Processes and Techniques - Principles, Methods, Equipment and Applications (2nd Edition) William Andrew Publishing/Noyes (2002), ISBN: 978-0-8155-1442-8.319-348.

[6] D. M. Mattox, Ion Plating, Handbook of Deposition Technologies for Films and Coatings, Noyes Publications Mill Road, Park Ridge, New Jersey 07656,(1994) ISBN: 0-8155-1337-2, 346-391.

[7] J. R. McNeil, J. J. McNally, and P. D. Reader, Ion Beam Deposition, Handbook of Thin-Film Deposition Processes and Techniques -

Principles, Methods, Equipment and Applications (2nd Edition) William Andrew Publishing/Noyes (2002), ISBN: 978-0-8155-1442-8 463-497.

[8] J. Carlsson, Chemical Vapor Deposition, Handbook of Deposition Technologies for Films and Coatings, Noyes PublicationsMill Road, Park Ridge, New Jersey 07656,(1994) ISBN: 0-8155-1337-2 400-456.

[9] A. Sherman, Plasma-Assisted Vapor Deposition Processes: Handbook of Deposition Technologies for Films and Coatings, Noyes Publications Mill Road, Park Ridge, New Jersey 07656,(1994) ISBN: 0-8155-1337-2.485-505.

[10] C. A. Moore, Z. Yu, L. R. Thompson, G. J. Collins- Laser and Electron Beam Assisted Processing, Handbook of Thin-Film Deposition Processes and Techniques - Principles, Methods, Equipment and Applications (2nd Edition) William Andrew Publishing/Noyes (2002), ISBN: 978-0-8155-1442-8 .349-377.

[11] M. Schwartz, Deposition from Aqueous Solutions: An Overview, Handbook of Deposition Technologies for Films and Coatings, Noyes Publications Mill Road, Park Ridge, New Jersey 07656,(1994) ISBN: 0-8155-1337-2.506-597.

[12] R. F. Bunshah, Metallurgical Applications, Handbook of Deposition Technologies for Films and Coatings, Noyes PublicationsMill Road, Park Ridge, New Jersey 07656,(1994) ISBN: 0-8155-1337-2.766-787.

[13] D. P. Norton, Pulsed Laser Deposition of Complex Materials: Progress toward Applications, Pulsed laser deposition of thin films:

applications-led growth of functional materials, Wiley-Interscience,(2007) ISBN-10: 0-471-44709-9.3-28.

[14] D. B. Chrisey and G. K. Hubler, Pulsed laser deposition of Thin Films,John Wiley and Sons Inc,New York (1994) ISBN 0-471-59218-8.229-253.

[15] S. Johnson, M.Haluska, R. J. Narayan , R. L. Snyder-In situ annealing of hydroxyapatite thin films, Materials Science and Engineering **C 26** (2006) 1312 – 1316.

[16] F. J. Garcia, Sanz, M. B. Mayor, J. L. Arias, J. Pou, B. Leon,M. Perez-Amor-Hydroxyapatite coatings: a comparative study between plasma-spray and pulsed laser deposition techniques, Journal of Materials Science: Materials in Medicine **8** (1997) 861- 865.

[17] X. Liua, P. K. Chub, C. Dinga, Surface modification of titanium, titanium alloys and related materials for biomedical applications, Materials Science and Engineering **R 47** (2004) 49–121.

[18] J.Cl. Puippe, Surface Treatments of Titanium Implants, European Cells and Materials **5. Suppl. 1**,(2003) 32-33.

[19] John A Disegi, Anodizing Treatments for Titanium Implants, 0-7803-3869-3/97 10.0001 9971EEE.

[20] Donald M. Mattox, Non-Elemental Characterization of Films and Coatings, Handbook of Deposition Technologies for Films and Coatings, Noyes PublicationsMill Road, Park Ridge, New Jersey 07656,(1994) ISBN: 0-8155-1337-2.669-702.

[21] P.S. Vanzillottaa, G. A. Soaresa, I. N. Bastosb, R. A. Simãoa, N. K. Kuromotoa, Potentialities of Some Surface Characterization Techniques for the Development of Titanium Biomedical Alloys, Materials Research, **7 No. 3** (2004) 437-444.

[22] Veeco Dektak 6M stylus profiler,Manual 2004.

[23] PEJ Flewitt and R K Wild, Physical methods for materials characterization, IOP Publishing Ltd,(2003) 138.

[24] D. K Schroder, Semiconductor material and device characterization, Wiley interscience publication,(1998) 170.

[25] B.D Cullity, S.R.Stock, Elements of X-ray diffraction,Third edition,Prentice hall New Jersey(2001) 170.

[26] M.J.Buerger, X-ray Crystallography, John Wiley and sons, New York(1962) 29.

[27] C.Kittel,Introduction to solid state physics,seventh edition,Wiley Eastern Limited(1996) 29.

[28] A.A. Thorpe, T. G. Nevell, S. A. Young, J. Tsibouklis, Surface energy characteristics of poly_methylpropenoxyfluoroalkylsiloxane/ film structures, Applied Surface Science **136** (1998) 99–104.

[29] R. B. Shaevich, Measurement of the specific free surface energy of solids, Measurement Techniques, **50, No. 10**, (2007) 1121-1123.

[30] Claudio Della Volpe, Marc Brugnara, Devid Maniglio, Stefano Siboni and Tenzin Wangdu, About the possibility of experimentally measuring an equilibrium contact angle and its theoretical and practical consequences, Contact Angle, Wettability: and Adhesion, VSP(2006) Netherlands,ISBN 90-6764-436-6 .19-99.

[31] Pedro César Garcia Oliveira, Gelson Luis Adabo, Ricardo Faria RIBEIRO, Sicknan Soares da ROCHA,Fabiano Araújo Ávila, Accácio Lins do Valle, Influence of the final temperature of investment heating on the tensile strength and Vickers hardness of CP Ti and TI-6AL-4V alloy, J Appl Oral Sci. **15** (2007) 44-8.

[32] George F. Vander Voort, Micro indentation Hardness Testing, ASM Handbook Vol 8- ASM International Materials Park, OH 44073 (2000), ISBN 0-87170-389-0.470-478

[33] P L. Menezes , Kishore , S.V. Kailas, Influence of surface texture on coefficient of friction and transfer layer formation during sliding of pure magnesium pin on 080 M40 (EN8) steel plate, Wear **261** (2006) 578–591.

[34] J.L. Ariasa, M.B. Mayora, J.Pou , Y.Leng , B. Leona, M. Perez-Amor, Micro- and nano-testing of calcium phosphate coatings produced by pulsed laser deposition, Biomaterials **24** (2003) 3403–3408.

[35] V. H. Bulsara,S.Chandrasekar and T. N. Farris, Scratch Testing, ASM Handbook vol 8- ASM International Materials Park, OH 44073 (2000), ISBN 0-87170-389-0.670-690.

[36] P. Fermo1, A. Piazzalunga1, R. Vecchi, G. Valli, and M. Ceriani, A TGA/FT-IR study for OC and EC quantification applied to carbonaceous aerosol collected in Milan (Italy), Atmos. Chem. Phys. Discuss, **5,** (2005) 4335–4371.

[37] A. R.Kumar and S. Kalainathan, Growth and characterization of nano-crystalline hydroxyapatite at physiological conditions, Cryst. Res. Technol. **43, No. 6**, (2008) 640 – 644.

Chapter 3

MECHANISM OF PROTEIN ADHESION TO IMPLANT SURFACES

This chapter gives an introduction to bioadhesion and biofilm formation. The chapter also describes the common protein adhesion molecular family. Integrins which are the cell adhesion molecules are highlighted here

3.1 Introduction to Bioadhesion of Biomaterials

Bioadhesion, i.e. biofilm formation resulting in a fouling surface, is required for biomaterial to be considered as a part of the body (e.g., orthopaedic prosthesis, hard tissue) to enhance its incorporation and its biomechanical response [1-9]. Bioadhesion takes place in three steps: the deposition and attachment of a protein layer, followed by cell deposition. The important parameter corresponds to the formation of a water monolayer on the substrate as in fig 3.1. Because of its low wettability (and high water contact angle), a substrate with a low surface energy could interact neither with bio molecules nor with water molecules. There is no affinity, only electrostatic repulsion of the proteins. Hence, the organization of the bio molecules at the interface is not uniform, and cell aggregates are formed [2].

Conversely, with high surface energy materials, a low-cohesion monomolecular layer of water is formed spontaneously and characterized by several features: the water tension is higher than that of a protein, and the hydrophilic surface affinity with the small water molecules is stronger than with

more complex molecules. Therefore, a front of small and mobile water molecules is created during wetting and leads to water spreading on the surface, and monolayer formation. Sometimes, interface swelling is observed within the first few seconds. Hydrogen bonds are established immediately between the polar groups of the polymer and the water molecules. Salt ions (Na+, Cl–) enhance the phenomenon. Then, the anchoring of hydrophilic bio-molecules (protein derivatives, i.e., BSA) by hydrogen bonds takes place, but without any adhesion to the substrate.

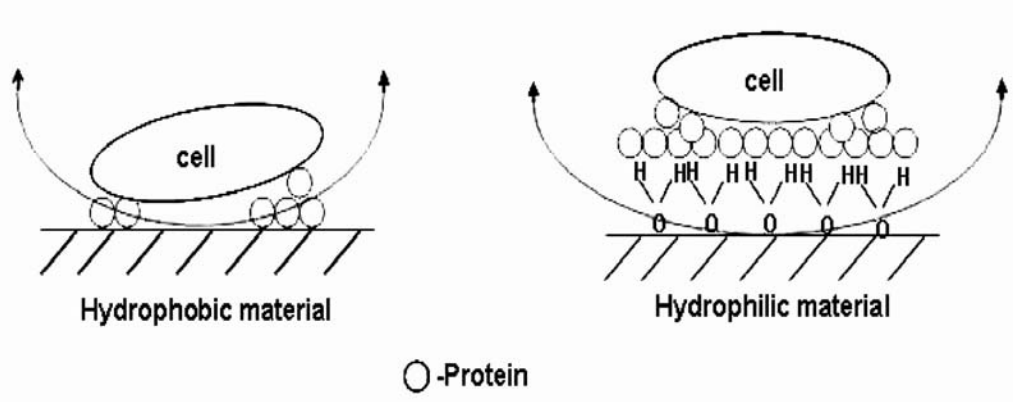

Fig 3.1 Adhesion behaviour of hydrophobic and hydrophilic materials

With such materials, the interface is defined by the aqueous top layer of substrate and by the surface of the cells or bacteria, with a protein layer in between. In conclusion, the deposition of a water monolayer on a hydrophilic substrate prohibits the formation of a stable bio molecular layer and cells cannot be deposited. Therefore a more hydrophobic surface favours protein adhesion and thereby cell adhesion [2, 3].

3.1.1 Osteoblasts adhesion on metal surface through protein ligand–receptor binding mechanism.

It is well recognized that osteoblasts (bone cells) preferentially adhere to specific amino acid sequences such as arginine–glycine–aspartic acid (RGD) and heparin-sulphate ligand binding regions in adsorbed proteins as depicted in fig 3.2 [6,13]. Accordingly, how specific amino acid sequences are exposed in adsorbed proteins to associate with binding to integrin receptors in cell membranes is critical to whether cell adhesion will occur on an implant surface. Thus, the efficacy of bone regeneration is determined mainly by surface characteristics such as the chemical composition and physical properties of the implant that controls initial protein adsorption [6].

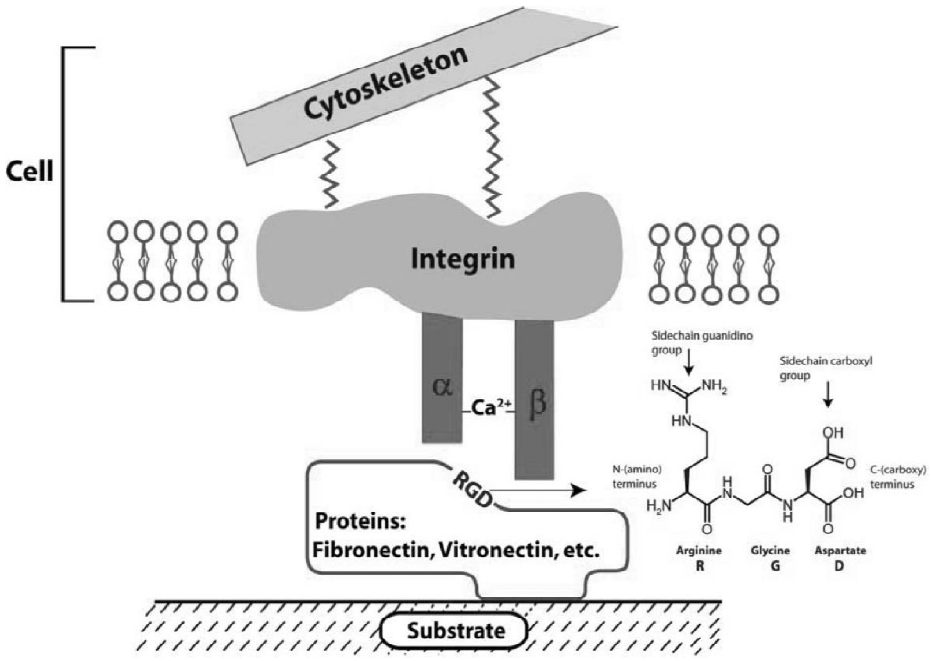

Fig: 3.2 Initial protein interactions leading to cell recognition of implants.

These properties alter the adsorption of proteins which mediate the adhesion of desirable (osteoblast) and undesirable (fibroblast) cells. It is believed that the lack of attention paid to understanding cellular recognition to proteins initially adsorbed on biomaterial surfaces to date could be one of the key reasons why current implant do not, on average, last longer than 15 years. It is this new direction aimed at intelligently designing implant surfaces to control protein interactions important for subsequent cell adhesion that may provide answers to those problems which have plagued current orthopedic implants.

3.1.2 Protein Adhesion molecular family

A brief description of the common families of protein adhesion molecules are described here [10, 11, 12]. The majority of adhesion molecules can be grouped into families.

i) Cadherin

The cadherin proteins[10] comprise a very large superfamily which can be divided into two subfamilies, the classic cadherins and the protocadherins.The classic cadherins can be subdivided into four subfamilies, the type I classic cadherins, the type 11 classic cadherins, the desmosomal cadherins and the modified or other classic cadherins. The first cadherin to be identified was E-cadherin (cadherin-1),w hich acts as the prototype for the type I classic cadherins, namely N-cadherin (cadherin-2), Pcadherin (cadherin-3) and R-cadherin (cadherin-4) **.**Structurally the protocadherins differ from the classic cadherins in that they do not have propeptide sequences and the extracellular domains contain more than five cadherin repeats (usually six or seven).

The characteristic feature of the classic cadherins is their ability to mediate Ca2+ dependent homophilic adhesion with specificity being generated by sequence differences at the adhesive face of the N-terminal domain.

Structural studies combined with mutagenesis suggest that binding can be regulated by the cadherins switching between non-binding monomers and adhesive competent dimers in the plane of the membrane. some of the protocadherins can mediate Caz+-dependent homophilic cell adhesion'2J38'3. In addition the CNR protocadherins contain an RGD motif in their N-terminal cadherin repeat, which is predicted to be located on a protruding loop thereby implicating this subclass of Pcdha protocadherins as counter-receptors for integrins on neighbouring cells.

ii) Immunoglobulin superfamily

The immunoglobulin superfamily (IgSF) [10] represents a large group of proteins with the common feature that they all contain one or more extracellular Ig domains. All cells in the body express such molecules and in leucocytes, where the cell surface proteins have been most thoroughly characterized, 34% of the transmembrane and membrane-associated proteins are IgSF members. Unlike the cadherins, which essentially mediate homophilic interactions via the antiparallel binding of the N-terminal cadherin repeats with the equivalent domain on neighbouring cells, the IgSF members show a broad range of ligand interactions. These include integrins (e.8. ICAMs), sialic acid (members of the siglec subfamily), extracellular matrix components (e.g. contactin-1) and homophilic interactions (e.g. CD31, P (O), CEACAM family). In some cases, more than one ligand has been identified.

iii) Integrins Cell adhesion molecules of focal adhesion contacts:

Integrins are so called because they ‘integrate’ the extracellular matrix with the intracellular cytoskeleton and hence deliver ‘outside-in’ signals from the external environment to the cell to modify cellular structure and functions: cell adhesion, motility, proliferation, apoptosis, induction of gene transcription and differentiation [10]. To achieve this, integrins are recruited into complex

structures, focal adhesion contacts (or related structures at cel1:cell contacts, which can involve integrins interacting with counter-receptors). The function of the integrin receptor is itself modulated by signals from within the cell delivered via other receptor systems ('inside-out'signalling) through complex cytoskeletal interactions with their cytoplasmic tails.

Integrin ligand specificity: Physicochemical analysis of integrins in conjunction with cross-linking studies with radioactively labelled RGD and other peptide probes has revealed that the ligand binding site of the functional integrin heterodimer resides in its globular head. In the main, integrins act as cell surface receptors for ECM proteins. Some integrins are promiscous and can bind a number of ligands (e.g. recognize vitronectin, fibrinogen, fibronectin, denatured collagen and other proteins, whereas others show a more restricted binding pattern. Conversely, several ECM proteins are recognized by a number of different integrin receptors.

iv) Selectins

The three selectins, E-selectin (CD62E), L-selectin (CD62L) and P-selectin (CD62P), are related both structurally and functionally [10]. They have been extensively studied due to their role in the inflammatory response and their potential use as therapeutic targets. All three selectins are type I transmembrane proteins with an N-terminal C-type selectin domain followed by an EGF repeat and a variable number of complement control protein (CCP) domains. The human E-selectin, L-selectin and P-selectin have six, two and nine CCP domains, respectively. However, the number of CCP domains in E- and P-selectin varies from four to six and from six to nine, respectively, in other species. Selectins, as their names indicate, bind carbohydrates with all three selectins binding to the tetrasaccharide sialyl-Lewisx (sLex) and its stereoisomer, in which the positions of the linkages of fucose and galactose are

exchanged. In addition, both E- and P-selectin can bind sulpho-LeX and sulpho-LeA and Lselectin binds with high efficiency to sulphated sLeX epitopes in which additional sulphate residues are attached to the galactose and N-acetylglucosamine residues.

3.1.3 Surface topography of implants for favourable protein adhesion

One of the major research topics in orthopedic tissue engineering is topography, particularly with respect to optimizing cell colonization. Surface roughness is an immensely studied subject by numerous investigators with the goal of improving the performance of bone implants [3, 6, 13]. Specifically, compared with smooth surfaces, micron surface roughness (from 1 to 100 μm surface features) on titanium substrates created by sandblasting, etching, machining and the use of micron-sized metal bead coatings has enhanced osteoblast functions such as adhesion, proliferation, production of alkaline phosphatase, and deposition of calcium-containing mineral. Other strategies for improving the biocompatibility and osteogenic capacity of metal implants include surface modification with inorganic mineral coatings, particulates, or cements containing a diversity of calcium salts (mainly calcium phosphates, sulfates or carbonates). The idea behind all of these strategies is to make the metal surface more acceptable to bone cells and, by doing so, trick the body into rapid integration of the implanted structure rather than fibrous encapsulation. Recent studies have provided information that nanometer crystalline hydroxyapatite (HA) and amorphous calcium phosphate compacts could be chemically functionalized with the arginine–glycine–aspartic acid (RGD) peptide sequence using the aforementioned maleimide chemistry. Results showed that the immobilization of the cell adhesive RGD sequence increased osteoblast adhesion compared to those non-functionalized and those functionalized with the non-cell adhesive control peptide[6,14,15,16]. In this work various modified Ti surfaces were subjected to cell viability studies to measure their cell adhesion properties.

References:

[1] J. H. Boss, Biocompatibility: Review of the Concept and Its Relevance to Clinical Practice,Biomaterials and Bioengineering Handbook, CRC USA, (2000) 978-0824703189 1-54.

[2] G. Legeay and F. Poncin-Epaillard, Surface Engineering by Coating of Hydrophilic Layers:Bioadhesion and Biocontamination, Adhesion – Current Research and Application. Wulff Possart, WILEY-VCH Verlag GmbH & Co. KGaA, Weinheim (2005) ISBN: 3-527-31263-3, 175-184.

[3] A.J. García and C.D. Reyes, Bio-adhesive Surfaces to Promote Osteoblast Differentiation and Bone Formation, J Dent Res **84(5)** (2005) 407-413,.

[4] U. Bakowsky, C. Ehrhardt, C. Loehbach, P. Li, C. Kneuer, D. Jahn, D. Hoekstra, and C.-M. Lehr, Adhesion Molecule-Modified Cardiovascular Prostheses:Characterization of Cellular Adhesion in a Cell Culture Modeland by Cellular Force Spectroscopy, Bioadhesion and Biocontamination, Adhesion – Current Research and Application. Wulff Possart, WILEY-VCH Verlag GmbH & Co. KGaA, Weinheim (2005) ISBN: 3-527-31263-3, 157-164.

[5] M. Cannas, M. Bosetti, M. Santin, and S. Mazzarelli, Tissue Response to Implants: Molecular Interactions and Histological Correlation, Biomaterials and Bioengineering Handbook, CRC, USA (2000) 978-0824703189 1-54.

[6] G.Balasundaram, T. J Webster, A perspective on nanophase materials for orthopaedic implant applications, Journal of materials chemistry **16** (2006) 3737-3745.

[7] N. J. Hallab, R. M. Urban, and J. J. Jacobs, Corrosion and biocompatibility of Orthopedic Implants, Biomaterials in Orthopedics, Marcel Dekker, Inc., 270 Madison Avenue, New York, NY 10016, U.S.A (2004) ISBN: 0-8247-4294-X 63-91.

[8] M. Niinomi, T. Hattori, and S. Niwa, Material Characteristics and Biocompatibility of Low Rigidity Titanium Alloys for Biomedical Applications, Biomaterials in Orthopedics, Marcel Dekker, Inc., 270 Madison Avenue, New York, NY 10016, U.S.A (2004) ISBN: 0-8247-4294-X 41-62.

[9] L. V. Carlsson, W. Macdonald, C. M. Jacobsson, and T. Albrektsson, Osseointegration Principles in Orthopedics: Basic Research and Clinical Applications, Biomaterials in Orthopedics, Marcel Dekker, Inc., 270 Madison Avenue, New York, NY 10016, U.S.A (2004) , ISBN: 0-8247-4294-X 223-239.

[10] K. Kendall, Molecular Adhesion and Its Applications, Kluwer Academic Publishers New York (2004) ISBN: 0-306-46520-5 275-300 275-301.

[11] R. P. McEver, P-selectin glycoprotein ligand-1 (PSGL-1), Adhesion Molecules: Function and Inhibition, Birkhäuser Verlag AG, P.O. Box 133, CH-4010 Basel, Switzerland, (2007) ISBN 978-3-7643-7974-2 3-27.

[12] C. M Isacke ,M.A.Horton, The adhesion molecule. Academic press USA (2000) ISBN 0-12-356505-7 149-210.

[13] G. Balasundaram, Michiko Sato, Thomas J. Webster-Using hydroxyapatite nanoparticles and decreased crystallinity to promote osteoblast adhesion similar to functionalizing with RGD Biomaterials **27** (2006) 2798–2805.

[14] J.M.Fernandez-Pradas, L.Cleries, E.Martinez , G.Sardin , J.Esteve , J.L.Morenza-Influence of thickness on the properties of hydroxyapatite coatings deposited by KrF ablation. Biomaterials **22** (2001) 2171-2175.

[15] D. D. Deligianni, Nikoleta D.Katsala, Petros G. Koutsoukos , Yiannis F. Missirlis -Effect of Surface Roughness of Hydroxyapatite on Human Bone Marrow Cell Adhesion,Proliferation,Differentiation and Detachment. Biomaterials **22** (2001) 87-96.

[16] Bacakova–Cell adhesion on Artificial Materials for Tissue Engineering. Pysiol. Res **53 (suppl.I)** (2004) S35- S45.

Chapter 4

IN-VITRO CELL VIABILITY TESTS

This chapter discusses the in-vitro cytotoxicity test that have been adopted in the present work to assess the cell viability of the modified implant materials. The chapter describes MTT assay and fluorescence microscopy analysis used for quantifying cell adhesion

4.1 Introduction to in vitro models of cytotoxicity testing

The usefulness of mammalian cell cultures for biocompatibility testing is confirmed by experimental studies which found a good correlation between in vitro and in vivo tests. The rationale is that in vitro models employing human cells to study the interactions between the cell system and the biomaterial/device allow for a reasonable prediction of the performance in vivo of the biomaterial/device [1].

It has to be acknowledged that isolated cell systems are more sensitive to toxic materials than body tissues. Nevertheless, there is an increasing demand for reliable in vitro methods for two main reasons: (1) cellular mechanisms of toxicity can be described using biochemical assays; (2) valid alternatives to animal models are needed. Using such testing methods the materials can be screened according to their grade of toxicity and discarded, if this is the case, prior to further testing [1,2].

A number of characteristics and functions of cells can be verified after challenge with biomaterials: morphology, membrane integrity, cytoskeleton, surface molecules, viability, proliferation, protein synthesis, oxidative response, motility, secretion, response to growth factors and cytokines, cell-cell interactions and recently, gene expression.

Adhesion of cells onto biomaterials is considered a positive phenomenon for implant outcome: such process is known to influence cell activities. Cell adhesion onto foreign surfaces is inspected mainly by cell count, while electron microscopic techniques / fluorescence microscopy and computer-assisted measurement are used for the assessment of spreading and morphology. The ability of surface topography to determine orientation and alignment of cells and to modify bone cell response has been demonstrated in several studies [2-12].

4.1.1 Cell Viability tests

Historically, the hemolysis test was the very first test for the assessment of the damage induced by biomaterials to red blood cells. The test is simple, but nearly every substance not "physiological" is able to induce massive red blood cell lysis [1, 2]. The uptake of neutral red (NR) and the exclusion of propidium iodide (PI) are used for routine evaluation of cell viability after challenge with materials or extracts. The uptake of NR, initially developed for toxicological and immunological purposes was then modified to meet biocompatibility needs. Although it is suitable for quantitative evaluation through spectrophotometric measurement of the amount of dye inside the cells, it is often used as a qualitative method [2]. It must be considered that the results may be affected by consistent alteration of medium ph, being NR a sensitive probe for monitoring the intra-cellular pH[2,4].

The staining of nucleic acids with PI is commonly used in a number of flow cytometry tests: this dye stains dead cells after crossing the injured membrane. Since these methods rely on different mechanisms and different cell compartments, that is viable and dead cells are stained by NR and PI respectively, the entire cell population is covered and different steps of toxicity mechanism may be detected. Results from PI and NR assay methods show a good correlation; nevertheless occasional disagreement between the two methods was found with NR detecting toxicity where PI was negative. This can be explained by the fact that a delay of cell growth may decrease NR uptake, but not necessarily result in PI uptake if the cell membrane is intact. Another method is the exclusion of trypan blue, with qualitative or quantitative assessment [1].

Quite recently the MTT [9,10,11] test has become very popular in biocompatibility testing with cell culture systems Yellow **MTT** (3-(4,5-Dimethylthiazol-2-yl)-2,5-diphenyltetrazolium bromide, a tetrazole) is reduced to purple formazan in living cells. A solubilization solution (usually either dimethyl sulfoxide, an acidified ethanol solution, or a solution of the detergent sodium dodecyl sulfate in diluted hydrochloric acid) is added to dissolve the insoluble purple formazan product into a colored solution. The absorbance of this colored solution can be quantified by measuring at a certain wavelength (usually between 500 and 600 nm) by a spectrophotometer. The absorption maximum is dependent on the solvent employed.

MTS [1,2] is a more recent alternative to MTT. MTS (3-(4,5-dimethylthiazol-2-yl)-5-(3-carboxymethoxyphenyl)-2-(4-sulfophenyl)-2H-tetrazolium), in the presence of phenazine methosulfate (PMS), produces a water-soluble formazan product that had an absorbance maximum at 490-500 nm in phosphate-buffered saline. It is advantageous over MTT in that (1) the

reagents MTS + PMS are reduced more efficiently than MTT, and (2) the product is water soluble, decreasing toxicity to cells seen with an insoluble product.

These reductions take place only when reductase enzymes are active, and therefore conversion is often used as a measure of viable (living) cells. Changes in metabolic activity can give large changes in MTT or MTS results while the number of viable cells is constant. When the amount of purple formazan produced by cells treated with an agent is compared with the amount of formazan produced by untreated control cells, the effectiveness of the agent in causing death, or changing metabolism of cells, can be deduced through the production of a dose-response curve.

4.1.2 Fluorescence microscopy [10, 11, 12]

DAPI or **4, 6-diamidino-2-phenylindole** is a fluorescent stain that binds strongly to DNA (De-oxy ribonucleic acid). It is used extensively in fluorescence microscopy. Since DAPI will pass through an intact cell membrane, it may be used to stain both live and fixed cells [10].

For fluorescence microscopy, DAPI is excited with ultraviolet light. When bound to double-stranded DNA its absorption maximum is at 358 nm and its emission maximum is at 461 nm. (This emission is fairly broad, and appears blue/cyan.). DAPI will also bind to RNA, though it is not as strongly fluorescent. Its emission shifts to around 500 nm when bound to RNA. Fig 4.1 shows DAPI bound to minor groove of DNA.

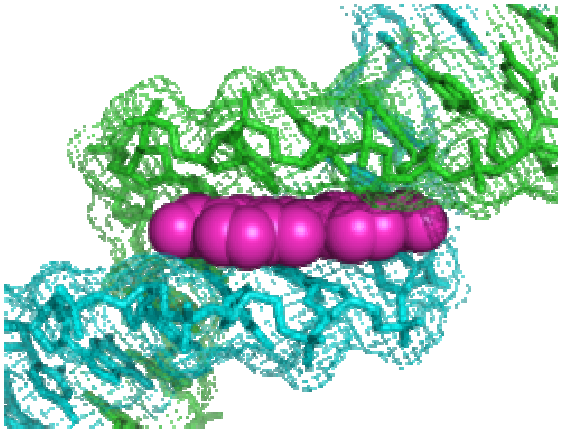

Fig: 4.1 DAPI (magenta) bound to the minor groove of DNA (green and blue)

DAPI's blue emission is convenient for microscopists who wish to use multiple fluorescent stains in a single sample. There is fluorescence overlap between DAPI and green-fluorescent molecules like fluorescein and green fluorescent protein (GFP), or red-fluorescent stains like Texas Red, but using spectral unmixing or taking images sequentially can get around this.

Apart from labelling cell nuclei, the most popular application of DAPI is in detection of mycoplasma or virus DNA in cell cultures. Because DAPI easily enters live cells and binds tightly to DNA, it is toxic and mutagenic. Care should be taken in its handling and disposal.

MTT assay and DAPI fluoresense microscopic studies were conducted in this research to assess the cell viability of the different surface modified implant material as per the following proceedure.

For MTT assay, all the samples were transferred to a fresh plate and 800 µL of MTT reagent was added to each well and incubated for 2 hours at 37^0C. MTT transformed to dark blue formazan by mitochondrial dehydrogenises enabling cell viability to be assessed. 800 µL of lysis buffer (20%Sodium

Dodecyl Sulphate 50% Dimethyl Formamide 30% Distilled water) was added to each well, mixed and incubated at 37oC for 4 hours. 200 µL of each sample was transferred to a fresh 96 well plate and the optical density of the solution was measured at 570nm in an ELISA microplate reader (Biorad USA). Analysis of optical variance was used to evaluate difference in cell viability between the groups [2, 8, 11, 12].

For confocal imaging osteosarcoma cells were grown on the samples in culture medium for 48 hours. After which the cells were fixed with 4% Paraformaldehyde (PFA), washed twice in 1X Phosphate Buffered Saline (pH 7.4) (PBS) and incubated in DAPI (4', 6-Diamidino-2-phenyindole) (1:1000) for 10 minutes at room temperature (28^0C). Cells were imaged for nuclear visualization thereafter using a confocal microscope (Leica TCS SPE Germany).

References:

[1] F. A. Barile-Principles of toxicology testing, CRC Press USA (2008), ISBN-10: 0-8493-9025-7, 1-27 & 147-194.

[2] M. Theiszovaa, S. Jantovaa, J. Draguňovab, P. Grznarovaa, M. Palouc-Comparison the Cytotoxicity of Hydroxyapatite Measured By Direct Cell Counting And MTT Test in Murine Fibroblast NIH-3T3 Cells, Biomed Pap Med Fac Univ Palacky Olomouc Czech Repub. **149(2)** (2005) 393–396.

[3] J. L. Ong, D. L. Carnes, K. Bessho-Evaluation of titanium plasma-sprayed and plasma-sprayed hydroxyapatite implants in vivo, Biomaterials **25** (2004) 4601–4606.

[4] L. Bačáková, E. Filová, F. Rypáček, V. Švorčík, V. Starý- Cell Adhesion on Artificial Materials for Tissue Engineering, Physiol. Res. **53 (Suppl. 1)** (2004) S35-S45.

[5] J. Suha, Bong-C. Janga, X. Zhub, J.L. Ongc, K. Kimc, Effect of hydrothermally treated anodic oxide films on osteoblast attachment and proliferation, Biomaterials **24** (2003) 347–355.

[6] L. C. Baxter, V. Frauchiger, M. Textor, I. Gwynn and R. G. Richards-Fibroblast and Osteoblast Adhesion and Morphology on Calcium Phosphate Surfaces, European Cells and Materials. **4.** (200 2) 1 - 1 7.

[7] S. Oh, C. Daraio, L. Chen, T. R. Pisanic, R.R. Fin ones, S. Jin - Significantly accelerated osteoblast cell growth on aligned TiO2 nanotubes, Wiley InterScience. DOI: 10.1002/jbm.a.30722.

[8] M.D. Ball, S. Downes, C.A. Scotchford, E.N. Antonov, V.N. Bagratashvili,V.K. Popov, W.-J. Lo, D.M. Grant, S.M. Howdle-

Osteoblast growth on titanium foils coated with hydroxyapatite by pulsed laser ablation, Biomaterials **22** (2001) 337-347.

[9] Y. Fuse, I. Hirata, H. Kurihara and M. Okazaki-Cell Adhesion and Proliferation Patterns on Mixed Self-assembled Monolayers CarryingVarious Ratios of Hydroxyl and Methyl Groups, Dental Materials Journal **26(6)** (2007) : 814－819.

[10] D. S.Baskin,H. Ngo ,V. V Didenko- Thimerosal Induces DNA Breaks,Caspase-3 Activation,Membane Damage and Cell Death in Cultured Human Neurons and Fibroblasts,Toxicological sciences **74** (2003) 1-8.

[11] J. Jakubowska, M. Stasiak, A. Szulawska, A. Bednarek and M. Czyz-Combined effects of doxorubicin and STI571 on growth, differentiation and apoptosis of CML cell line K562,Acta Biochima Polonica **54**. **4** (2007) 839–846.

[12] H. K. Patra, S. Banerjee, U. Chaudhuri, P Lahiri, A. K. Dasgupta, -Cell selective response to gold nanoparticles, Nanomedicine: Nanotechnology, Biology and Medicine **3** (2007) 111– 119.

Chapter 5

PULSED LASER DEPOSITION AND CHARACTERIZATION OF HYDROXYAPATITE THIN FILMS ON $TiAl_6V_4$ ALLOYS AND THE ANALYSIS OF PARAMETERS FOR GOOD OSEOINTEGATION

Polycrystalline hydroxyapatite thin films were grown on $TiAl_6V_4$ (Ti) substrates using pulsed laser deposition and subsequent hydrothermal annealing at a lower substrate temperature of 200^0C.The films showed good characteristics and cell adhesion properties.

5.1Introduction

Hydroxyapatite, ($Ca_{10}(PO4)_6(OH)_2$), (HA) has good biocompatibility and is being widely used as a coating material to improve the durability and biocompatibility of implant and alternative bone. HA is the main chemical constituent of human bone. It has been developed and made available for experimental or clinical application because of its excellent biocompatibility, faster bone regeneration, and direct bonding to regenerated bone without intermediate connective tissue [1]. $TiAl_6V_4$ plasma-sprayed with HA is one of the materials currently used as artificial joints. Despite the strong bonding between the HA coating itself and the bone structure, it has been recognized that the mechanical stability of the interface between the HA coating and the metallic substrate could be a problem either during surgical operation or after implantation [1-16]. It has been suggested that establishment of a thin, adherent

coating without structural defects will help solve the coating delamination problem [17, 18, 19].

Various deposition techniques, such as RF magnetron sputtering, chemical routes like sol–gel, ion beam sputtering, pulsed laser deposition and electrophoretic deposition have been applied for thin film depositions of HA [20-25]. The pulsed laser deposition (PLD) method was introduced in 1992 for high quality HA coating and has become a widely used technique for the deposition of thin films due to the advantages of simple system setup, a wide range of deposition conditions, a wider choice of materials and higher instantaneous deposition rates [1-3]. This method has demonstrated capability and reproducibility for preparation of stoichiometric high crystalline layers of complex materials. Amorphous hydroxyapatite films are obtained at deposition temperatures below 400°C by PLD [3]. These films exhibit rapid in vivo degradation, and are unsuitable for orthopaedic or dental applications that require biological fixation of the implant to bony tissue. However, amorphous films prepared at low deposition temperatures can be subsequently annealed to crystalline nature. Several researchers have described protocols for obtaining highly crystalline HA films that involve room temperature pulsed laser deposition and post deposition annealing at temperatures of 350- 500 °C to get crystalline HA films [3-6]. In other studies, the substrates of Ti and/or Ti-alloy were maintained at temperatures between 500 and 800^0C in water vapor atmosphere in order to generate a HA coating with a high degree of crystallinity for high biocompatibility [17, 19]. The condition of high substrate temperature promoted the oxidation of the substrate surface prior to the growth of the HA layer. The oxidation layer degraded the adhesion of the coating to the substrate making them unsuitable for orthopaedic applications [18]. Therefore, various methods are being assessed to deposit HA at lower temperatures as adhesive

coatings and induce film crystallinity subsequently [18]. It is seen that the presence of OH^- group is critical in stabilizing the HA structure and inducing crystallinity [18]. In this study $TiAl_6V_4$ (Ti) substrates have been coated by PLD method at different substrate temperatures ranging from 150-500^oC in O_2 atmosphere and the films were subjected to a hydrothermal annealing at 100^oC to get polycrystalline films. It was observed that amorphous films deposited at a substrate temperature of 200^oC can be converted to polycrystalline films by subsequent hydrothermal annealing at 100^0C. This substrate temperature is comparatively much lower to previously reported cases. Adhesion studies of the obtained coatings yielded a good bonding strength. Standard MTT assay studies show the greater cell adhesion characteristics of the film. The properties of the obtained coatings suggest that the method can be adopted for coating $TiAl_6V_4$ implants to make them more biocompatible and bioactive.

5.2 Experimental

5.2.1 Preparation of HA discs and substrates

Targets used for the laser deposition were prepared from pressing and sintering of HA powder prepared by the wet method [26]. The powder was subjected to cold isostatic pressing under a pressure of 120MPa and sintered at 1200°C for 2hrs in air. $TiAl_6V_4$ discs of 15mm diameter cut from cylindrical rods were used as substrate. Before coating, the substrate surface was mechanically polished through No.600 grit, cleaned ultrasonically and sand blasted using 100-150 pm Silica sand.

5.2.2 Deposition parameters

A standard PLD system was used for the deposition. The ablation target and substrate, which was 4 cm from the target and parallel to the target, were placed in a stainless steel vacuum chamber. While the substrate was stationary,

the target was rotating during the entire deposition process at a speed of 10 rpm. The Nd:YaG laser (Model X spectra physics USA) with a wavelength of 355nm and pulse duration of 9 ns was guided into the chamber using an anti-reflection coated convex lens through a quartz window. Stabilized output energy density of 1.6 J/cm^2 per pulse with a repetition rate of 10 Hz was used. The laser beam was made to fall on to the target at an angle of 45^0. Prior to deposition, the chamber was evacuated to a base pressure of 3 x 10^{-6} m bar by a combined rotary and diffusion pumping system and oxygen was bled into the chamber to maintain an operating pressure of 2 x 10^{-3} m bar. Substrates were heated with in - built heater and coatings were done on substrates at the temperature range of 150 to 500^0 C. Coating duration for all the films was kept uniform at 2 hrs. The as deposited samples were amorphous as observed by X Ray Diffractometer (XRD).These samples were subjected to a hydrothermal annealing in the presence of 20 ml of water in a sealed hydrothermal parr bomb (100 ml) for two hours at a temperature of 100^0 C[27].

5.2.3 Cell Culture

Osteosarcoma cell line KHOS-NP (R-970-5) [NCCS] were grown in culture medium 50 ml Dulbecco's modified essential media plus 10% foetal bovine serum plus one milli molar Non essential amino acids(50 mlDMEM+10%FBS+1mM NEAA) in a T-25 flask and incubated at 37^{o}C for 2 days in a 5% $C0_2$ incubator (Thermo). Approximately 5x10^5cells were plated on to control titanium discs and HA coated discs at 200^0C followed by hydrothermal treatment in 12 well plates. The culture was incubated for 72 hours at 37^{o}C in 5% CO_2 incubator. The samples with attached cells were used for MTT assay.

5.3 Results and Discussion:

The thickness, average roughness, micro-hardness and Ca/P ratios [16-28] of the films grown at different substrate temperatures are tabulated in table 5.1. As the substrate temp increased the coating thickness decreased which is in line with expectations as re-evaporation of HA from the substrates can occur at higher substrate temperatures [3].

Table 5.1: Film thickness, Average roughness, Ca/P ratio of the films and micro hardness of the substrates at different substrate temperatures. Surface roughness and micro hardness of the control sample is shown in row 7 of the table

Sl No	Description	Substrate Temperature ^{0}C	Coating Thickness μm	Average Roughness Ra μm	Ca/P Ratio	Vickers Micro Indentation HV number	Remarks
1	$TiAl_6V_4$ Sample 1	150^{0}C	4.5	0.59	-	-	Prima-facie poor adhesion
2	Sample 2	200^{0}C	4	0.6 um	1.88	357.8	Best coating. Near stoichiometric Ca/P ratio
3	Sample 3	300^{0}C	3	0.67 um	2	352.4	Higher Ca/p ratio
4	Sample 4	350^{0}C	2	0.69	2.1	366.6	Low thickness high Ca/P ratio
5	Sample 5	400^{0}C	1	0.7	2.2	344.2	Low thickness high Ca/P ratio
6	Sample 6	500	1	0.71	2.5	395.6	Low thickness High ca/p ratio
7	Control Sample $TiAl_6V_4$	NA	NA	0.3um	NA	356.8	Nil

The film coated at 150^{0}C showed very poor material characteristics and thickness and peeled off on physical contact and was not used for further micro structural study. This shows the requirement of a higher substrate temperature for the proper deposition of an adherent film of HA on the substrate. The film

coated at 200^0C showed the maximum thickness of 4 μm. The measured average surface roughness for the plain polished surface is 0.3 μm .The measured average surface roughness of the HA films ranges from 0.6 to 0.72μm which is greater than that of the substrate and will aid in cell adhesion. The micro hardness measurements of the substrates shows minimal deviation from the micro hardness of the control sample at lower substrate temperatures and a slightly higher value at 500^0C showing that the mechanical properties of the alloy are not altered within the range of temperatures. The Ca/P ratio of the substrates deviated more from the stoichiometric value of 1.67 with increase in substrate temperature due to the preferential evaporation of phosphorous at higher temperatures [3]. The value was near stoichiometric at a substrate temperature of 200^0C. The structural evolution of the as deposited and hydrothermal treated coatings is shown in fig 5.1 (a & b). Above 200^0C the coatings have a mixture of slight crystalline and amorphous phases. The films after the hydrothermal treatment showed distinct crystalline peaks of HA with preferred orientation of (300) [31].

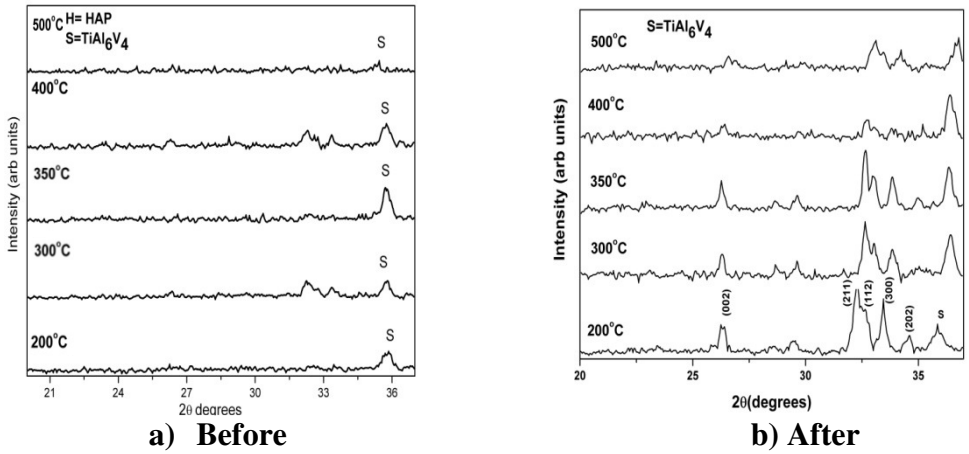

a) Before **b) After**

Fig 5.1 a& b XRD spectrum of coatings at different substrate temperatures before and after the hydrothermal treatment

SEM micrographs of all the samples are shown in fig 5.2. Broad face morphology of the coated films after the hydrothermal treatment showed that the HA coatings comprised of numerous spheroidal and needle like aggregates of different sizes

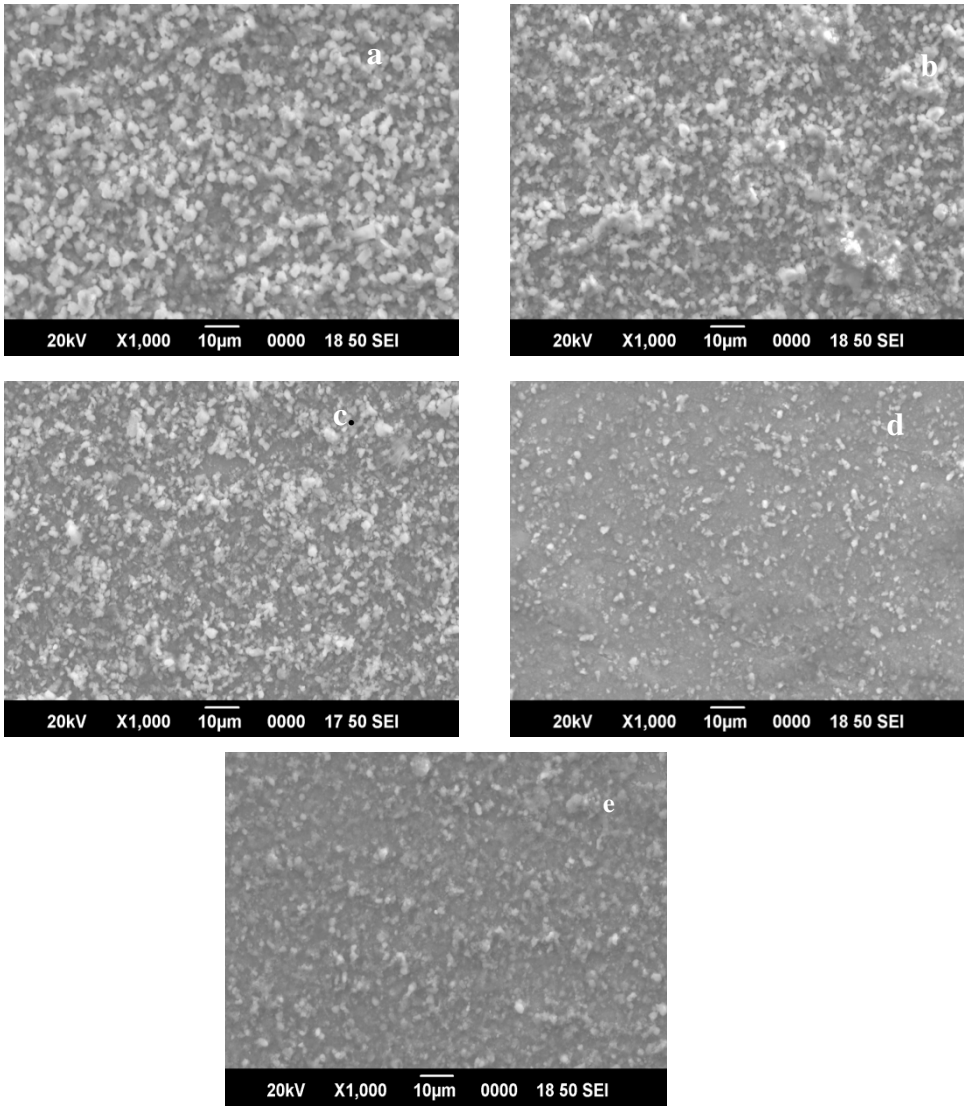

Fig 5.2 SEM images of HA films coated on $TiAl_6V_4$ substrates at different substrate temperatures a) 200^0C b) 300^0C c) 350^0C d) 400^0C e) 500^0C

The films at substrate temperatures from 200–350^{0}C showed dense coatings as compared to the films coated at higher temperatures which is in agreement with the measured thickness values. Many crevices and voids were observed to be distributed over the entire coated surface.

The EDX spectra of the HA coated sample is shown in fig 5.8. TGA of HA (fig 5.4) shows water loss from 35^{0}C and the separation of OH- group within a temperature of 300^{0}C.

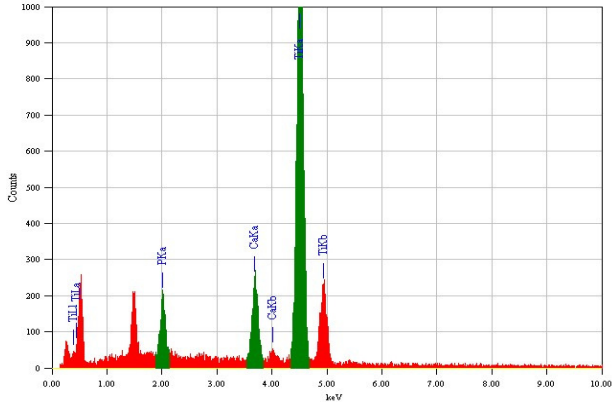

Fig 5.3 EDX Spectra of film coated at a substrate temperature of 200^{0}C

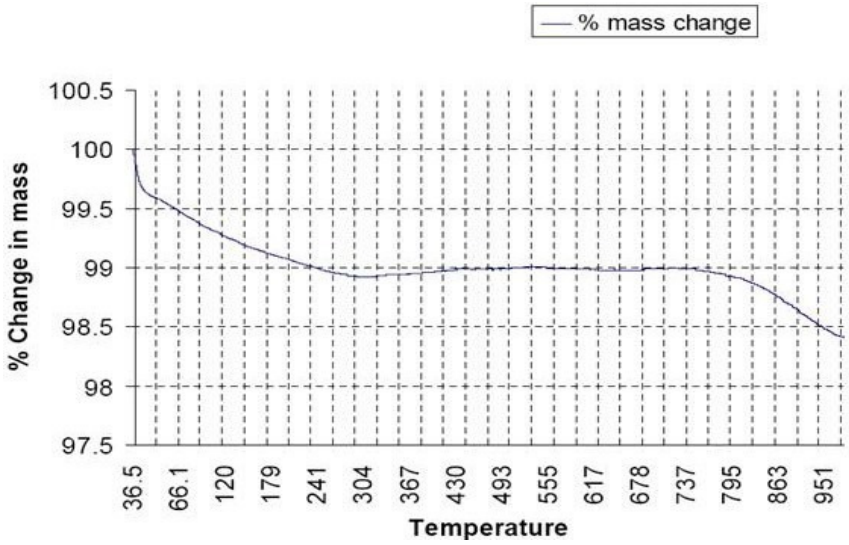

Fig 5.4 Thermo Gravimetric Analysis Curve for Hydroxyapatite

The plot between Coefficient of Friction and load for the micro-scratch analysis of the coating at 200^0C is shown in fig 5.5.

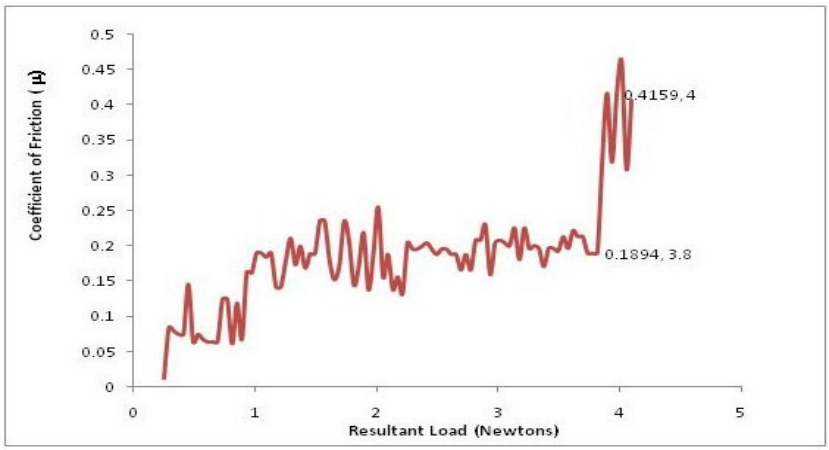

Fig: 5.5 The plot between Coefficient of Friction and load for the micro-scratch analysis of the coating deposited at 200^0C.

The critical load was calculated as close to 4 N from the graph which is in line with implant requirements [29]. Variance Analysis graph for MTT assay of the sample coated at 200^0C and the control sample is shown in fig 5.6.

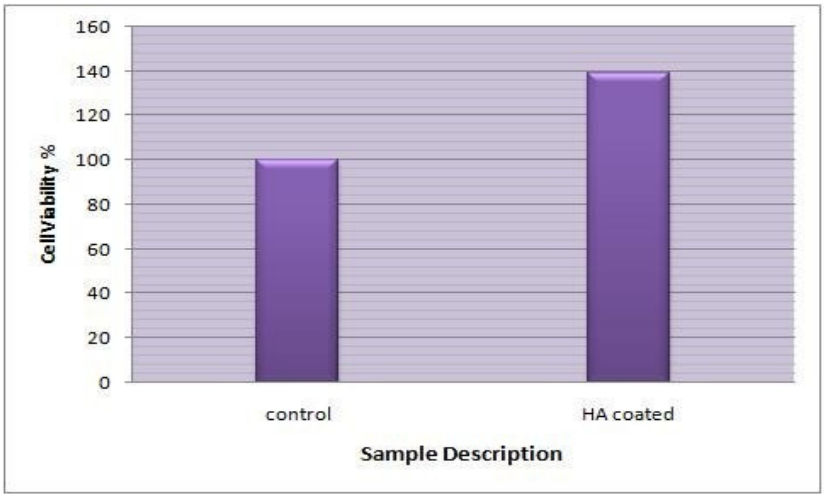

Fig 5.6 Variance Analysis graph for MTT assay of the sample coated at 200^0C and the control sample.

The coated sample showed 40% higher adhesion of cells. The Poly crystalline HA thin film coatings with adequate thickness, roughness and near stoichiometric ratio obtained on $TiAl_6V_4$ alloy at a low substrate temperature of 200^0C followed by a hydrothermal treatment at 100^0C for two hours has shown good delamination strength adequate surface roughness and sufficient thickness for use as a coating for orthopedic implants. The standard MTT assay for assessing the cell viability confirms the higher bioactive nature of the coating.

5.4 Conclusion:

The substrate temperature affects the growth rate and roughness of the HA films. Polycrystalline films of near stoichiometric ratio with sufficient delamination strength and good cell adhesion capabilities can be obtained at lower substrate temperature of 200^0C followed by hydrothermal treatment. Since studies are going on for a long time to deposit HA films at low temperatures to get a high delaminating strength, the above coating method can be adopted for thin film deposition of HA on to $TiAl_6V_4$ alloys to get highly biocompatible implants at lower substrate temperature. Further in vivo studies and modifications in coating set up will be required to consider implementation of the above method in producing commercial bioactive orthopedic implants.

References:

[1] C.F.Koch, S.Johnson, D.Kumar, M.Jelinik, D.B.Chrisey, A.Doraiswamy, C. Jin, R.J.Narayan, I.N.Mihailescu, Pulsed Laser Deposition of Hydroxyapatite thin films. Materials Science & Engineering **C 27** (2007) 484-494

[2] Q. Bao , C. C. , D. Wang , Q. Ji , T. Lei, Pulsed Laser Deposition and its Current Research Status in Preparing Hydroxyapatite Thin Films .Applied Surface Science **252** (2005) 1538-1544

[3] H. Kim , S. Lee , Y. Kim, D. Kim, W. Lee, Influence of Substrate Temperature on the Growth Rate and composition of Calcium Phosphate Films Prepared by Using Pulsed Laser Deposition. Journal of the Korean Physical Society **49(6)** (2006) 2418-2422

[4] W. Lee, S.Lee, H. Kim, Characteristics of Calcium Phosphate films Prepared by Pulsed Laser Deposition under various Water Vapor Pressures .Journal of the Korean Physical Society **47(1)** (2005) 152-156.

[5] Y. Cao, J. Weng, J. Chen, J. Feng, Z. Yang and X. Zhang, Water vapour-treated hydroxyapatite coatings after plasma spraying and their characteristics . Biomaterials **17** (1996) 419-424

[6] J.M.Fernandez-Pradas, L.Cleries , E.Martinez , G.Sardin , J.Esteve, J.L.Morenza, Influence of thickness on the properties of hydroxyapatite coatings deposited by KrF ablation. Biomaterials **22** (2001) 2171-2175.

[7] D. D. Deligianni , N. D.Katsala , P. G. Koutsoukos , Y.F. Missirlis, Effect of Surface Roughness of Hydroxyapatite on Human Bone

Marrow Cell Adhesion, Proliferation, Differentiation and Detachment. Biomaterials **22** (2001) 87-96

[8] L.Cleries , E.Martinez , J.M.Fernandez-Prasad , G.Sardin , J,Esteve , J.L Morenza, Mechanical Properties of Calcium Phosphate Coatings Deposited by Laser Ablation. Biomaterials **21** (2000) 967-971.

[9] Y. Suda , H. Kawasaki , T. Oshima , S. Nakashima , S.i Kawazoe , T. Toma, Hydroxyapatite Coatings on Titanium Dioxide Thin Films Prepared by Pulsed Laser Deposition Method .Thin Solid Films **506-507** (2006) 115-119

[10] H. Zeng, W.R. Lacefield-XPS,EDS and FTIR Analysis of Pulsed Laser Deposited Calcium Phosphate Bioceramic Coatings: The Effect of Various Process Parameters. Biomaterials **21** (2000) 23-30.

[11] S.R.Sousa, M.A.Barbosa, Effect of Hydroxyapatite Thickness on Metal Ion Release from Ti6Al4V Substrates .Biomaterials **17** (1996) 397-404.

[12] W. Mroz, M. Jeydynski, J.Hoffman, M.Jelinek, B. Major, A. Prokopiuk, Z. Szymanski, Effect of Reactive Atmosphere on Pulsed Laser Deposition of Hydroxyapatite Thin Films. Journal of Physics: Conference Series **59** (2007) 720-723

[13] S.Grigorescu, C.Ristoscu, G.Socol, E. Axente, F.Feugeas, I.N.Mihailescu, Hydroxyapatite Pulsed Laser Deposited Thin Films Behaviour When Submitted to Biological Simulated Tests Romanian Reports in Physics, **57/ 4** (2005) 1003-1010.

[14] B.Feng , Y. Chen, X.D Zhang, Effect of Water Vapor Treatment on Apatite Formation on Precalcified Titanium and Bond Strength of Coatings to Substrates .J Biomed Mater Res **59** (2002) 12-17.

[15] A. Bigi, B. Bracci, F.Cuisinier, R.Elkaim, M.Fini, I.Mayer, I.N.Mihailescu , G.Socol , L.Sturba , P. Torricelli - Human osteoblast response to pulsed laser deposited calcium phosphate coatings .Biomaterials **26** (2005) 2381- 2389.

[16] Wei-Qi Yan, T. Nakamura, K. Kawanabe, S. Nishigochi, M. Oka and T. Kokubo, Apatite layer coated titanium for use as bone bonding implants. Biomaterials **18** (1997) 1185-1190.

[17] M Katto, K Ishibashi, K Kurosawa, A Yokotani, S Kubodera, A Kameyama,T Higashiguchi, T Nakayama, H Katayama, M Tsukamoto and N Abe, Crystallized hydroxyapatite coatings deposited by PLD with targets of different densities. Journal of physics: conference series **59** (2007) 75-78.

[18] [18] L.Cleries, J.M.Fernandez-Pradas, G.Sardin, J.L.Morenza, Dissolution behaviour of calcium phosphate coatings obtained by laser ablation. Biomaterials **19** (1998) 1483-1487.

[19] J.L.Arias, F.J. Garcia-Sanz,M.B.Mayor,S.Chiussi,J.Pou, B.Leon, M.Perez-Amor, Physiochemical properties of calcium phosphate coatings produced by pulsed laser deposition at different water vapour pressures .Biomaterials **19** (1998) 883-888.

[20] R. B.Heimann, R. Wirth- Formation and transformation of amorphous calcium phosphates on titanium alloy surfaces during atmospheric plasma spraying and their subsequent in vitro performance .Biomaterials **27** (2006) 823-831.

[21] H.Li, K.A.Khor, P.Cheang -Titanium dioxide reinforced hydroxyapatite coatings deposited by high velocity oxy-fuel (hvof) spray. Biomaterials **23** (2002) 85-91.

[22] E.S.Thian, N.H.Loh, K.A.Khor,S.B.Tor, Microstructures and Mechanical properties of Powder Injection molded Ti6Al4V/HA powder. Biomaterials **23** (2002) 2927-2938.

[23] Y.W.Gu, N.H.Loh, K.A.Khor, S.B.Tor, P.Cheang, Spark Plasma Sintering of hydroxyapatite powders. Biomaterials **23** (2002) 37-43.

[24] E.S.Thian, J.Huang, S.M.Best, Z.H.Barber , W.Bonfield, Magnetron co-sputtered silicon-containing hydroxyapatite thin films-an in vitro study. Biomaterials **26** (2005) 2947-2956.

[25] M. Manso, C. Jimenez , C. Morant, P. Herrero, JM Martinez-Duart, Electrodeposition of hydroxyapatite coatings in basic conditions. Biomaterials 21 (2000) 1755-1761.

[26] Hideki Aoki, Medical Applications of HAP Takayama Press ,Tokyo 1994.179-181.

[27] K. Byrappa, M. Yoshimura - Handbook of Hydrothermal Technology Noyes Publications Park Ridge, New Jersey, U.S.A. William Andrew Publishing LLC Norwich, New York, U.S.A.(2001) ISBN 0-8155-1445-X.161-182.

[28] G. Revankar, ASM Metals Handbook Vol 8. ASM International. Handbook Committee. ASM International Materials Park, OH 44073-0002 (2000) ISBN 0-87170-389-0 416-564.

[29] J.L.Arias, M.B.Mayor, J.Pou, Y.Leng, B.Leon, M.Perez-Amor, Micro and nano-testing of calcium phosphate coatings produced by pulsed laser deposition. Biomaterials **24** (2003) 3403-3408.

[30] S. Oh, C. Daraio, L.Chen, T. R. Pisanic, R.R. Fin˜ ones, S. Jin, Significantly accelerated osteoblast cell growth on aligned TiO_2 nanotubes, Wiley InterScience. DOI: 10.1002/jbm.a.30722.

[31] International centre for Diffraction data 01-1008

Chapter 6

ANODIZATION OF $TiAl_6V_4$ IMPLANT MATERIAL AND STUDY OF PARAMETERS FOR OSSEO INTEGRATION

Ti substrates were anodized to different degrees of anodization and their surface parameters compared for cell adhesion capabilities. The results were cross checked with cell viability studies. It was seen that the dependence of cell adhesion was more on the surface properties like roughness porosities etc compared to the wetabilility of the surfaces.

6.1. Introduction

Titanium and its alloys are the materials of choice for most dental and orthopaedic implants due to its biocompatibility and excellent mechanical properties [1-3].Among the Titanium alloys $TiAl_6V_4$ (Ti) is the most commonly used implant material [1-3]. Bone response and tissue integration with the implant material depends on the physical and chemical properties of the surface. Different surface modification techniques have been developed for increasing the surface properties of (Ti), anodization being one of them [4]. It has been well established that the adhesion of osteoblasts on to an implant surface is by the interaction of cell adhesion protein molecules and these molecules favor surfaces with comparatively lesser wetability, higher roughness and porosities [5-8]. Anodized surfaces exhibit these characteristics but these parameters vary with varying degree of anodization. In this study Ti samples have been acid anodized at different voltages to

varying degree of anodization and the influence of their surface properties and contact angle measurements were studied to assess their protein adhesion characteristics as compared to a control surface as well as an acid etched surface (deoxidized). The results have been counterchecked using a cell viability study of osteoblast cells on the surface by an MTT assay and confocal imaging.

6.2 Experimental

6.2.1 Preparation of substrate

Medical grade Ti disks of 15 mm diameter and 2mm thickness were cleaned ultrasonically in acetone for 20 minutes and later cleaned in 70% ethanol solution and washed with distilled water. The samples were etched in knolls reagent (2ml HF (40%) and 4 ml HNO3 (66%) in 1000 ml of water) and rinsed in distilled water and dried in air. One set of etched sample was used for comparative studies.

6.2.2 Anodization parameters

Ti was anodized in 200 g/L sulfuric acid, 5% trisodium phosphate, and 5% sodium bicarbonate (baking soda) [9,10].The electrolyte was contained in a chemical resistant tank with fume extraction. (Section 2.2 of chapter 2). A D.C. electrical supply with voltage regulation from 2 to 100 volts and sheet lead cathodes were provided. The parts to be treated was immersed in the processing solution and connected as the anode to the electrical D.C. source. The temperature of the bath was maintained in the range of 20- 26°C throughout the duration of treatment. The cell voltage was varied between 50-75 volts and three anodized samples were obtained at 55 volts with yellow surface appearance (sample labelled as yellow), 60 volts with pink surface appearance (sample labelled as pink) and 75 volts with

blue surface appearance (sample labelled as blue) respectively. The time of treatment was 15 minutes for each sample. Immediately after removal from the anodizing bath, parts were washed thoroughly in clean running water, rinsed in clean hot water and allowed to dry.

6.2.3 Cell Culture

Osteosarcoma cell line KHOS-NP (R-970-5) [NCCS] were grown in culture medium of DMEM+10%FBS+1mM NEAA (chapter 5 section 5.2) in a T-25 flask and incubated at 37oC for 2 days in a 5% C02 incubator (Thermo). ~ 5x105cells were plated on to three samples each of anodized, etched and plain polished control samples of Ti in 12 well plates. The culture was incubated for 72 hours at 37^{o}C in 5% CO2 incubator. The samples with attached cells were used for MTT assay and confocal microscopy.

6.3 Results and Discussion

The plots of contact angles against surface nature for the various implant surfaces (as measured by method mentioned in section 2.3 chapter 2) are shown in fig 6.1. As can be seen the contact angle for the anodized sample (blue) at 75 volts is the highest in all fluids, whereas the samples anodized at lower voltages (pink and yellow) have lesser or comparable contact angles to that of the control sample as as well as the etched (deoxidized) sample. The plot of surface roughness and surface thickness [11] of the samples (as measured by method mentioned in section 2.3 of chapter 2) are shown in fig 6.2 and fig 6.3. It is seen that the surface roughness and thickness varies almost linearly with the degree of anodization.

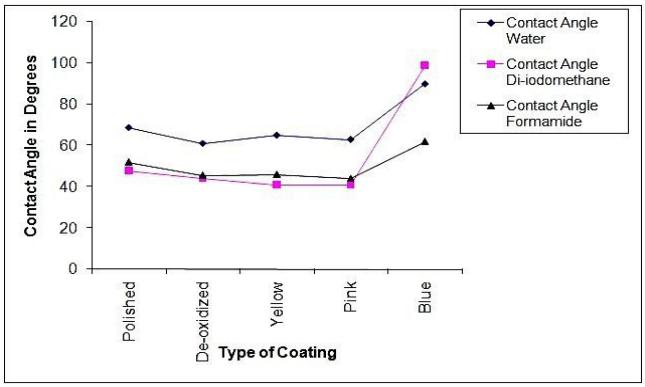

Fig 6.1 Plot of contact angles of the various samples in different mediums.

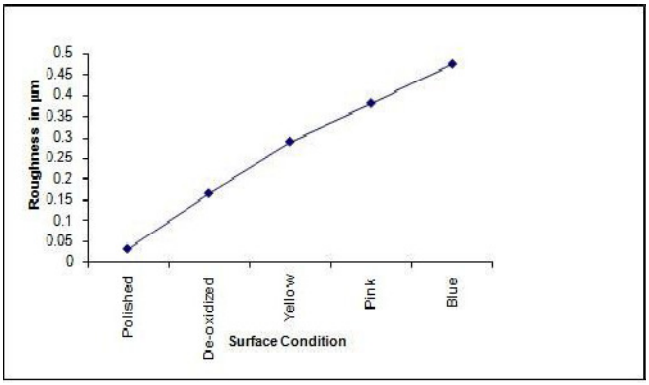

Fig 6.2 Plot of average surface roughness of the various samples

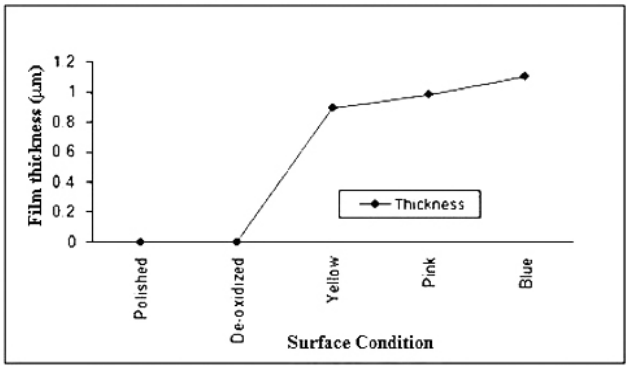

Fig 6.3 Plot of anodized surface thickness of various samples

The anodized oxide layer thickness also increases linearly with the anodization voltages. The scanning electron micrographs (as measured by method mentioned in section 2.3 of chapter 2) of the various surfaces are shown in fig 6.4.The sample anodized at the highest voltage of 75 volts exhibit highest microporosities and surface asperities followed by the ones anodized at lower voltages. Etched sample (deoxidized) shows distinct etch line topography.

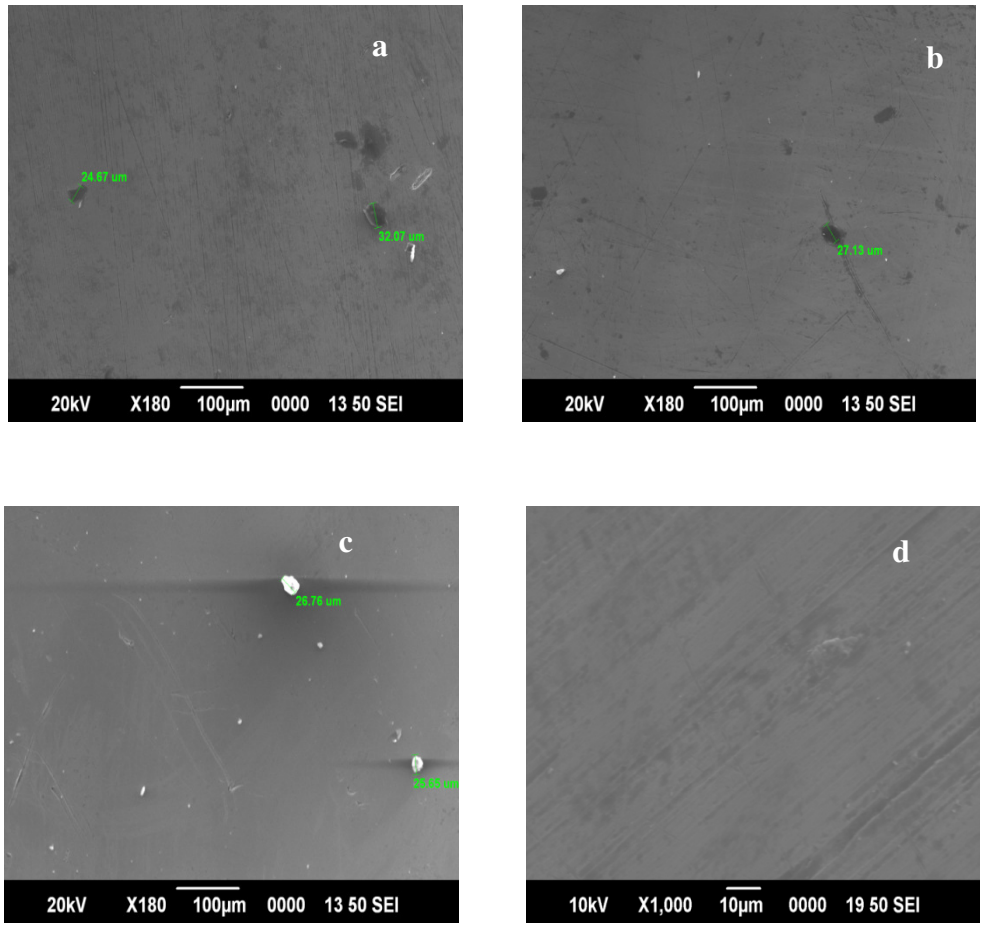

Fig 6.4 SEM micrographs of anodized and etched samples a). Ti anodized at 75 volts, b).Ti anodized at 60 volts, c).Ti anodized at 55 volts, d).HF etched Ti.

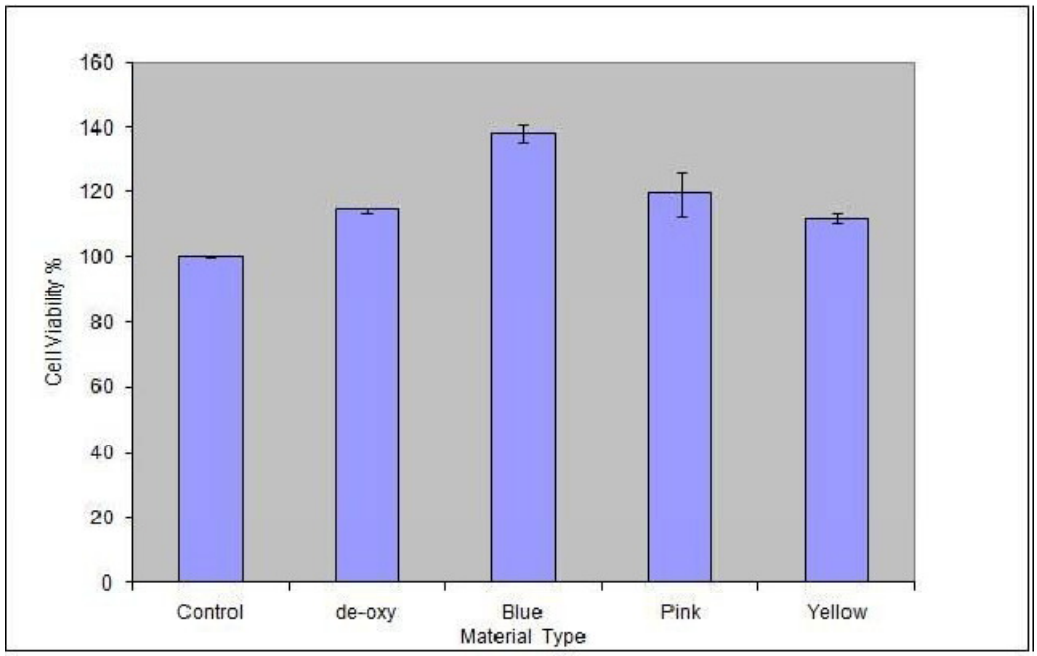

Fig 6.5 Optical variance analysis plot to assess the cell viability of the samples

Variance analysis plot for the different samples subjected to MTT assay (as mentioned in section 4.1 of chapter 4) is shown in fig 6.5. It is seen that the sample anodized at highest voltage of 75 volts (blue) exhibits maximum cell viability followed by the sample anodized at lower voltages (pink and yellow) and the etched (deoxidized) and control sample.

The confocal images of the adhered nucleus to the various samples are shown in fig 6.6.

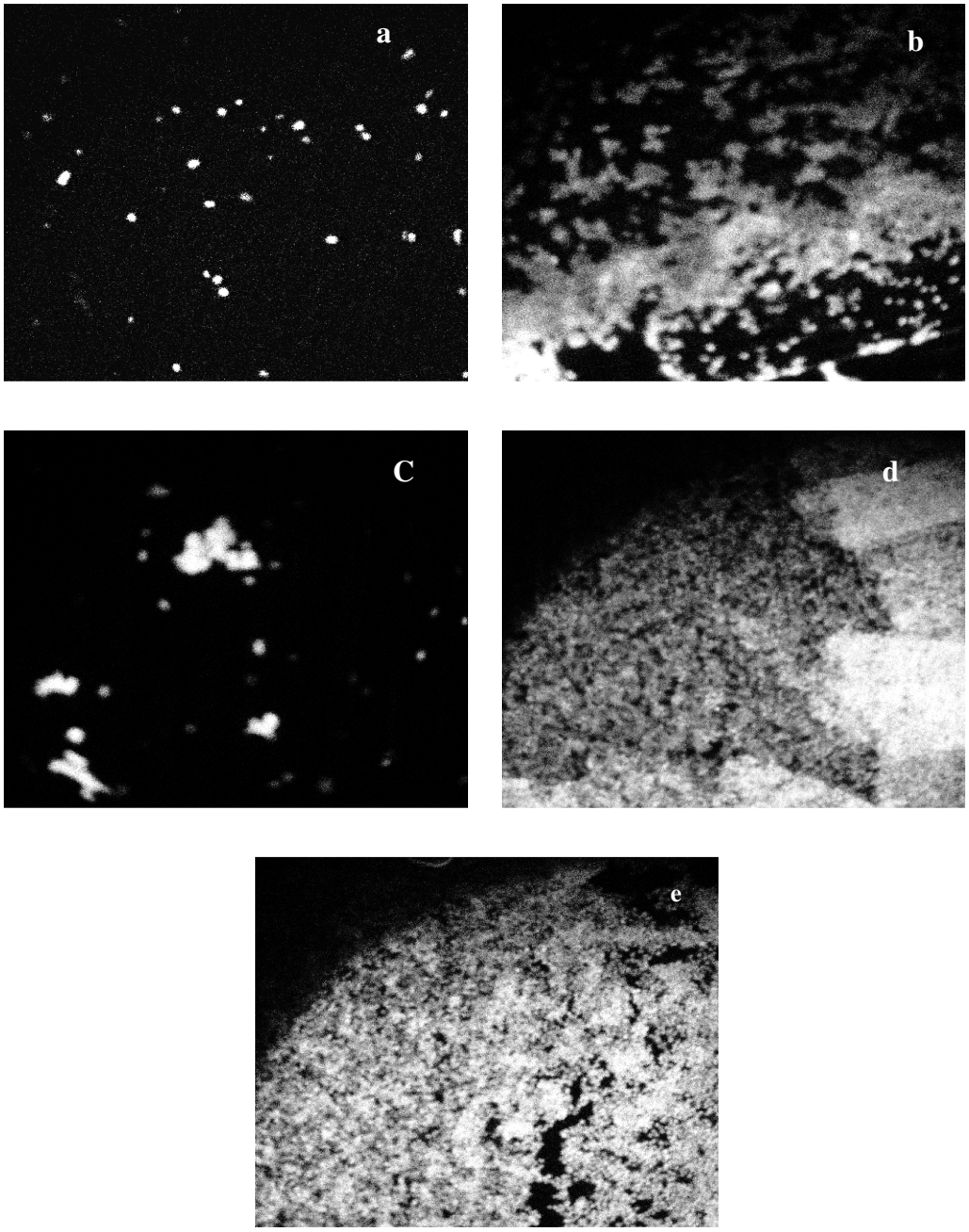

Fig 6.9-6.13 Confocal Visualization of nuclear density on various samples.a) Control TiAl6V4 b) Etched Sample c) Anodized at 55V (Yellow), d) Anodized at 60 V(Pink),e) Anodized at 75 V(Blue).

The nuclear density as shown by the white patches is maximum for the blue sample and decreases for the pink and yellow samples. The etched sample showed nuclear density just lower than the pink sample. The nucleus density confirms the maximum cell adhesion characteristics of the sample anodized at 75 V followed by the sample anodized at lower voltages and comparable nuclear density for the etched sample to that of the pink sample. The cell viability of the control sample is found to be the lowest.

As made clear in previous studies, adhesion of cells on to substrates occur through adhesion molecules which are proteins [5-6] .These proteins favour adhesion to hydrophobic, rough and porous surfaces. Since the Ti surface anodized at 75 V (blue) exhibits highest hydrophobic nature, surface roughness and maximum porosities, it presents the ideal condition for cell adhesion and is established in the cell viability study. However even though the wettability of the other anodized (pink and yellow) and etched samples are only comparable or even less than that of the plain polished control sample they exhibited higher cell adhesion than the control sample. This can be attributed to the higher roughness and porous natures of these samples in relation with the control sample. Hence even though the adhesion protein molecules which determine the adhesion characteristics of cells on to an implant surface is known to favour a hydrophobic surface, the other surface conditions like roughness, micro-porosities, thickness are seen to override the dependence of cell adhesion on hydrophobicity of an anodized implant surface.

6.4 Conclusion:

Ti substrates were anodized to varying degrees and their surface parameters for cell protein adhesion like wettability, roughness, micro-porosity and thickness were studied and the influence of wettability on cell adhesion was

compared with the other surface parameters thro a MTT assay and confocal imaging of adhered nuclear density. An anodized surface which has the highest hydrophobic nature also exhibited maximum roughness and porosity and was seen to exhibit the highest cell adhesion characteristics. However other anodized surfaces which exhibited lesser hydrophobic nature than the control Ti surface also exhibited good cell adhesion. This shows the dependence of cell adhesion more on the surface parameters like roughness, micro porosities and thickness within this range than on the wetability of the surface. This factor can be considered for selection of anodized implant material for orthopaedic use.

References:

[1] C.F.Koch, S.Johnson, D.Kumar, M.Jelinik, D.B.Chrisey, A.Doraiswamy, C. Jin, R.J.Narayan, I.N.Mihailescu, Pulsed Laser Deposition of Hydroxyapatite thin films. Materials Science & Engineering **C 27** (2007) 484-494.

[2] A. Bigi, E. Boanini, B. Bracci, A.Facchini, S Panzavolta, F. Segatti, L. Sturba, Nanocrystalline hydroxyapatite coatings on titanium: a new fast biomimetic method.. Biomaterials **26** (2005) 4085-4089.

[3] C.K.Wang, J.H.Chern Lin, C.P. Ju, H.C. Ong and R.P.H.Chang, Structural characterization of pulsed laser deposited hydroxyapatite film on titanium substrate. Biomaterials **18** (1997) 1331-1336.

[4] H.Oh, J.Lee, Y. Jeong, Y. Kim,C. Chi, Microstructural characterization of biomedical titanium oxide fabricated by electrochemical method. Surface and Coatings Technology **198** (2005) 247-252.

[5] G.Legeay and F.Poncin-Epaillard Surface Engineering by coating of Hydrophilic Layers, Bioadhesion and Biocontamination. Adhesion – current research and application, Wiley-VCH GmbH & Co KGaA, Weinheim (2005) ISBN: 3-527-31263-3,175-188.

[6] K.Kendall, Molecular Adhesion and its Applications Kluwer Academic Publishers, New York, (2004) ISBN 0-306-46520-5,275-301 41-183.

[7] S.R.Sousa, M.A.Barbosa, Effect of Hydroxyapatite Thickness on Metal Ion Release from Ti6Al4V Substrates .Biomaterials **17** (1996) 397-404

[8] D. D. Deligianni, N. D.Katsala, P. G. Koutsoukos , Y. F. Missirlis,Effect of Surface Roughness of Hydroxyapatite on Human Bone Marrow Cell

Adhesion, Proliferation, Differentiation and Detachment. Biomaterials **22** (2001) 87-96.

[9] J.Cl.Puippe, Surface Treatments of Titanium implants. European Cells and Materials **5/1** (2003) 32-33.

[10] X. Liua,, P. K. Chub, C. Dinga, Surface modification of titanium, titanium alloys,and related materials for biomedical applications Materials Science and Engineering **R 47** (2004) 49–121 .

[11] P.S Vanzillotta, G.A.Soares, I.N.Bastos, R.A.Simao, N.K.Kuromoto, Potentialities of some surface characterization techniques for the development of titanium biomedical alloys. Materials Research, 7/3 (2004) 437-444.

[12] D E Pacham, Handbook of Adhesion. John Wiley and Sons Ltd, West susex, England. (2000) ISBN -13 978-0-471-80874-9 79-85.

[13] A.A. Thorpe, T. G.Nevell, S. A.Young, J. Tsibouklis, Surface Energy characteristics of poly (methylpropenoxyfluoroalkylsiloxane) film structures. Applied surface science **136** (1998) 99-104.

[14] S.Oh, C.Daraio, L.Chen, T.R. Pisanic, R. R. Fin˜ ones, S. Jin, Significantly accelerated osteoblast cell growth on aligned TiO2 nanotubes, Wiley InterScience. DOI: 10.1002/jbm.a.30722

[15] J.Y. Suh, B. Jang, X. Zhu, J.L.Ong, K. Kim, Effect of hydrothermally treated anodic oxide films on osteoblast attachment and proliferation. Biomaterials **24** (2003) 347-355.

Chapter 7

COMPARISON OF SURFACE PARAMETERS OF SURFACE MODIFIED $TiAl_6V_4$ IMPLANT SURFACES FOR SUITABILITY OF PROTEIN ADHESION AND THEIR IN-VITRO CELL VIABILITY STUDIES

The various surface parameters of $TiAl_6V_4$ surfaces modified by chemical etchng, anodizing and deposition of hydoxyapatite has been compared for their suitability for cell adhesion. Cell viability studies on the various surfaces were also conducted on these surfaces. Hydroxyapatite coated surfaces showed very good characteristics for cell adhesion followed by anodized and etched surfaces.

7.1 Introduction

Biocompatibility of orthopaedic implants depends on the ability of surface tissues to bond directly on to the implant material. Cellular attachment is dependent on many parameters including surface roughness, wetability, film thickness and other surface properties. It has been established that the adhesion of cells on to the surfaces of orthopedic implants depends on the ability of the surfaces to accommodate protein molecules. Protein adhesions are found to be effective in cases of higher surface roughness, macro porosity and hydrophobic nature of implant materials [1-5].

Various surface alteration techniques have been applied to Ti to make it more biocompatible. Studies have been made on the adhesion characteristics of

modified Ti implants based on their surface properties like roughness, film thickness, porosity etc [6-8].Work on the wetability nature of modified surfaces to predict cell adhesion are still in progress. It has been established that theoretically molecular proteins favour a more hydrophobic surface in relation to other surface properties [9].A comparison of various surface parameters and cell viability tests have been made to assess the biocompatibility of hydroxyapatite coated surfaces in relation to the anodized and etched surfaces .

7.2 Experimental

Pulsed Laser deposition Thin films of hydroxyapatite prepared by the wet method [10] were deposited on to a $TiAl_6V_4$ (Ti) **[11-17]** substrate at by pulsed laser deposition under oxygen atmosphere at a substrate temperature of 200^0C and hydrothermally annealed in a sealed hydrothermal parr bomb (100 ml) for two hours at a temperature of 100^0 C.(Refer chapter2)

Anodzation $TiAl_6V_4$ substrates were anodized in 200 g/L sulfuric acid, 5% trisodium phosphate, and 5% sodium bicarbonate (baking soda) for 15 minutes and three anodized samples were obtained at 55 volts with yellow surface appearance (sample labelled as yellow), 60 volts with pink surface appearance (sample labelled as pink) and 75 volts with blue surface appearance (sample labelled as blue) respectively[18] Refer chapter 2).

7.3 Results and Discussion:

The surfaces were characterized and subjected to biological tests as mentioned in section 2.3 of chapter 2 and section 4.1 of chapter 4 [19, 20, 21].The measurements of average surface roughness, film Thickness and contact angle of the various surface modified Ti substrates are shown in table 7.1.The Average surface roughness of the anodized film varied from 0.29 μm for the yellow sample to 0.474 μm for the blue sample. The surface roughness

for HA coated film was the highest at 0.68 μm compared to 0.032 μm for the control Ti. The thickness of the anodized films coated at 50-75 volts varied as 0.89, 0.98 and 1.1μm.

Table 7.1: Contact angle and roughness measurements of surface modified Ti samples and control sample

Material labeled as	Treatment	Roughness μm	Thickness μm	Contact angle in water in degrees	Contact angle in Di-iodomethane in degrees	Contact angle in Formamide in degrees	Surface Material
Blue	Anodized 75v	0.474	1.1	90	99	60	Titanium dioxide TiO_2
Pink	Anodized 60 v	0.38	0.98	63	41	45.6	TiO_2
Yellow	Anodized 55 v	0.29	0.89	65	41	46	TiO_2
Polished	Plain polished	0.032	NA	68.8	48	61	TiO_2
HA Coated	PLD Coated	0.68	4	85	71.5	70	Hydroxyapatite $Ca_{10}(PO_4)_6(OH)_2$

The contact angle in water and Di-iodomethane was the highest for the sample anodized at a voltage of 75 volts whereas for that in formamide the contact angle was maximum for HA coated sample. In all cases the sample coated with HA was either having the highest contact angle or the next best of all the samples. Since formamide has a ph value almost close to that of blood (7.3), the contact angle measured in formamide can be safely assumed to be the nature that the sample will be exhibiting with blood. In previous studies, mechanism of cell adhesion is seen to be due to the adhesion of protein molecules present on the surface of the cells known as adhesion molecules [1-6]. A larger contact angle theoretically increases the protein adhesion chances by exposing surfaces with lesser wetting. The adhesion nature is depicted in fig 7.1 wherein protein molecules are seen to get direct adhesion sites on the surface compared to a more hydrophilic surface. Protein adhesion molecules

from the extra cellular matrix (ECM) will get increased chances of adhesion to a HA coated surface and act as a ligand site for binding of cell adhesion molecules present the osteoblasts thereby enhancing osseointegration.

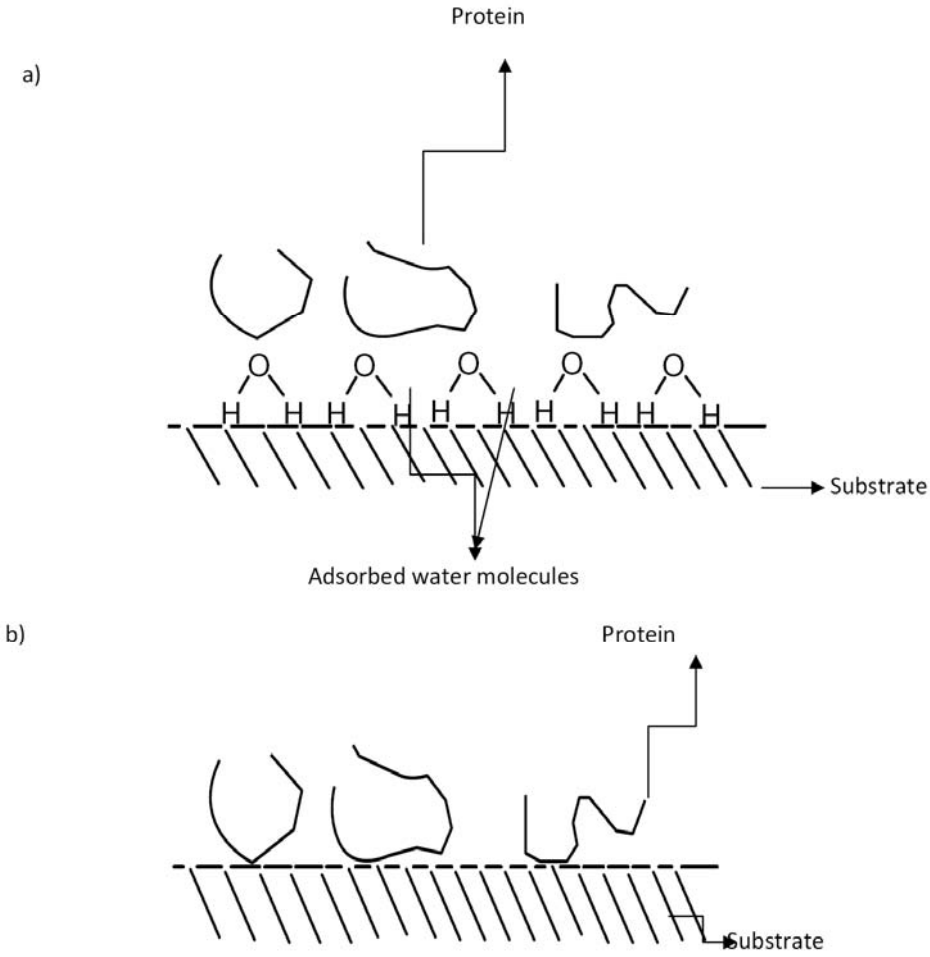

Fig 7.1 Depiction of adhesion characteristics of protein molecules on to a hydrophobic and hydrophilic substrate. a) Protein adhesion hindered by adsorbed water molecules on a Hydrophilic substrate b) Direct contact of protein molecules on a hydrophobic substrate.

Since higher roughness within a range of 0.22-0.78 increases cell adhesion [7], HA coated Ti samples will show a better cell adhesion characteristic compared to other surface modified Ti samples. The blue Ti also shows a higher roughness and contact angle compared to other Ti samples. The contact angle of control Ti is higher than that of the yellow and pink samples but the roughness values of the anodized surfaces are much higher and also they exhibit micro porosity which will aid in cell adhesion by mechanical interlocking.

The plot of contact angles in different medium and roughness for different samples are shown in fig 7.2.The marked groupings shows HA with the highest number of scores within a sample space of roughness greater than 0.5 μm and contact angle in formamide and water respectively being greater than or equal to 70 degrees and 80 degrees respectively. The blue anodized sample exhibited comparable groupings to the HA coated sample. The pink and yellow samples did not have scores in this region, this is more so due to its higher wettabilty nature even though the roughness is close to this range.

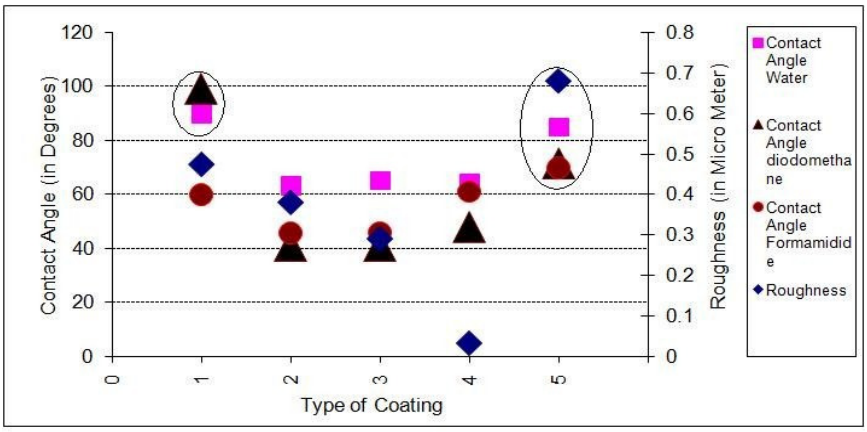

Fig 7.2 Plot of contact angles and roughness for different surface modified Ti samples 1. Ti anodized at 75 volts (Blue), 2. Ti anodized at 60 volts (Pink), 3. Ti anodized at 55 volts (Yellow), 4. Ti Plain Polished (control), 5. Ti HA coated

The cell viability plots based on the analysis of optical variance method after MTT assay is shown in fig 7.3. The maximum cell viability percentage is shown by the HA coated Ti. The blue anodized sample exhibits comparable cell viability. The cell viability of the pink and yellow sample is seen to be much greater than the control Ti.

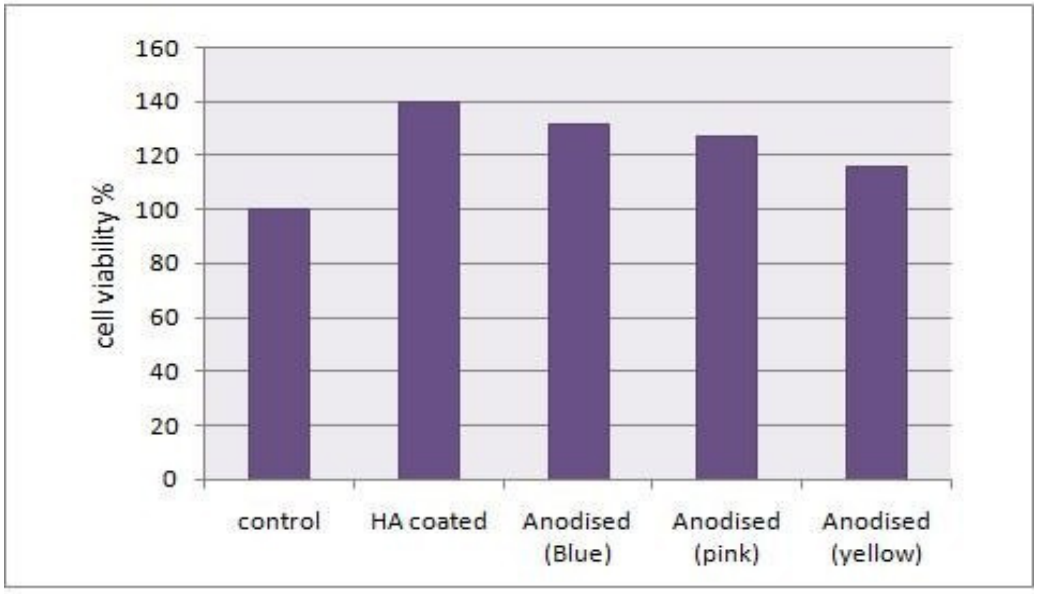

Fig 7.3 Cell viability by the optical variance method

The nuclear visualization thro confocal imaging of all the samples are shown in figs 7.4.The HA coated sample shows highest nuclear density shown by the number of spots followed by the blue, pink and yellow samples. The control Ti shows the least nuclear visibility. This shows that the HA coated Ti which returned all physical attributes required for protein adhesion is giving the highest cell viability perecentage in the cell viability tests. However the blue anodized sample also returned comparable physical properties required for protein adhesion and gives a comparable cell viability result to the HA sample. Even though the contact angle measurements of the pink and yellow sample is only comparable to the control Ti sample they returned a much higher cell viability result than the control Ti. The other

physical properties of roughness and microporosities of the yellow and pink surfaces play an important role in this result compared to the wettability of the surfaces.

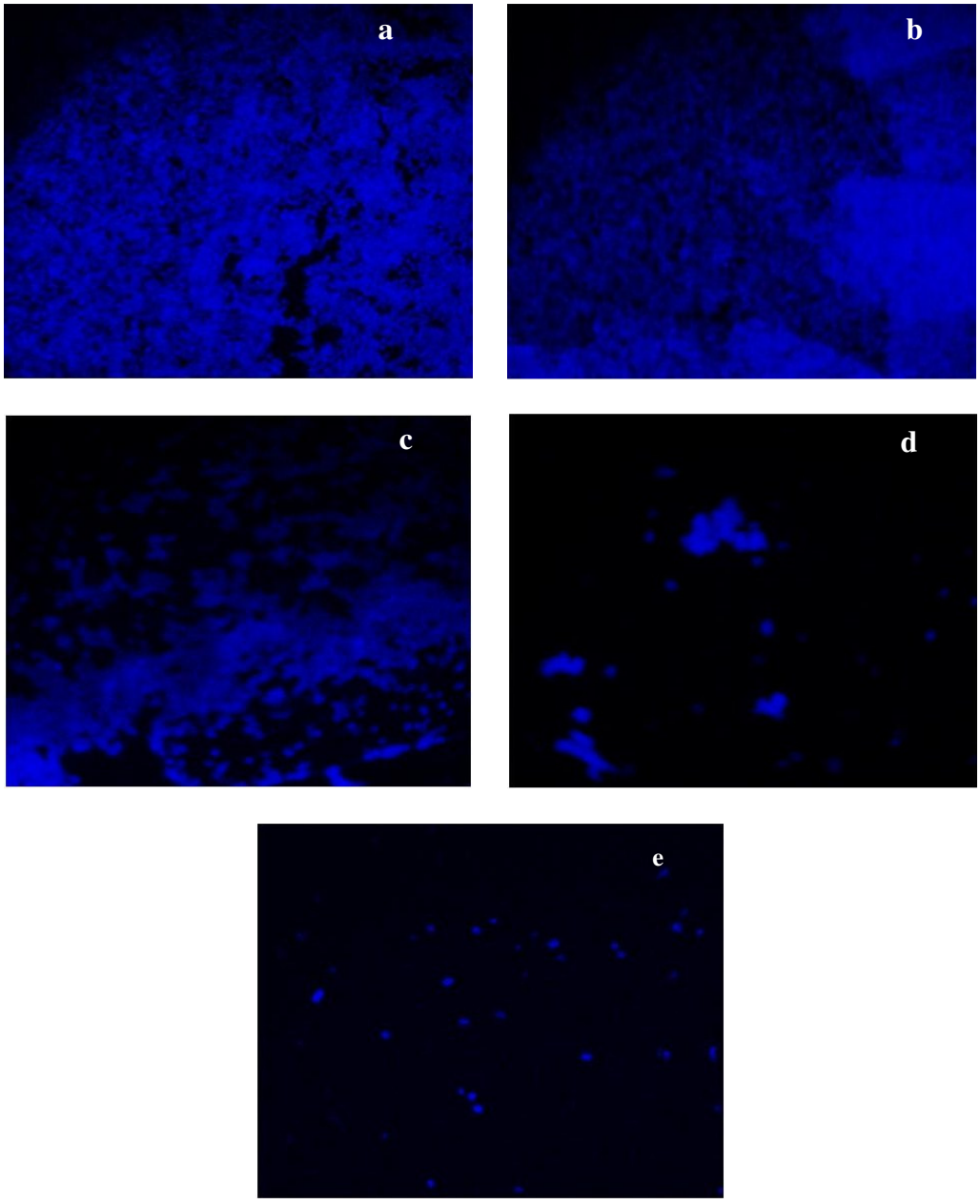

Fig 7.4 Confocal images of nuclear visualization a) HA Coated, b) Blue, 6) Pink, c) Yellow, d) Control Ti

7.4. Conclusion:

Ti surfaces coated with Pulsed laser deposited HA shows better surface properties like roughness and more hydrophobicity required for protein adhesion compared to anodized Ti samples and will give good osseointegration. This is confirmed by the in-vitro cell viability analysis. However the anodized blue surface also exhibited comparable surface properties to HA coated implants and showed good cell viability in the in-vitro studies. The other anodized pink and yellow surfaces also showed appreciable cell viability in comaparison with control Ti surfaces even though their wetability was on the higher side. This shows that surfaces anodized to the correct level can return comparable osseointegration to HA coated surfaces. The surface roughness and microporosities of the anodized surfaces plays a greater role in the cell adhesion compared to wetability. Further in vitro studies are required to assess the actual cell adhesion parameters of the modified implants.

References:

[1] C. M.Isacke, M. A.Horton. The adhesion Molecule, Facts book, Academic Press London (2000) ISBN 0-12-356505-7. 2-307.

[2] J. .B.Park, J. D Bronzino, Biomaterials Principles and Applications, CRC Press USA ISBN 0-8493-1491-7 117-141.

[3] D.E.Pacham, Handbook of Adhesion second edition, John Wiley and Sons,Ltd England (2005) ISBN 0-471-80874-1(HB) 1-112.

[4] K. Kendall, Molecular Adhesion and its Applications, Kluwer academic publications New York (2004) ISBN 0-306-46520-5 41-183.

[5] M. J .Parnham, Adhesion Molecules Functions and Inhibitions, Birkhauser Verlag Berlin (2007) ISBN 978-3-7643-7974-2 2-27.

[6] J. Suh, B.Vheol Jang, X. Zhu, J. L.Ong, K. Kim, Effect of hydrothermally treated anodic oxide films on osteoblast attachment and proliferation. Biomaterials **24** (2003) 347-355.

[7] D. D Deligianni, N. D Katasala, P. G Koutsoukos, Y. F Misirlis, Effect of surface roughness of hydroxyapatite on human bone marrow cell adhesion, proliferation, delamination and detachment strength. Biomaterials **22** (2001) 87-96.

[8] Y. Sul, C. B Johansson, K. Roser, T. Albrektsson, Qualitative and quantitative observations of bone tissue reactions to anodized implants. Biomaterials **23** (2002) 1809-1817.

[9] G.Legeay, F.Poncin-Epaillard, Surface Engineering by Coating of Hydrophilic Layers. Adhesion Current Research and Applications

.Wiley VCH Verlag Gmbh & Co KGaA Germany (2005).ISBN 3-527-31263-3 175-185.

[10] Hideki Aoki, Medical Applications of Hydroxyapatite, Takayama Press, 1994.

[11] A.Bigi,B.Bracci,F.Cuisinier,R.Elkaim,M.Fini,I.Mayer,I.N.Mihailescu ,G.Socol,L.Sturba,P.Torricelli, Human Osteoblast response to pulsed laser deposited calcium phosphate coatings. Biomaterials **26** (2005) 2381-2389.

[12] Q. Bao, C. Chen, D. Wang, Q. Ji, T. Lei, Pulsed laser deposition and its current research status in preparing hydroxyapaptite thin films. Applied Surface Science **252** (2005) 1538-1544.

[13] Y.Suda, H.Kawasaki, T.Ohshima, S. Nakashima, S. Kawazoe, T. Toma, Hydroxyapatite coatings on titanium dioxide thin films prepared by pulsed laser deposition method Thin Solid Films **506-507** (2006) 1115-119.

[14] J.M.Fernandez-Pradas, L.Cleries, E.Martinez, G.Sardin, J.Esteve, J.L.Morenza, Influence of thickness on the properties of hydroxyapatite coatings deposited by KrF laser ablation. Biomaterials **22** (2001) 2171-2175.

[15] W. Lee, S. Lee, H. Kim, D. Kim, Characteristics of calcium phosphate films prepared by pulsed laser deposition under various vapor pressures. Journal of the Korean Physical Society 47 (2005) 152-156.

[16] W.Mroz, M.Jedynski, J.Hoffman, M.Jelinek, B.Major, A.Prokopiuk, Z.Szymanski, Effect of reactive atmosphere on pulsed laser deposition of hydroxyapatite thin films. Journal of Physics. Conference Series **59** (2007) 720-723.

[17] S Bharathi, M K Sinha, D Basu, Hydroxyapatite coating by biomimetic method on titanium alloy using concentrated SBF Bull. Mater. Sci **28/ 6** (2005) 617–621.

[18] John A Disegi, Anodizing Treatments for Ttanium Implants .DOI-7803-3867-3/97 10.00 1997 IEEE.

[19] N. M. Jennett, R. Jacobs and J. Meneve, Advances in adhesion measurement good practice: Use of a certified reference material for evaluating the performance of scratch test Adhesion Aspects of Thin Films **2** VSP Netherlands (2005) 179-203.

[20] A.A. Thorpe, T. G. Nevell, S.A. Young, John Tsibouklis, Surface energy characteristics of poly_methylpropenoxyfluoroalkylsiloxane/ film structures. Applied Surface Science **136** (1998). 99–104.

[21] K.Bordji, J.Y.Jouzeau, D.Mainard, E.Payan, P.netter, K.T.Rie, T.Stucky, M.Hage-Ali, Cytocompatibility of Ti-6Al-4V and Ti-5Al-2.5Fe alloys according to three surface treatments, using human fibroblasts and osteoblasts. Bioamaterials **17** (1996)929-940.

Chapter 8

MOLECULAR LEVEL ANALYSIS OF ADHESION MECHANISM OF PROTEINS ON CALCIUM BINDING SITES OF HA USING QUANTUM MECHANICAL CALCULATIONS

Spartan 02, a molecular dynamics software, is used to analyze the bonding parameters of proteins from the extra cellular matrix on to a hydroxyapatite coated $TiAl_6V_4$ implant surface on the basis of their polarity (net electrostatic charge, Qr) and the energies of the molecular orbitals E_HOMO (energy of thehighest occupied molecular orbital), and E_LUMO (energy of the lowest unoccupied molecular orbital.

8.1 Quantum Chemical Calculations

Quantum chemical calculations use quantum mechanics to study and predict the chemical properties and behavior of molecules. Quantum mechanics describes molecules in terms of interactions among nuclei and electrons, and molecular geometry in terms of minimum energy arrangements of the nuclei. All quantum chemical calculations ultimately trace back to the time-independent Schrödinger wave equation (eqn 8.1), which can be generalized as a multi nuclear, multi electron system [12-14].

$$\hat{H}y = Ey \quad \text{.....} 8.1$$

Here E is the electronic energy in atomic units, y is a many electron wave function and $\hat{H}$ is the Hamiltonian operator, which in atomic units is given by

$$\hat{H} = -\frac{1}{2}\sum_{i}^{electons}\nabla_i^2 - \frac{1}{2}\sum_{i}^{nuclei}\frac{1}{M_A}\nabla_A^2 - \sum_{i}^{electrons}\sum_{A}^{nuclei}\frac{Z_A}{r_{iA}} + \sum_{i<j}^{electons}\frac{1}{r_{ij}} + \sum_{A<B}^{nuclei}\frac{Z_A Z_B}{R_{AB}} \quad \text{.....8.2}$$

Z is the nuclear charge, M_A is the ratio of the mass of nucleus A to the mass of an electron. R_{AB} is the distance between the nuclei A and B, r_{ij} is the distance between electrons i and j and r_{iA} is the distance between electrons i and nucleus A.

The many-electron Schrödinger equation cannot be solved exactly and hence approximations need to be introduced. One way to simplify Schrödinger equation is to assume that the nuclei do not move. This is called Born-Oppenheimer approximation, and leads to "electronic" Schrödinger equation(eqn 8.3)

$$\hat{H}^{el}y^{el} = E^{el}y^{el} \quad \text{.....8.3}$$

Hamiltonian for the "electronic" wave equation is given by (eqn 8.4)

$$\hat{H}^{el} = -\frac{1}{2}\sum_{i}^{electons}\nabla_i^2 - \sum_{i}^{electrons}\sum_{A}^{nuclei}\frac{Z_A}{r_{iA}} + \sum_{i<j}^{electons}\sum\frac{1}{r_{ij}} \quad \text{.....8.4}$$

The Hartree- Fock and semi empirical techniques used in this study are approximate methods to solve "electronic" wave equation. Equation 8.3 is a typical eigen value problem, the solution of which yields multi electron eigen functions (ψ^{el}) and the corresponding energy levels (E^{el}).

The Hartree- Fock method is also described as an *ab initio* ("from the beginning") method. In this method the many electron wave function (ψ^{el}) is expressed as a function of molecular orbitals (ψ_i). Molecular orbitals are expressed as linear combinations of a finite set (a basis set) of prescribed functions known as basis functions as shown in Eq. 8.5.

$$\psi_i = \sum_m c_{mi}\phi_m \quad \text{.....8.5}$$

c_m are unknown coefficients determined iteratively in Hartree- Fock procedure.

The set of molecular orbitals leading to lowest energy are obtained by a process referred to as "Self- consistent- field" or SCF procedure [12]. In the present study 6-31G, a basis set consisting of six Gaussian type basis functions, was used for calculations.

Semi empirical methods are simplified versions of Hartree-Fock theory using empirical (derived from experimental data) corrections in order to improve performance [12]. In the present study, the semi-empirical

method is used. The quantum chemical descriptors used in the present study are

Qr: Net electrostatic charge- Atomic charges chosen to best match the electrostatic potential at points surrounding a molecule, subject to overall charge balance [12, 13]

E_HOMO: Energy of the Highest Occupied Molecular Orbital. E_HOMO represents the energy of the least tightly held electrons in the molecule.

E_LUMO: Energy of the Lowest Unoccupied Molecular Orbital. LUMO describes the easiest root to the addition of more electrons to the system.

FMO (Frontier Molecular Orbital): Highest occupied molecular orbital (HOMO) and lowest unoccupied molecular orbital (LUMO) are the frontier orbitals.

In this study the electrostatic attraction and the tendency of adhesion of protein molecules on to a HA coated surface due to HOMO–LUMO interactions of calcium binding sites are done in a qualitative manner using the popular quantum chemical descriptors namely Qr. - net electrostatic charge and ΔE- orbital energy gap between HOMO and LUMO. The abundance of positive calcium binding sites to electron deficient sites of the protein molecules presents a strong case for adhesion of these cell adhesion ligands on to the HA coated surface compared to a normal Ti surface[5-15]. The proteins strand of fibronectin with the Argine-Glycine-Asparitic acid (RGD) [15-20] highlighted is chosen for this study.

8.2 Molecular modelling

Different molecular modelling packages use different molecular data input which includes both textual type data input and graphical data input. Spartan 02, the molecular modelling package used in this study, has a powerful graphical user interface for model building. Protein molecules are built from *sp*2 and *sp*3 hybridized carbon and oxygen atoms and hydrogen atoms. The atoms can be selected from the model kit available with the package and placed on the work area. Bonds can be formed by clicking on the appropriate free valences of the atoms which are already placed on the work area. The Calcium and Phosphorous atoms can be modelled by selecting atoms with appropriate free valences from the model kit. Calculation options can be set up by selecting "Calculations" from the"Setup" menu. Calculations can be performed for "Equilibrium Geometry" using the "Hartree-Fock" or "Semi-Empirical" method using basis sets such as "6-31G*" or "PM3" by making appropriate selections in the dialogue box. The orbital's _like HOMO and LUMO_, their energies, and atomic charges can be obtained by checking the appropriate boxes in the dialogue box. Calculations can be started by clicking the "Submit" button on the dialogue box. Output can be obtained by selecting the appropriate display functions. Molecular modelling of hydroxyapatite and the RGD strand of fibronectin has been made using the semi-empirical calculations and their frontier orbital's compared for favourable bonding characteristics.

8.3 Results and Discussion

Hydroxyapatite molecule has been modelled by selecting the atoms with the appropriate valences from the tool kit. The modelled molecule is shown in fig 8.1.

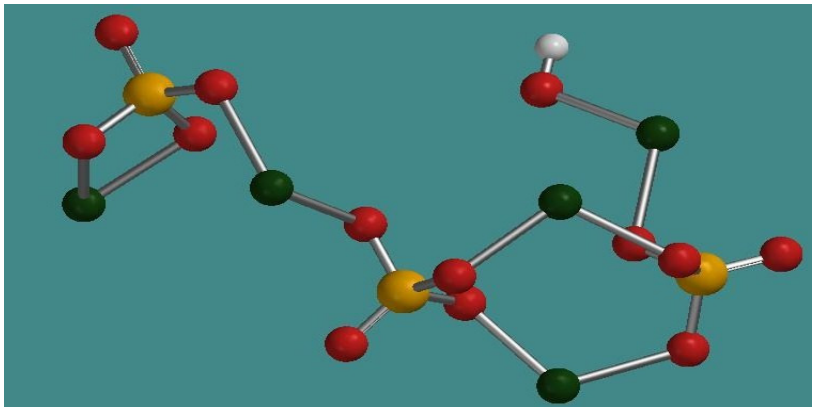

Fig 8.1 Hydroxyapatite molecule –Yellow-Phosphorous, Green-Calcium, Red- Oxygen and White –Hydrogen

Figure 8.2 shows the Argenine-Glycine-Aspartic acid strand of the protein fibronectin from the extracellular matrix

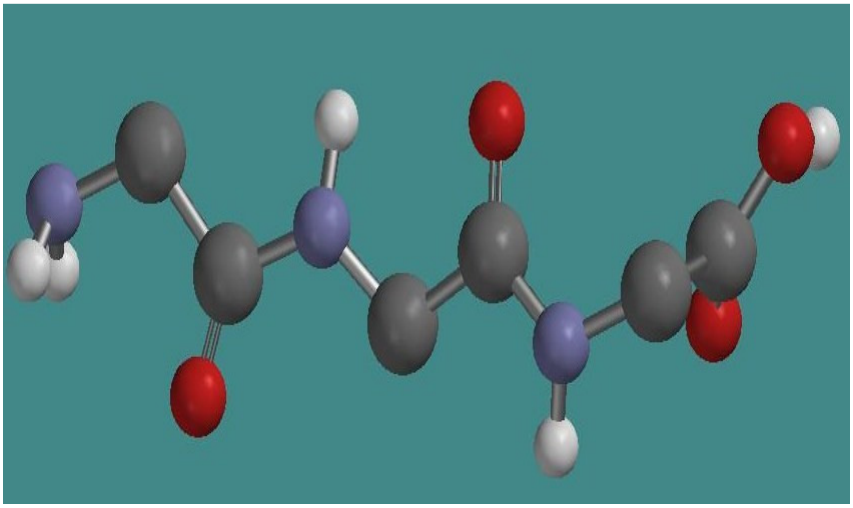

Fig 8.2 Modelled RGD strand –Grey-Carbon atoms, Blue-Nitrogen, Red-Oxygen and White-Hydrogen atoms.

The charge density of the hydroxyapatite molecule was calculated and visualized using the package and the same is shown in figure 8.3.The blue areas indicate net positive charge and the red areas indicate net negative charge. It is seen that in various orientations the net positive charge was carried near the

calcium atoms in the molecule and provided a case for electron deficient areas which can readily accept electrons from electron rich sites.

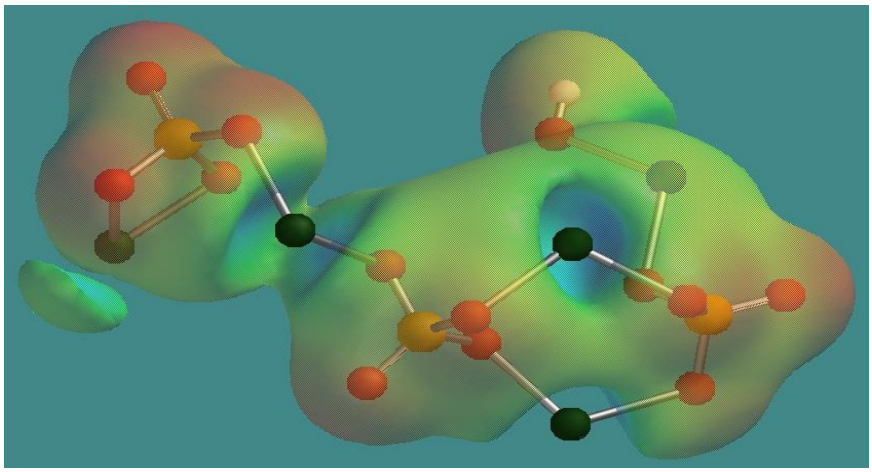

Fig 8.3 Charge density of hydroxyapatite molecule clearly showing the electron deficient calcium sites

Similarly the charge density of the RGD strand was visualised and same is depicted in fig 8.4.It is seen that the oxygen sites returned a net negative charge in the molecule and will readily associate with electron deficient sites of other molecules of conducive nature.

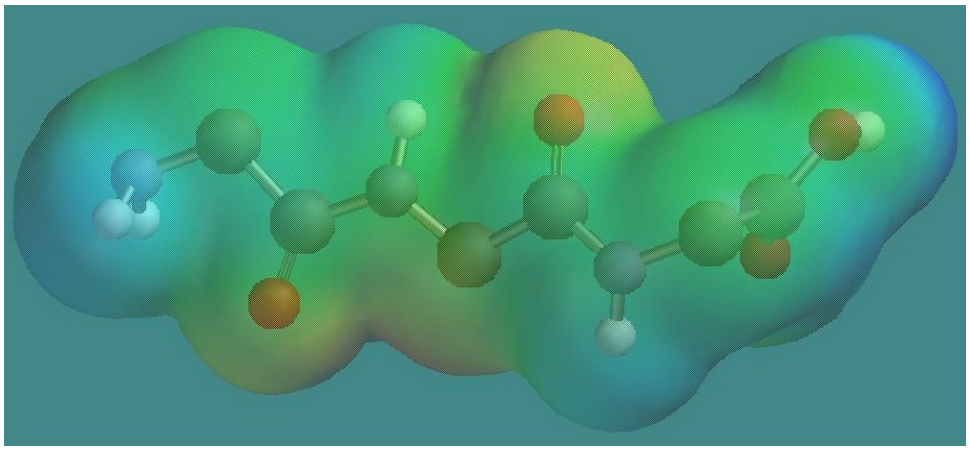

Fig 8.4 Charge density of RGD strand showing electron rich areas near the oxygen atoms.

The Lowest unoccupied molecular orbital LUMO for Hydroxyapatite and the Highest occupied molecular orbital HOMO for RGD strand were modelled and the same is shown in Figures 8.5 and 8.6. It can be seen that unoccupied orbital states existed near the calcium atoms of hydroxyapatite and occupied states existed at the oxygen sites of the RGD strand and according to the molecular orbital theory this presents a strong case for a HOMO-LUMO interaction to proceed and a satisfactory condition to exist for RGD containing proteins to adhere to Hydroxyapatite .

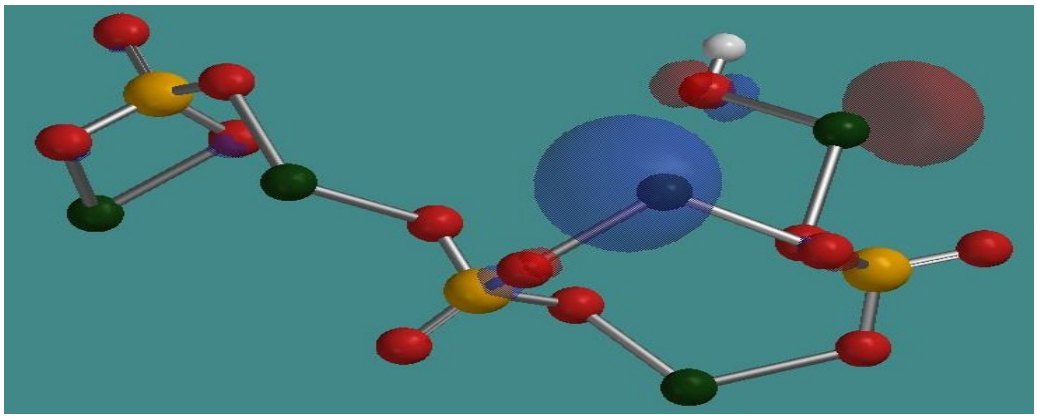

Fig 8.5 LUMO simulation of hydroxyapatite showing the LUMO near to calcium sites

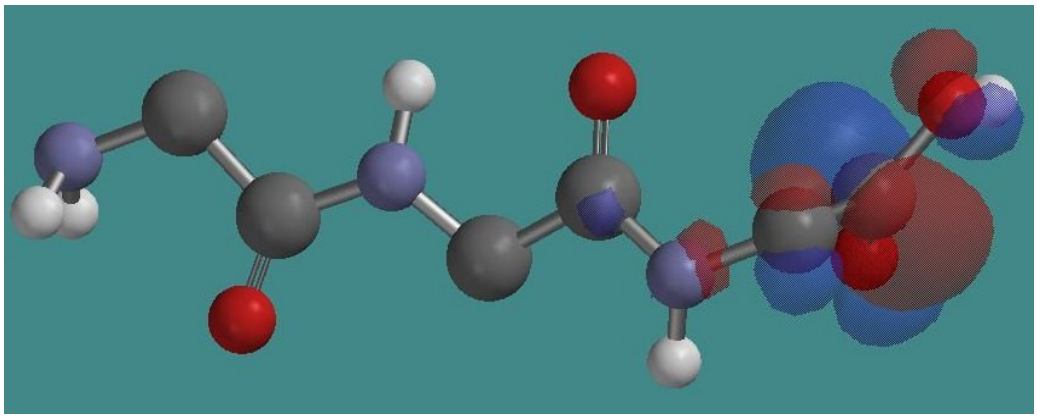

Fig 8.6 HOMO of RGD strand shows the HOMO near to the oxygen sites of the strand.

From the above study it is seen that the charge densities and the HOMO LUMO orbitals present a strong case for favourable RGD adhesion on to Hydroxyapatite.

8.4 Conclusion

The molecules of hydroxyapatite and RGD strand of the Extracellular matrix protein fibronectin was studied for favourable HOMO LUMO interactions and charge density polarities using the molecular dynamics modelling software Spartan 2 .Based on the charge density distribution and the HOMO –LUMO evolution a favourable condition exists for the binding of the RGD strands on to Hydroxyaatite surface. The RGD strand in turn acts as ligand sites for the binding of cell adhesion molecules on to them from bone cells .Thereby a favourable case for good osseointegration is obtained in case of Hydroxyapatite coated implants.

References:

[1] W.J.Hehre, A Guide to Molecular Mechanics and Quantum Chemical Calculations Wavefunction Irvine CA (2003) 21–88.

[2] W.J.Hehre, The Molecular Modelling Workbook for Organic Chemistry, Wavefunction Irvine CA (1998)13–29.

[3] F.P.Bowden, D Tabor The Friction and Lubrication of Solids, Oxford Classic Texts, Oxford U. P, New York, (2001). 285–298.

[4] N. H. Jayadas, K. P. Nair, Study of the Anti-Wear Properties of Coconut Oil Using Quantum Chemical Calculations and Tribological Tests, Journal of tribology **128** (2006) 654-659.

[5] K. Kendall Molecular Adhesion and its Applications, Kluwer academic publications New York (2004) ISBN 0-306-46520-5 275-300.

[6] R. P. McEver, P-selectin glycoprotein ligand-1 (PSGL-1), Adhesion Molecules: Function and Inhibition, Birkhäuser Verlag AG, P.O. Box 133, CH-4010 Basel, Switzerland, (2007)ISBN 978-3-7643-7974-2 3-27.

[7] C. M Isacke, M. A.Horton, The adhesion molecule. Academic press, USA(2000) ISBN 0-12-356505-7 149-210.

[8] G. Balasundaram, M.Sato, T. J. Webster, Using hydroxyapatite nanoparticles and decreased crystallinity to promote osteoblast adhesion similar to functionalizing with RGD, Biomaterials **27** (2006) 2798–2805.

[9] J.M.Fernandez-Pradas, L.Cleries, E.Martinez, G.Sardin, J.Esteve, J.L.Morenza, Influence of thickness on the properties of hydroxyapatite coatings deposited by KrF ablation. Biomaterials **22** (2001) 2171-2175.

[10] D. D. Deligianni, N. D.Katsala, P.G. Koutsoukos, Y. F. Missirlis, Effect of Surface Roughness of Hydroxyapatite on Human Bone Marrow Cell adhesion, Proliferation, Differentiation and Detachment. Biomaterials **22** (2001) 87-96.

[11] Bacakova, Cell adhesion on Artificial Materials for Tissue Engineering. Pysiol. **53/1** (2004) S35- S45.

[12] J. H. Boss, Biocompatibility: Review of the Concept and Its Relevance to Clinical Practice,Biomaterials and Bioengineering HandbookCRC USA (2000) 978-0824703189 1-54.

[13] G. Legeay and F. Poncin-Epaillard, Surface Engineering by Coating of Hydrophilic Layers:Bioadhesion and Biocontamination, Adhesion – Current Research and Application. Wulff Possart, Wiley-VCH Verlag GmbH & Co. KGaA, Weinheim (2005) ISBN: 3-527-31263-3 175-184.

[14] A.J. García and C.D. Reyes, Bio-adhesive Surfaces to Promote Osteoblast Differentiation and Bone Formation, J Dent Res (2005) **84(5)** 407-413, 2005.

[15] U. Bakowsky, C. Ehrhardt, C. Loehbach, P. Li, C. Kneuer, D. Jahn, D. Hoekstra, and C.-M. Lehr, Adhesion Molecule-Modified Cardiovascular Prostheses:Characterization of Cellular Adhesion in a Cell Culture Modeland by Cellular Force Spectroscopy Bioadhesion and Biocontamination, Adhesion – Current Research and Application. Wulff Possart, Wiley-VCH Verlag GmbH & Co. KGaA, Weinheim (2005) ISBN: 3-527-31263-3 175-184.

[16] M. Cannas, M. Bosetti, M. Santin, and S. Mazzarelli, Tissue Response to Implants: Molecular Interactions and Histological

Correlation, Biomaterials and Bioengineering Handbook, CRC, USA (2000) 978-0824703189 1-54.

[17] G. Balasundaram, T. J Webster, A perspective on nanophase materials for orthopaedic implant applications, Journal of materials chemistry**16** (2006) 3737-3745.

[18] N. J. Hallab, R. M. Urban, and J. J. Jacobs, Corrosion and biocompatibility of Orthopedic Implants, Biomaterials in Orthopedics, Marcel Dekker, Inc., 270 Madison Avenue, New York, NY 10016, U.S.A (2004) ISBN: 0-8247-4294-X 63-91 .

[19] M.Niinomi, T. Hattori, S. Niwa, Material Characteristics and Biocompatibility of Low Rigidity Titanium Alloys for Biomedical Applications, Biomaterials in Orthopedics, Marcel Dekker, Inc., 270 Madison Avenue, New York, NY 10016, U.S.A (2004) ISBN: 0-8247-4294-X 41-62.

[20] L. V. Carlsson, W. Macdonald, C. Magnus Jacobsson, and T. Albrektsson, Osseointegration Principles in Orthopedics: Basic Research and Clinical Applications, Biomaterials in Orthopedics, Marcel Dekker, Inc., 270 Madison Avenue, New York, NY 10016 U.S.A (2004) ISBN: 0-8247-4294-X 41-62.

Chapter 9

SUMMARY AND OUTLOOK

1. Summary

Interactions between orthopaedic implants and adjacent tissues are dependent, in part, on surface properties of the implant materials [1]. Mineralizing tissues have demonstrated the ability to bond directly to titanium and Titanium alloys especially $TiAl_6V_4$ (Ti) and that the overall success of cellular attachment, whether occurring in vitro or in vivo, is dependent on many parameters, including surface roughness, oxide composition and thickness, presence of contaminants and other surface properties [2–8]. By altering the surface chemistry of Ti through different sterilizing treatments, differences in the rate of human fibroblast attachment have been observed [9, 10]. Other implant surface modifications have included sandblasting [11], acid etching [12], the combination of sandblasting and acid etching [13], deposition of Ti coatings using plasma spraying [14], and deposition of calcium phosphate or hydroxyapatite (HA) coatings [15].

Hydroxyapatite, $(Ca_{10}(PO4)_6(OH)_2$ HA has good biocompatibility and is being widely used as a coating material to improve the durability and biocompatibility of implant and alternative bone.Among the various HA coating methods, the pulsed laser deposition (PLD) method was introduced in 1992 for high quality HA coating [16,] using excimer lasers and some harmonics of Nd:YAG lasers .In the previous studies, the substrates of Ti

and/or Ti-alloy were maintained at temperatures between 500 and 800ºC in water vapor atmosphere in order to generate a HA coating with a high degree of crystallinity for high biocompatibility [16]. The condition of high substrate temperature promoted the oxidation of the substrate surface prior to the growth of the HA layer. The oxidation layer degraded the adhesion of the coating to the substrate [16]. Therefore, crystallized HA coatings should be deposited at lower temperatures in order to obtain a high adhesive coating. A new HA coating has been developed on a $TiAl_6V_4$ implant material in this study using PLD combined with a hydrothermal treatment at a lower substrate temperature of 200^0C.The coating has returned good surface characteristics required for biocompatibility as well as sufficient bonding strength of more than 1KN.The coating was subjected to cell viability studies in vitro and returned good viability results of 40% higher osteoblast adhesion compared to uncoated $TiAl_6V_4$ sample. This suggests the use of this procedure to coat Ti orthopaedic implants for medical uses.

Anodization is another surface modification technique that can be used on implant surfaces. It is an electrochemical method which produces rough, thick and porous oxide films by spark discharging. A thick (2 mm), rough and porous oxide layer containing phosphorus (P) was reported to form on Ti surfaces after anodization with a H_3PO_4 electrolyte solution [17, 18]. Despite the extensive physical and chemical characterization of anodized oxides available in the literature [17-22], there is little data on the biological responses to anodized oxide surfaces with respect to the degree of anodization and comparison of cell attachment on HA surfaces with anodized Ti surfaces. Ti surfaces were anodized to various degrees of anodization and were compared for cell viability and surface characteristics for favourable cell adhesion. The surface anodized to the highest degree returned good surface characteristics for

favourable osteoblast adhesion and also gave comparable cell viability results in the in-vitro analysis. This suggests a higher adoption of a higher degree of anodization for Ti implants for orthopaedic uses to give a biocompatible implant comparable to a HA coated one.

Interfaces between protein molecules and inorganic materials are important in areas such as biomaterials science, biomineralization, biosensor and biofuel cell technologies [23, 24, 25]. Before cells adhere to a biomaterial surface, protein will be adsorbed from body fluids, and thisadsorption may control subsequent cell adhesion and behavior. Many studies in the past have qualitatively demonstrated the complexities of protein adsorption and the influence of protein adsorption on cellular response [26-29]. It is now well recognized that the osteoblasts are preferentially adhered to specific amino acid sequence such as Arg-Gly-Asp (RGD, a specific recognition site for transmembrane integrins) loop in adsorbed proteins [23, 28, 29].

Several extracellular matrix (ECM) proteins are crucial in cell adhesion, partially through the RGD sequence. In addition, in humans, ECM plays an important role in promoting or inhibiting the growth of the apatitic mineral component of bone and tooth enamel. Among these ECM proteins, fibronectin (FN) is a key one that not only provides a substrate for cell anchorage but also serves as a regulatory protein in processes such as cell adhesion, motility and proliferation [29]. As HA coated implants returned good osteblast adhesion compared to uncoated implants the anchorage of RGD sequence on to the coating surface provides an interesting area of study at the molecular level. The molecular level analysis of the HOMO- LUMO evolution and the charge densities suggest a favourable condition for the binding of the RGD strand on to HA coated surfaces.

References:

[1] J. Suha, B. Janga, X. Zhub, L.J Ongc, K. Kim, Effect of hydrothermally treated anodic oxide films on osteoblast attachment and proliferation Biomaterials **24** (2003) 347–355

[2] C.Larsson, P.Thomsen, B.O Aronsson, M.Rodahl,J. Lausmaa, B.Kasemo, L.E. Ericson, Bone response to surface-modified titanium implants: studies on the early tissue response tomachined and electropolished implants with different oxide thicknesses. Biomaterials **17** (1996) 605–16

[3] B.Kasemo, Biocompatibility of titanium implants: surface science aspects. J Prosthet Dent **49** (1983) 832–7.

[4] R.E.Baier, A.E.Meyer, J.R. Natiella, J.M.Carter, Surface properties determine bioadhesive outcomes: methods and results. J Biomed Mater Res **18** (1984) 337–45.

[5] J.E.Lemons, Dental implant tissue interfaces the bone-implant interface workshop report. Illinois: Americal Academy of Orthopaedic Surgeons, 1985 136–48.

[6] J.H.Doundoulakis, Surface analysis of titanium after sterilization: role in implant-tissue interface and bioadhesion. J Prosthet Dent **58** (1987) 471–8.

[7] B.Kasemo, J.Lausmaa, The bone-biomaterial interface and its analogues in surface science and technology. The bone–biomaterials interface workshop (1991) 19–32.

[8] J.LOng, G.N.Raikar, L.C.Lucas, R.Connatser, J.C.Gregory, Spectroscopic characterization of passivated titanium in a physiologic solution. J Mater Sci: Mater Med **6** (1995) 113–9.

[9] J.C.Keller, R.A. Draughn, J.P.Wightman , W.J.Dougherty, S.D.Meletiou, Characterization of sterilized cp titanium implant surfaces.Int J Oral Maxillofac Implants **5** (1990) 360–7.

[10] C.M.Michaels, J.C.Keller, C.M.Stanford, In vitro periodontal ligament fibroblast attachment to plasma-cleaned titanium surfaces. J Oral Implantol **17** (1991) 132–9.

[11] A.Wennerberg, T.Albrektsson, B.Andersson . Bone tissue response to commercially pure titanium implants blasted with fine and coarse particles of aluminum oxide. Int J Oral Maxillofac Implants **11** (1996) 38–45.

[12] P.R. Klokkevold, R.D. Nishimura, M.Adachi, A.Caputo, Osseointegration enhanced by chemical etching of the titanium surface. Clin Oral Implants Res **8** (1997) 442–7.

[13] D. Buser, T.Nydegger, T.Oxland T,D.L. Cochran , R.K.Schenk, H.P.Hirt, D.Snetivy, L.P.Nolte, Interface shear strength of titanium.implants with a sandblasted and acid-etched surface: a biomechanical study in the maxilla of miniature pigs. J Biomed Mater Res **45** (1999) 75–83.

[14] S.L.Wheeler, Eight-year clinical retrospective study of titanium plasma-spraying and hydroxyapatite-coated cylinder implants. IntJ Oral Maxillofac Implants **11** (1996)340–50.

[15] P.Ducheyne, Q.Qiu, Bioactive ceramics: the effect of surface reactivity on bone formation and bone cell function. Biomaterials **20** (1999) 2287–303.

[16] M Katto, K Ishibashi, K Kurosawa, A Yokotani, S Kubodera, A Kameyama, T Higashiguchi, T Nakayama, H Katayama, M Tsukamoto and N Abe, Crystallized hydroxyapatite coatings deposited by PLD with

targets of different densities, Journal of Physics: Conference Series **59** (2007) 75–78

[17] P.Kurze, W.Krysman, H.G.Schneider, Application fields of ANOF layers and composites. Cryst Res Technol **21** (1986) 1603–9.

[18] W.W. Son, K.H.Kim, H.I. Kim, T.Hanawa, Y.S.Jeong, Formation of titanium oxide layer by anodizing method. Biomater Res **4** (2000) 66–72.

[19] W.W .Son, K.H.Kim, H.I.Kim , T.Hanawa, Y.S.Jeong YS, Formation of titanium oxide layer by anodizing method. Biomater Res **4** (2000) 66–72.

[20] H.Ishizawa, M. Ogino, Formation and characterization of anodic titanium oxide films containing Ca and P. J Biomed Mater Res **29** (1995) 65–72.

[21] H.Ishizawa, M.Ogino, Characterization of thin hydroxyapatite layers formed on anodic titanium oxide films containing Ca and P by hydrothermal treatment. J Biomed Mater Res **29** (1995) 1071–9.

[22] Zhu X, Kim KH, Jeong YS, Anodic oxide film containing Ca and P of titanium biomaterial. Biomaterials **22** (2002) 199–206.

[23] Jia-Wei Shen, Tao Wu, Qi Wang, Hai-Hua Pan, Molecular simulation of protein adsorption and desorption on hydroxyapatite surfaces, Biomaterials **29** (2008) 513–532.

[24] J.J.Gray, The interaction of proteins with solid surface. Curr Opin Struct Biol **14** (2004) 110–5.

[25] Xiong YJ, Shi L, Chen BW, Mayer MU, Lower BH, Londer Y, High-affinity binding and direct electron transfer to solid metals by the Shewanella oneidensis MR-1 outer membrane c-type cytochrome OmcA. J Am Chem Soc **128** (2006) 13978–9.

[26] R.Langer, D.A.Tirrell, Designing materials for biology and medicine.Nature **428** (2004) 487–92.

[27] M.M.Stevens, J.H.George, Exploring and engineering the cell surface interface. Science **310** (2005) 1135–8.

[28] J.A.Hubbell, Materials as morphogenetic guides in tissue engineering.Curr Opin Biotechnol **14** (2003) 551–8.

[29] B.G. Keselowsky, D.M.Collard, A.J.Garcia, A Integrin binding specificity regulates biomaterial surface chemistry effects on cell differentiation.Proc Natl Acad Sci USA **102** (2005) 5953–7.